AN INVESTIGATION OF RANONG CLAY FROM THAILAND

A THESIS

Presented to

The Faculty of the Graduate Division

by

Lek Uttamasil

In Partial Fulfillment

of the Requirements for the Degree

Master of Science in Ceramic Engineering

Georgia Institute of Technology

June, 1969

AN INVESTIGATION OF RANONG CLAY FROM THAILAND

Approved:

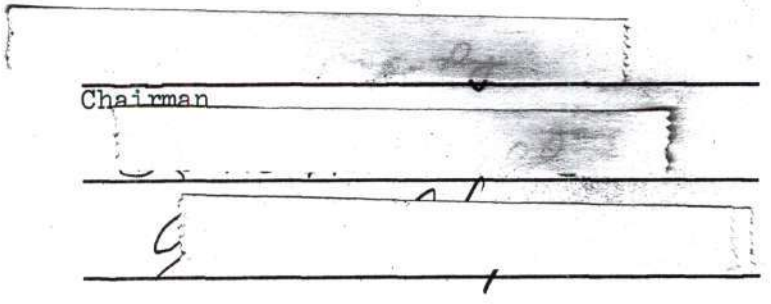

Chairman

Date approved by Chairman: June 3, 1969

In presenting the dissertation as a partial fulfillment of the requirements for an advanced degree from the Georgia Institute of Technology, I agree that the Library of the Institute shall make it available for inspection and circulation in accordance with its regulations governing materials of this type. I agree that permission to copy from, or to publish from, this dissertation may be granted by the professor under whose direction it was written, or, in his absence, by the Dean of the Graduate Division when such copying or publication is solely for scholarly purposes and does not involve potential financial gain. It is understood that any copying from, or publication of, this dissertation which involves potential financial gain will not be allowed without written permission.

7/25/68

ACKNOWLEDGMENTS

I wish to express my sincere appreciation to my thesis advisor, Dr. W. E. Moody, for his guidance, encouragement, generosity, patience, and invaluable advice. Profound appreciation and sincere gratitude are also given to Dr. Lane Mitchell and Dr. A. T. Chapman for their willingness to assist and advise.

I wish to give special thanks to the Applied Scientific Research Corporation of Thailand, Bangkok, Thailand for the clay sample.

I would also like to thank Dr. R. J. Gerdes for his assistance in the scanning electron microscopic experiments, Miss Jane Thacker for her excellent typing, and Mr. Thomas Mackrovitch for his laboratory assistance.

I am grateful to the financial aid of the Georgia Institute of Technology during a period when much of my study was taken.

Lastly, I wish to express my sincere appreciation to my family for encouraging this work.

TABLE OF CONTENTS

TABLE OF CONTENTS (Continued)

LIST OF TABLES

LIST OF TABLES (Continued)

LIST OF TABLES (Continued)

LIST OF ILLUSTRATIONS

LIST OF ILLUSTRATIONS (Continued)

LIST OF ILLUSTRATIONS (Continued)

SUMMARY

Ranong clay, from Ranong Province, Thailand was investigated for the identification of the type of clay minerals present and for its suitability for use as a paper or other type clay.

Ranong clay is found to belong to the kaolin group. It is composed of a mixture of a fairly well-crystallized kaolinite, metahalloysite with non-clay impurities of $2M_1$ muscovite and alpha quartz, and a small amount of the other minor impurities of potash feldspar, tourmaline, gibbsite, hydro-muscovite, organic materials, hematite, and amorphous materials. The mineral composition of Ranong clay is approximately 79.2 percent kaolinite, 7.8 percent metahalloysite, 7.5 percent quartz, and 5.5 percent muscovite.

Ranong refined clay consists mostly of a mixture of kaolinite and metahalloysite with a few percent of the impurities. It is a high quality clay with low grit content, a small amount of impurities, controllability of particle size, and good color.

Ranong refined clay may be suitable for use as a filler clay in the paper industry or in the ceramic industry. The metahalloysite causes high viscosity of Ranong refined clay and consequently makes it unsuitable for use in the high speed coating equipment presently used in the paper industry.

CHAPTER I

INTRODUCTION

Ranong clay is one of the clay deposits found at Hadd Som Paen area, Ranong Province, Thailand. This clay, belonging to residual clay type, occurred in the Late Cretaceous as a consequence of the weathering of granite rock.

Ranong clay, a by-product of the production of tin, has not been used extensively in the industry as the investigation and evaluation of this clay are still underway.

The purpose of this research was to identify the type of clay minerals present in Ranong clay and to investigate the properties of Ranong clay as to its feasibility for use as a paper clay or other type clay.

CHAPTER II

REVIEW OF LITERATURE

Clay

Clay is a natural, earthy, fine-grained material composed largely of the clay minerals according to Grim[1]. Most clays are plastic when wet and permanently hard when fired. Generally, there are two types of clay, one is residual clay remaining in place after weathering of parent rock, and the other is sedimentary clay that has been transported from the original location.

Mineral Composition and Structure of Clays

Clay is composed of extremely small crystalline particles of one or more clay minerals. These minerals are hydrous aluminum silicates which may be partially or completely proxied by magnesium or iron silicates as essential constituents. Most clays consist of a mixture of clay minerals. Varying amounts of non-clay minerals such as feldspar, mica, quartz, calcite, pyrite, and anatase are often found mixed with the clays. Furthermore, many clays contain organic materials, exchangeble ions, water, soluble salts, and allophane.

There are several classifications of clay minerals. Grim[1] suggested the classification which is based on the shape of clay minerals and expandable or nonexpandable character of 2:1 and 1:1 layer silicates, as shown in Table 1.

The structure and mineral composition of clay will be discussed

Table 1. Classification of the Clay Minerals[1]

I. Amorphous
   Allophane group

II. Crystalline

   A. Two-layer type (sheet structures composed of units of one layer of silica tetrahedrons and one layer of alumina octahedrons), 1:1 layer:
      1. Equidimensional
         Kaolinite group
            Kaolinite, nacrite, etc.
      2. Elongate
         Halloysite group

   B. Three-layer types (sheet structures composed of two layers of silica tetrahedrons and one central dioctahedral or trioctahedral layer), 2:1 layer:
      1. Expanding lattice
         a. Equidimensional
            Montmorillonite group
               Montmorillonite, sauconite, etc.
         b. Elongate
            Montmorillonite group
               Nontronite, saponite, hectorite
      2. Nonexpanding lattice
         Illite group

   C. Regular mixed-layer types (ordered stacking of alternate layers of different types)
      Chlorite group

   D. Chain-structure types (hornblende-like chains of silica tetrahedrons linked together by octahedral groups of oxygens and hydroxyls containing Al and Mg atoms)
      Attapulgite
      Sepiolite
      Palygorskite

according to the classification suggested by Grim[1].

In general, two units are involved in the structure of most clay minerals. One unit is in the form of octahedral sheet in which Al or Mg atoms occupy the octahedral interstices, and the other is built of silica tetrahedral sheet in which Si atoms occupy the tetrahedral interstices, forming the hexagonal networked sheet. The structure of clay minerals arises from the combination of these units in various ways.

Allophane is an amorphous substance of variable compositions found in clay minerals[2]. It contains variable proportions of silica, alumina, and water[3], and usually associates with halloysite. It may be colorless, blue, pale green, brown, or yellow.

Ross and Kerr[4] studied the kaolin group and proposed a nomenclature which has been generally accepted. Kaolinite is a common mineral of the kaolin group. It is hydrous alumium silicate having the approximate composition of $Al_2O_3 \cdot 2SiO_2 \cdot 2H_2O$. The crystallographic system of kaolinite, according to Brindley[5], is triclinic with axial dimensions of $a = 5.16A^\circ$, $b = 8.97A^\circ$, $c = 7.38A^\circ$, $\alpha = 91.8^\circ$, $\beta = 104.5^\circ$, and $\gamma = 90^\circ$. Structurally, kaolinite is composed of a single sheet of silica tetrahedrons forming a continuous series of ring structure and a single alumina octahedral sheet combining into kaolin unit layer, as shown in Figure 1 (after Grim (II)). In the latter, the hydroxyl ions occupy all the anion sites in the unshared level at the interval of b/3. In the level of octahedral-tetrahedral conjunction, only one-third of the anion sites are hydroxyl, and the remainder are oxygen. In order to satisfy the electrical neutrality, only two-thirds of the crystal alumina sites are occupied. Ideally, the occupied Al sites have a continuous hexagonal

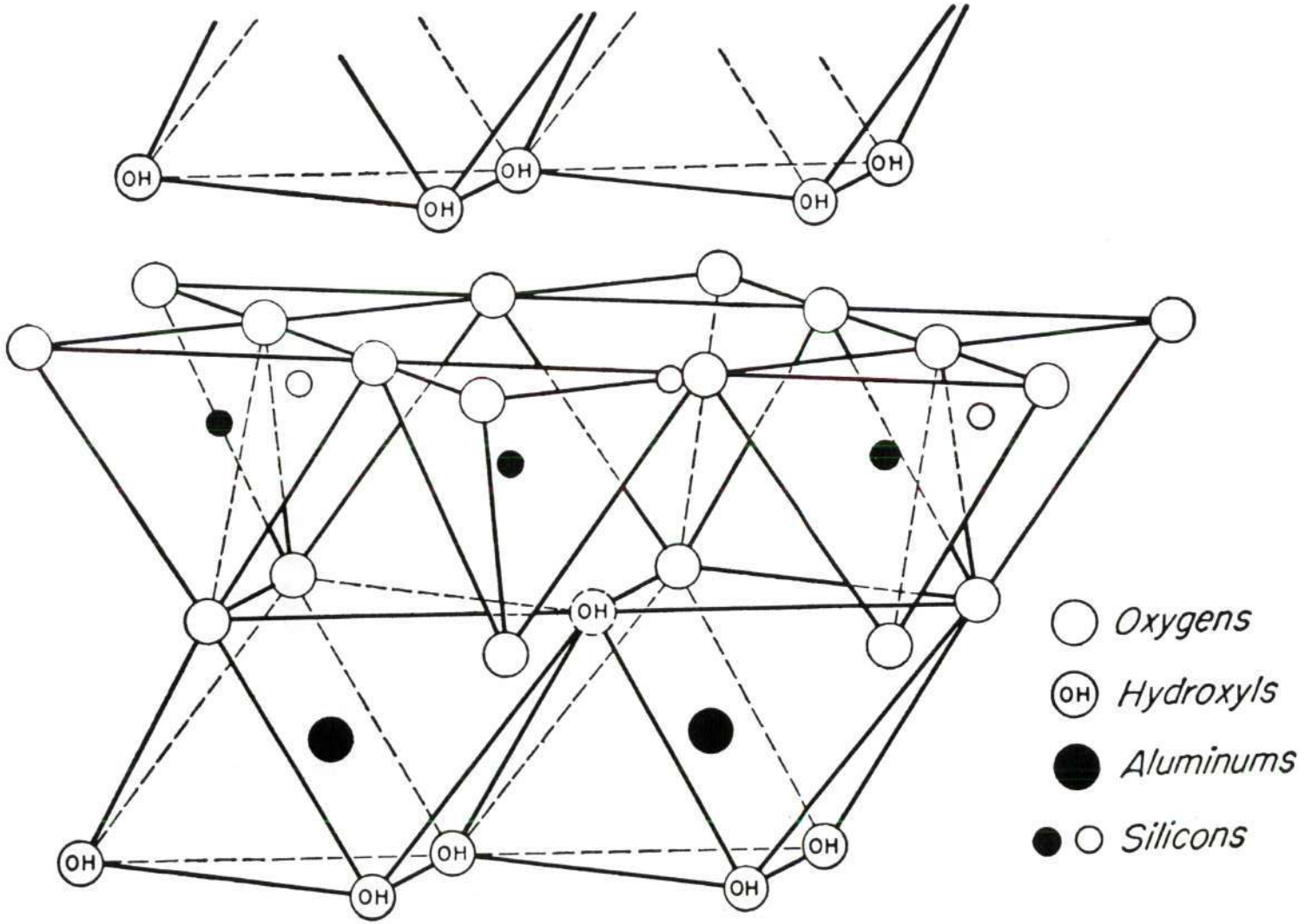

Figure 1. Diagramatic Representation of Kaolinite Structure after Grim (II).

structure in the a and b direction. However, it has some random distribution of Al ions among the octahedral sites. In general, kaolinite has a range of structure in terms of degree of crystallinity; namely, poorly-to-well crystallized structure. The poorly-crystallized kaolinite may be due to disorders such as random layer displacement, foreign ion substitution, ionic displacement, interlayer water, etc. Brindley[6] suggested that the poorly-crystallized kaolinite has disorder of nb/3, caused by the shift of the entire kaolin alumina layer. The other possibility was attributed to the shift of individual alumina ions along b (or 120° on either side) into vacant lattice sites. Brindley[5] suggested that the X-ray diffraction patterns of well-crystallized kaolinite would give four clear reflections in the "d" spacing range 3.5-2.5A°. He also pointed out that the partial resolution of the doublet, $11\bar{1}$, and $1\bar{1}\bar{1}$, with spacing 4.18 and 4.13 is an indication of well-crystallized kaolinite. The degree of nb/3 crystallinity index of kaolinite can be determined from the ratio of $(02\bar{1})/(060)$ reflection intensities of X-ray diffraction traces, according to Johns and Murray[7]. The range of the ratio varies from 0.0 for a poorly nb/3 crystallized kaolinite to 1.0 (or slightly more) for a nb/3 well-crystallized one.

Dickite and nacrite have a similar structure to kaolinite but differ from kaolinite with respect to the method by which the layers are stacked one upon the other[1].

Halloysite is an elongated mineral occurring in two forms[4,8], one is metahalloysite with a composition $Al_2O_3 \cdot 2SiO_2 \cdot 2H_2O$, and the other is a more hydrated form with an additional $2H_2O$. The latter form dehydrates to the former irreversibly at relatively low temperature ($\sim 60°C$).

The basal spacing is approximately 7.2A° for metahalloysite and 10.1A° for the hydrated form of halloysite. The structure of the hydrated form of halloysite is shown in Figure 2 (after Grim (II)). Hendricks and Jefferson[9] suggested that the water molecules in this layer had a definite configuration. Bates, et al[10] stated that the outside diameters of the tubular particles of halloysite range from 0.04 to 0.19 micron with a median value of 0.07 micron. The average wall thickness was about 0.02 micron. The tubes may range in length up to several microns. When dehydration takes place, this tubular form of dehydrated halloysite frequently collapses, splits, or unrolls. Collins[11] suggested that the halloysite does not always occur in tubular form and it is found sometimes in irregular or spherical units.

Smectite is used for the group name, and Montmorillonite as the aluminous member of this group. Smectite is composed of two silica tetrahedral sheets with a central alumina octahedral sheet combined together to form a common layer which is continuous in the a and b directions, as shown in Figure 3 (after Grim (II)). In the method of stacking of the silica-alumina-silica units, the oxygen layers of each unit are adjacent to oxygens of the neighboring units with the consequence that there is a very weak bond and an excellent cleavage between them. A chargewise unbalance in the lattice also arises. The water and other polar molecules can enter between the smectite units and cause expansion. Sodium, calcium, magnesium, iron, and other cations can also occur between the units, and these are generally exchangeable. A relationship exists between the thickness of the water layers and the type of exchangeable ions[1]. The theoretical formula for the smectite is

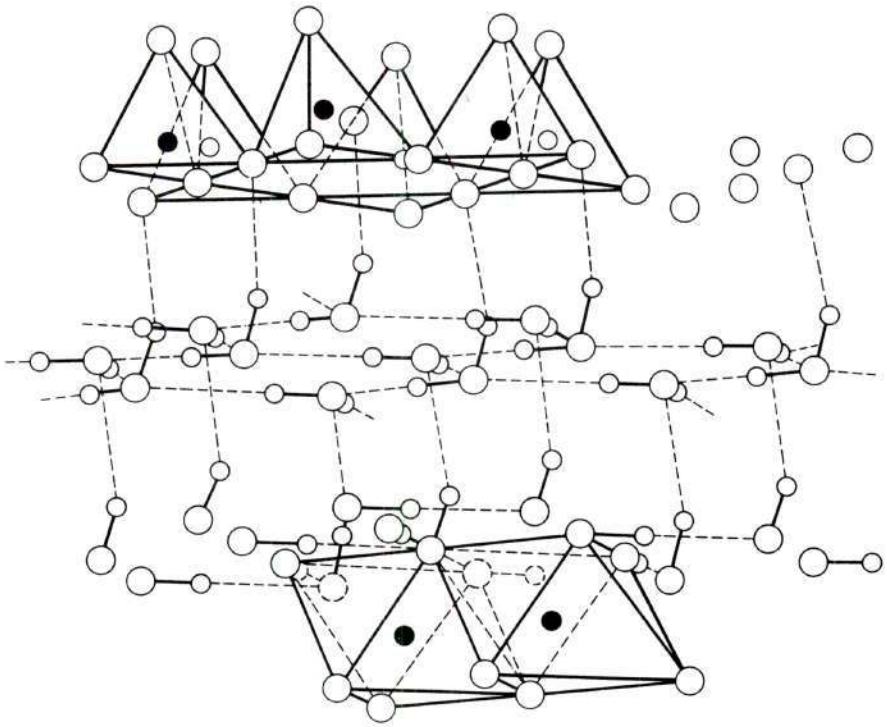

Figure 2. Diagramatic Representation of Halloysite 4 H_2O Structure after Grim (II).

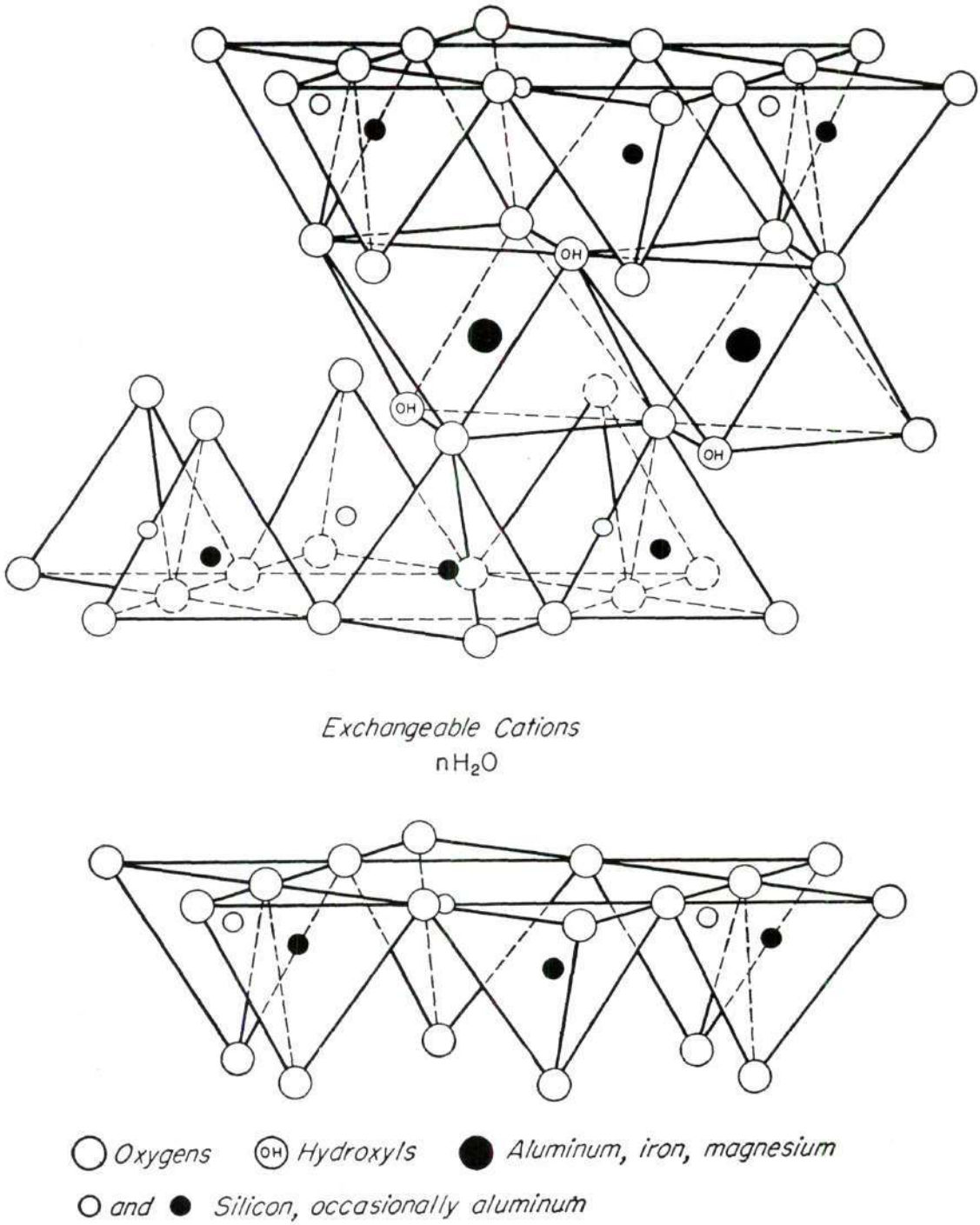

Figure 3. Diagramatic Representation of Smectite Structure after Grim (II).

$(OH)_4Si_8Al_4O_{20}$ n H_2O (interlayer). The smectite always differs from the theoretical formula because of substitutions in the lattice[12]. These substitutions are the basis of the other minerals in the smectite group. Montmorillonite, a common clay mineral in the smectite group, results from a moderately small amount of substitution of magnesium for aluminum ions. Sauconite results when the aluminum is replaced by zinc. Both montmorillonite and sauconite are equi-dimensional clay minerals. The shapes of nontronite, saponite, and hectorite are elongated. All these minerals belong to the smectite group. Nontronite occurs from the substitution of aluminum by iron. Saponite and hectorite result from the replacement of aluminum by magnesium. Hectorite also has lithium.

Illite is a name for the mica-like clay minerals[13]. The basic structural unit of illite is a layer composed of two tetrahedral sheets with a central octahedral sheet, as shown in Figure 4 (after Grim (II)). The tetrahedral tips in each silica sheet point toward the center of the unit and are combined with the octahedral sheet in a single layer with a substitution of hydroxyls by oxygens. This unit is similar to the smectite unit except that some aluminum ions replace silicon in the tetrahedral sheet, and this results in a charge deficiency. The charge deficiency is balanced by potassium ions which act as a bridge between the unit layers so that the illite minerals are not expandable.

Chlorite is one of the regular, mixed layer types of clay minerals. The structure of the true chlorites consists of alternate mica-like and brucite layers[5,14,15]. These layers are continuous in the a and b dimensions and are stacked in the c direction with basal cleavage between

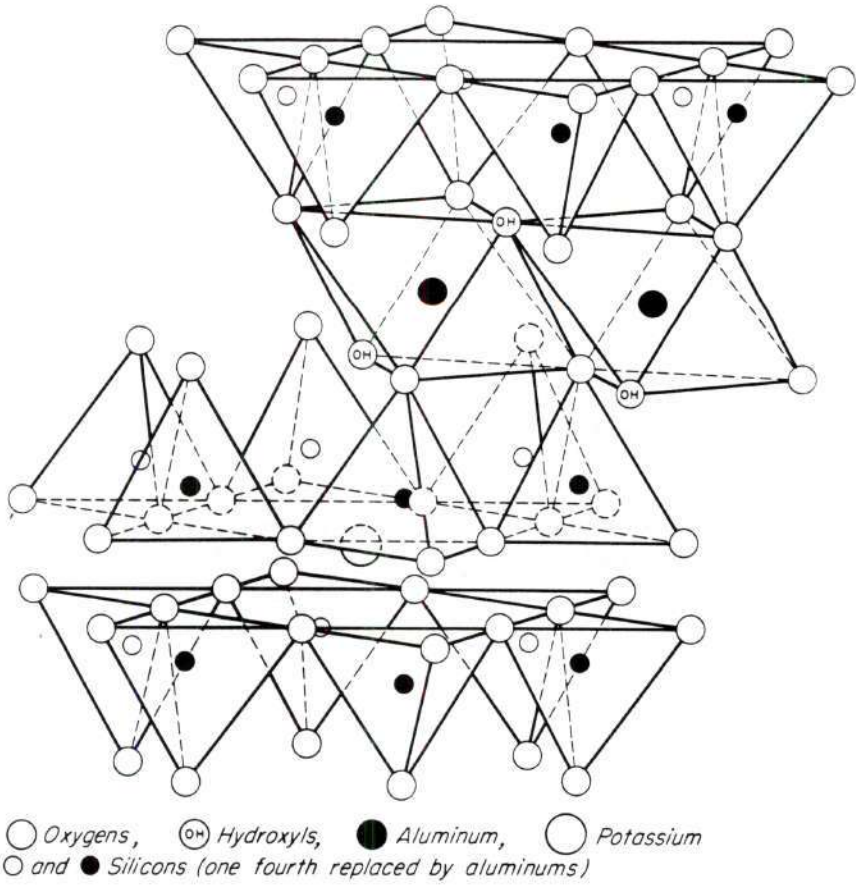

Figure 4. Diagramatic Representation of Illite Structure after Grim (II).

layers. The composition of the mica-like layers is $(OH)_4(Si \cdot Al)_8(Mg \cdot Fe)_6 O_{20}$. The brucite layer may be a magnesium or aluminum or iron hydroxide or a combination of three irons. The structure of chlorite is shown in Figure 5 (after Grim (II)). The various clay minerals in the chlorite group can be distinguished by the kind and amount of substitution in the brucite and the mica layers.

Vermiculite is one of the clay minerals with a c-axis dimension of $14A^{\circ}$, which does not expand when treated with polar molecules but usually collapses to about $10A^{\circ}$ on heating[16]. It has some of the structural characteristics of chlorite and some of smectite. Gruner[17] showed that vermiculite structure consists of a layer made of two silica tetrahedral sheets with a central magnesium, iron octahedral sheet separated by two layers of water molecules and adsorbed magnesium, and calcium ions. The structure of vermiculite is shown in Figure 6 (after Grim (II)).

Attapulgite, palygorskite, and sepiolite are fibrous clay minerals which belong to the chain-structure types. These minerals consist of double silica chains linked together by octahedral groups of oxygens and hydroxyls, containing Al and Mg atoms. Bradley[18] studied the structure of attapulgite, and its schematic representation is shown in Figure 7 (after Grim (II)).

Sepiolite[19] is hydrous magnesium silicate. The structure of this mineral is similar to, but differs in detail from the attapulgite. The schematic representation of the clay mineral as presented by Nagy and Bradley[19] is shown in Figure 8 (after Grim (II)). This scheme is that two pyroxene chains are linked to form an amphibole chain with an extra silica tetrahedron added at regular intervals of each side. Brauner and Preisinger[20] postulated the structure of sepiolite, in con-

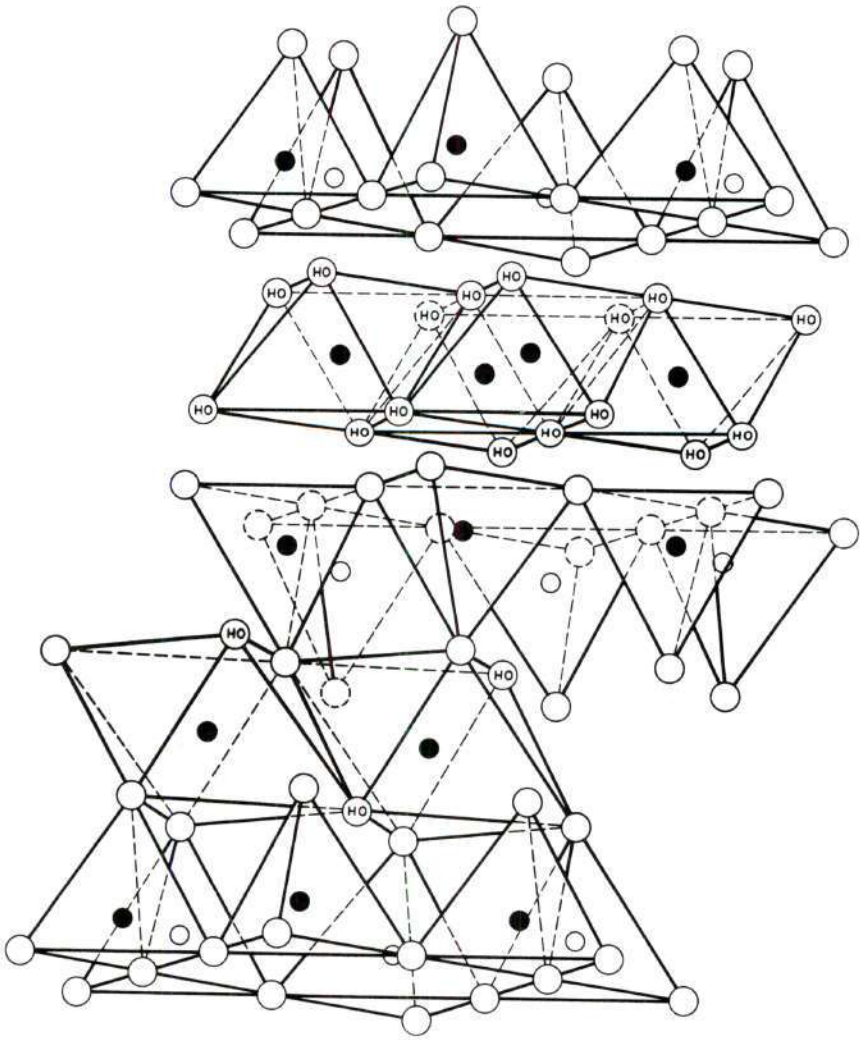

Figure 5. Diagramatic Representation of Chlorite Structure after Grim (II).

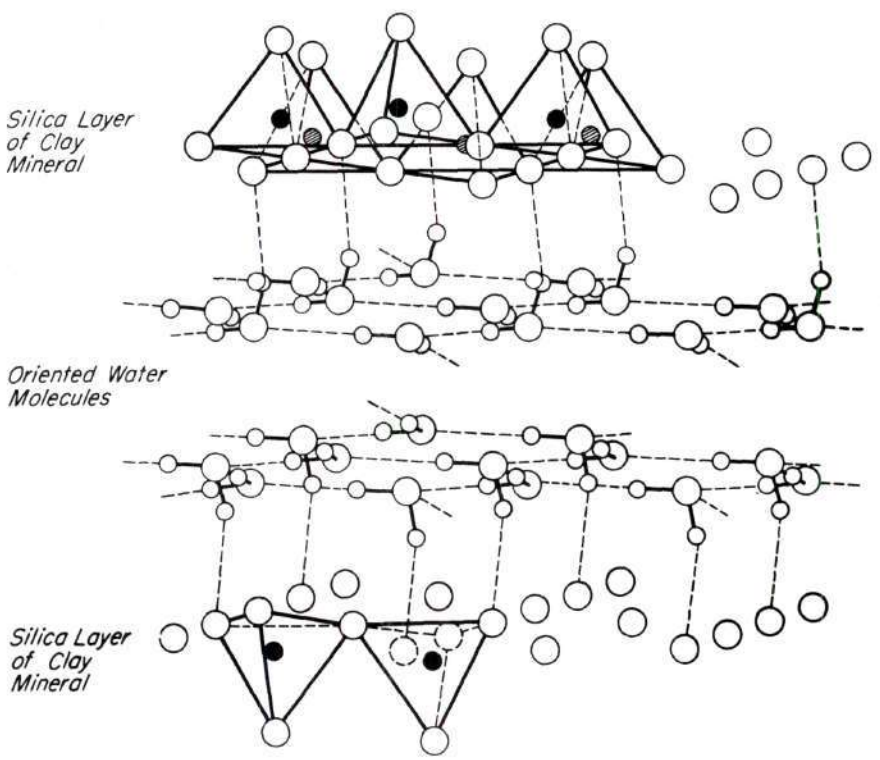

Figure 6. Diagramatic Representation of Vermiculite Structure after Grim (II).

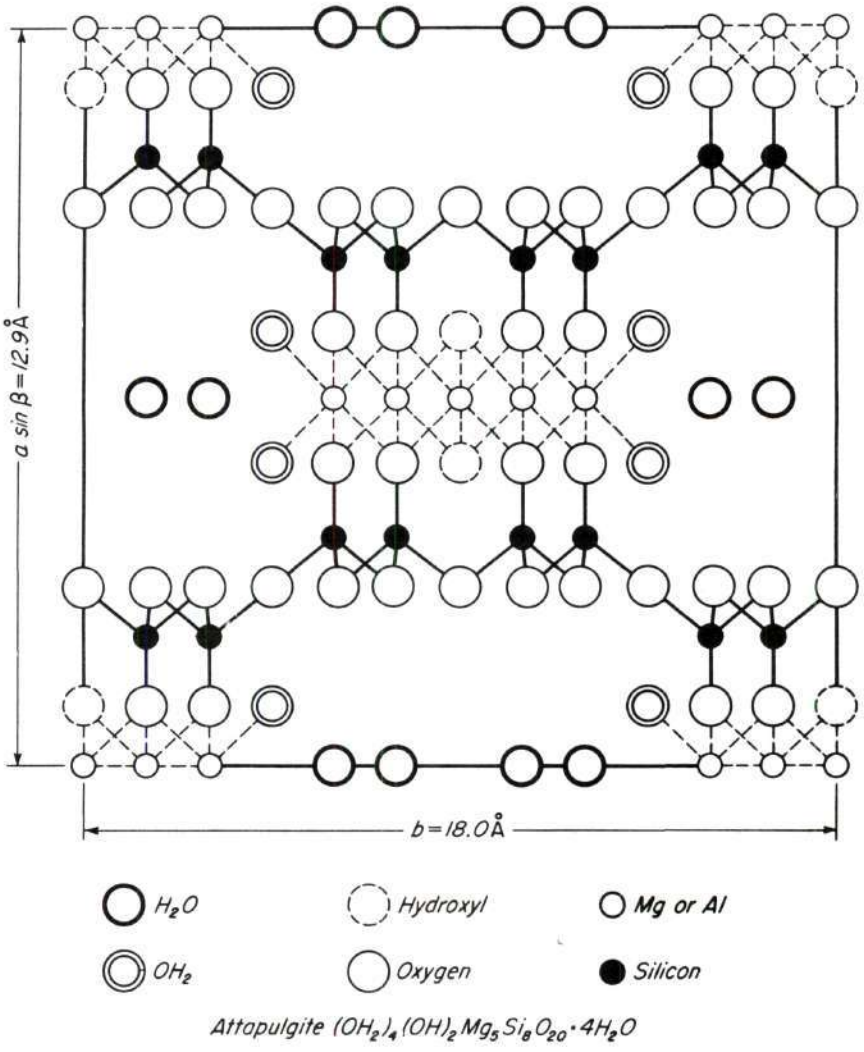

Figure 7. Schematic Representation of Attapulgite Structure after Grim (II).

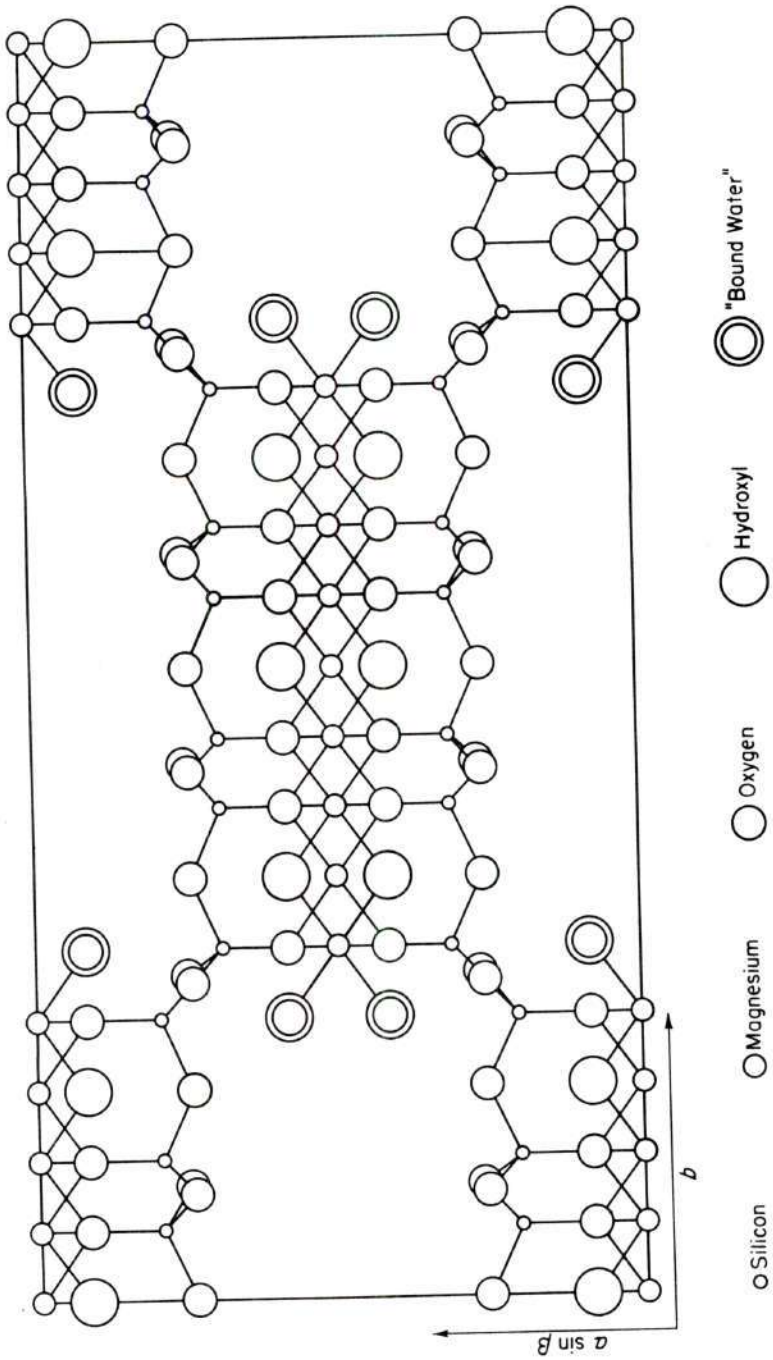

Figure 8. Schematic Representation of Sepiolite Structure after Grim (II).

trast to the previous one, as being composed of three pyroxene chains linked together to form two continuous amphibole chains.

Palygorskite is usually associated with smectite. Huggins, et al[21] suggested that palygorskite has the same structure as attapulgite and attapulgite is considered as simply short-fibered palygorskite.

Mixed layer minerals are found present in several clay materials. In general, there are many clay materials which are composed of more than one clay mineral, and the minerals may be mixed in different ways. The types of mixing may be by the interstratification of the clay mineral layers or by the combination of discrete clay minerals. The mixed-layer structures are of two different types; namely, a regular interstratification and a randomly irregular stratification of layers. The common mixed-layer minerals are mixed-layers of illite and montmorillonite, and of chlorite and vermiculite. The specific names for the mixed-layer minerals cannot be adopted since they have inherent variability. They can only be designated as mixtures of the layers involved according to Grim[1].

Methods of Identification of Clay Minerals

Several methods are available for identifying the clay minerals and also non-clay minerals which occasionally occur in clay minerals as the secondary minerals or impurities. They are X-ray diffraction analysis, electron microscopic analysis, differential thermal analysis, thermogravimetric analysis, infrared spectroscopic analysis, etc. In general, a combination of several methods is necessary. The X-ray and electron microscope yield the most rapid and best determinations. X-ray

diffraction analysis is now the most widely used for the identification and study of the crystalline characteristics of clay minerals. Electron diffraction with similar principles to X-ray diffraction is less widely used. It will be particularly more useful when used in conjunction with the electron microscope, since the morphology of clay minerals is related to their crystal structures.

Neutron diffraction so far has not been applied to any extent to clay minerals; however, it is a very important tool in the determination of the position of hydrogen atoms. The differential thermal analysis and thermogravimetric analysis will give clear-cut curves for relatively pure clay minerals. These are the more valuable tools for identification purposes, especially when used in conjunction with the other methods. The infrared spectroscopic analysis has useful applications in clay mineral analysis, in particular, for the determination of the relationship between the hydrogen and the hydroxyl bonds. However, the routine use of infrared analysis for mineralogical investigations has been largely neglected. The petrographic microscope is a reliable tool for identifying the clay minerals in the case of few coarse-grained clays, but most clays have grains too fine to permit positive identification. It should be noted that when immersion liquids are used for refractive index determinations, they may enter the crystal lattice of the swelling minerals and thereby change their indexes of refraction. The textural characteristics of a clay material can be revealed by a study of thin sections[22]. Grim[23] suggested that a preliminary study with the petrographic microscope will help in planning what other analyses should be made on clay materials. Piller[24] has given special

consideration to the use of phase contrast method. The spectroscopic analyses will give, qualitatively, and quantitatively, a rapid and positive idea for various elements present in the clay materials. Chemical analysis of the clay materials is important technologically, but it seems to have relatively little value for mineralogical identification. It can be used in conjunction with other techniques for identification such as X-ray diffraction etc. Kelly[25] indicated some interpretations could be made from chemical analysis of clays. He also mentioned some difficult problems involved. In the chemical methods, dye staining tests can also be used for identification purposes. A summary of characteristics of staining of clay minerals has been prepared by Grim[1]. Physical tests are able to aid identification of clays, and they are more invaluable to determine their degree of utility.

Industrial Utilizations of Clays

Clays are important industrial ceramic materials because of their unique properties and their low cost. They are used in the manufacture of a variety of products. Outside the ceramic industry, clays are the essential parts of paper, drilling fluids, and certain lubricating greases. They are applied in the formulation of insectides, ointments, adhesives, and rubber or synthetic plastics. They act as catalysts or catalyst supports in many processes, and they are used for clearing wine. Certain industrial uses of clays are shown in Table 2. The properties and mineralogical compositions of clays are specified for their uses in the aforementioned industries.

Clays find their major use in the paper industry where they are

Table 2. Some Industrial Utilizations of Clays

Industrial Products	
Paper	Refractories
Paint	Roofing Tiles
Foundries	Drain Tiles
Medicine	Terra Cotta
Cosmetics	Wall Tiles
Pesticides	Floor Tiles
Ink	Insecticides
Paste	Food Additives
Crayons	Sizing
Plasters	Catalysts
Whitewares	Rubber
Cement	Pencils
Insulators	Drilling Muds
Electrical Conduits	Oil Clarifiers
Bricks	Plastics
Porcelain Enamels	Adhesives
Aggregates	Textiles
Fertilizers	Detergents
Linoleum	Bleaching
Filter Aids	Absorbents

used as a filler in the interstices of a paper sheet to add ink receptivity and opacity. As a coater, they are used to coat the surfaces of a paper sheet to render sharp photographic pictures and bright printed colors. The adaptibility of the characteristics and properties of clays is invaluable in the paper industry. These are good whiteness, desirable brightness, chemical inertness, low abrasiveness, low viscosity, controllability of particle size, softness of texture, low adhesive demands, ability to produce high gloss, and satisfactory ink adsorption.

The type of clay used in the paper industry is a high quality kaolinite. In general, there are two processes involved in refining kaolin and removing its impurities; namely, the dry process and the wet process. The wet process usually gives much better quality products than the dry one, and the products can be sold at a higher price.

The physico-chemical properties of kaolinite are very important in selection for use in the paper industry. As a filler, the kaolin should have suitable brightness which varies from about 80 to 84 percent, although sometimes slightly lower values are acceptable. It should have low screen residue, low abrasiveness, and suitable particle size distribution. The properties of widely used kaolins are shown in Table 3 (after Grim (II)). The viscosity is not important but it should be easily dispersable.

For use as a coater, the brightness, viscosity, and particle size distribution of kaolin are very important. The brightness should be in the range of 80 to 85 percent or higher, and its particle size should be 80 percent finer than 2 microns or higher. According to Iannicelli and Millman[27], the acceptable viscosity values are not greater than 1000

Table 3. Properties of Some Kaolins Used in Paper Manufacture[26]

	Filler Clay		Coating Clay			
	A	B	C*	D	E	F*
Particle-size distribution, equivalent spherical diameter, % by weight:						
0-0.5μ	20	4	44	44	30	26
0.5-1μ	21	6	28	28	27	29
1-2μ	17	10	20	20	23	23
2-5μ	13	31	8	8	17	20
5-10μ	12	30	0	0	3	7
10-30μ	7	19	0	0	0	0
Maximum screen residue, wet, 325 mesh	0.15	0.15	0.005	0.01	0.01	0.008
GE brightness	82.5-84	80.5-83	86.5-88	86.5-88	85-86.5	85-86.5
pH	4.2-5.0	3.8-4.6	6.3-7.0	4.2-4.6	4.2-4.6	6.3-7.0
Maximum viscosity:**						
at 10 rpm	---	---	500	500	350	300
at 100 rpm	---	---	200	200	200	180

* Clays C and F are "predispersed."

** TAPPI procedure, Brookfield, R. V. F., 70 percent solids; No. 3 spindle.

centipoises, usually less than 200 centipoises as measured by means of completely defloculated suspension of 70 percent solid by a Brookfield viscosimeter. However, the specifications of kaolin for paper use vary according to the manufacturer's individual requirement. Besides the aforementioned properties, the coating properties such as ink acceptivity, pick, etc., may be investigated in order to assure the optimum uses of this material for the paper industry.

Ranong Clay, Thailand

There are several kaolin deposits in Thailand. Large deposits are found at Lamphan, Uttaradit, Chanthaburi, Surat Thani, and Ranong Province. The locations of these deposits are shown in Figure 9. Furthermore, white clay deposits are also found at Rayong, Cholburi, Prachinburi, and Chiengrai Province.

Ranong clay has been proved to be the most promising china clay deposit in Thailand[28]. It may be able to compete in world markets when it is carefully improved and developed. Some of the deposits of Ranong clay have been mined and supplied to the whiteware and refractory industries. One of the clay mines in Ranong Province, Thailand, is illustrated in Figure 10.

Location of Deposits

Ranong clay deposits are located at Ban Hadd Som Paen area, Ranong Province, Thailand. One of the deposits is shown in Figure 11. The deposits occur at the elevation of 250 meters above sea level.

Geologic Relations[29]

According to the geology, the parent rocks (porphyritic biotite

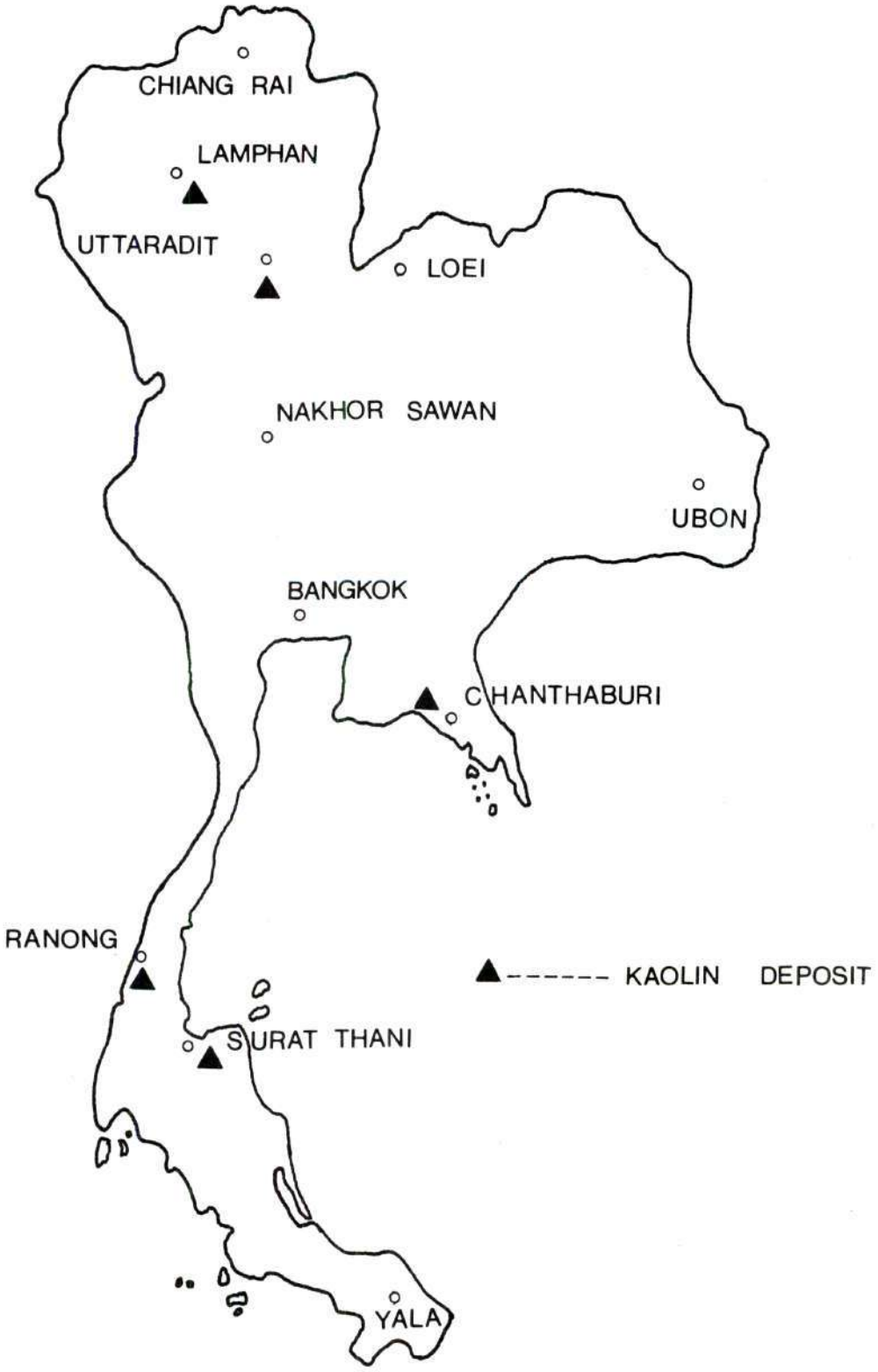

Figure 9. Outline Map Showing Kaolin Deposits in Thailand.

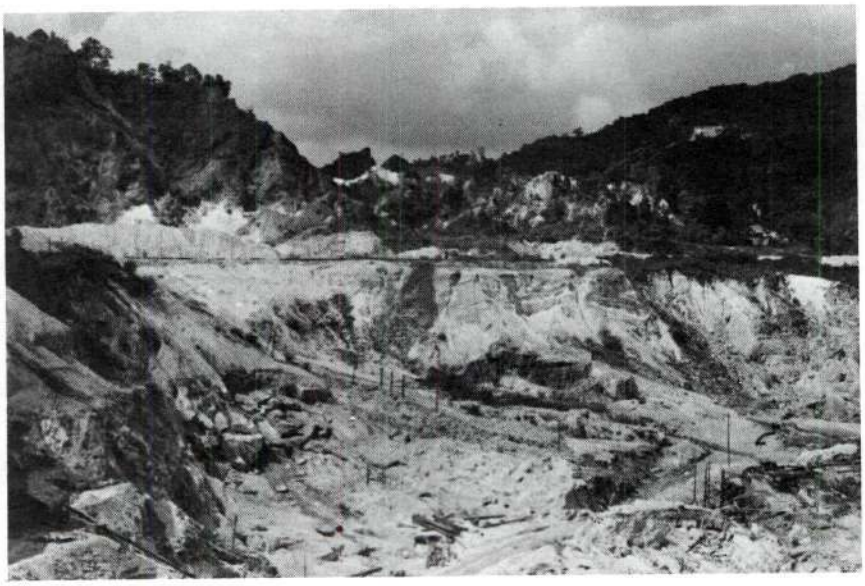

Figure 10. Ranong Clay Mine in Thailand.

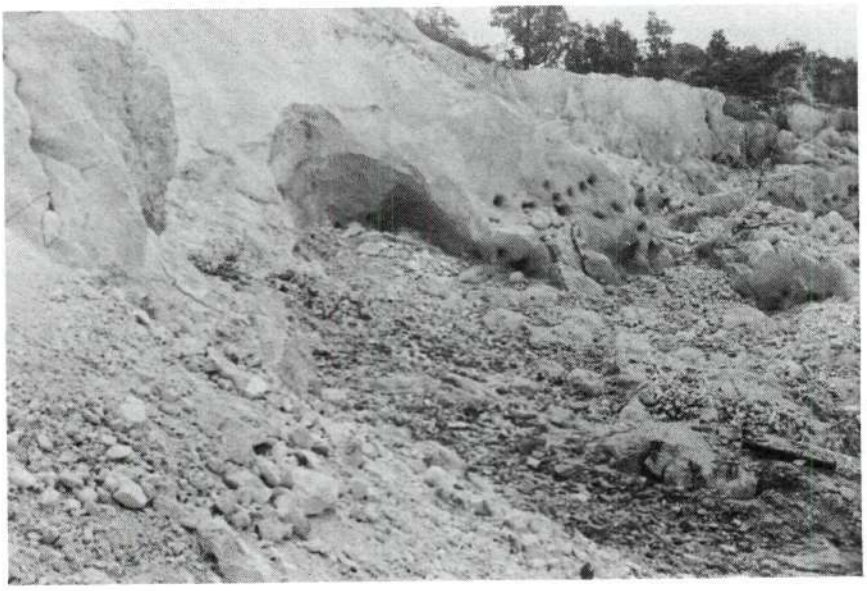

Figure 11. Ranong Clay Deposits.

granite) were created in Late Cretaceous by the intrusion of the biotite granite through the Phuket-series (name of rock series). The action of pneumatolysis altered the parent rocks into the coarse-grained tourmaline muscovite granite, and medium-grained tourmaline muscovite granite. Further action of this process generated feldspar. Ranong clay is believed to occur in Late Cretaceous, from the pneumatolysis of feldspar.

Ranong clay is considered to be a residual clay and occurs as shown in Figure 12. It can be seen that some of the kaolin clays are associated with the quartz veins. Beside quartz veins, it is reported that the cassiterite and wolfram minerals are found in Ranong clay deposits. The clay actually is a by-product of cassiterite mining operations.

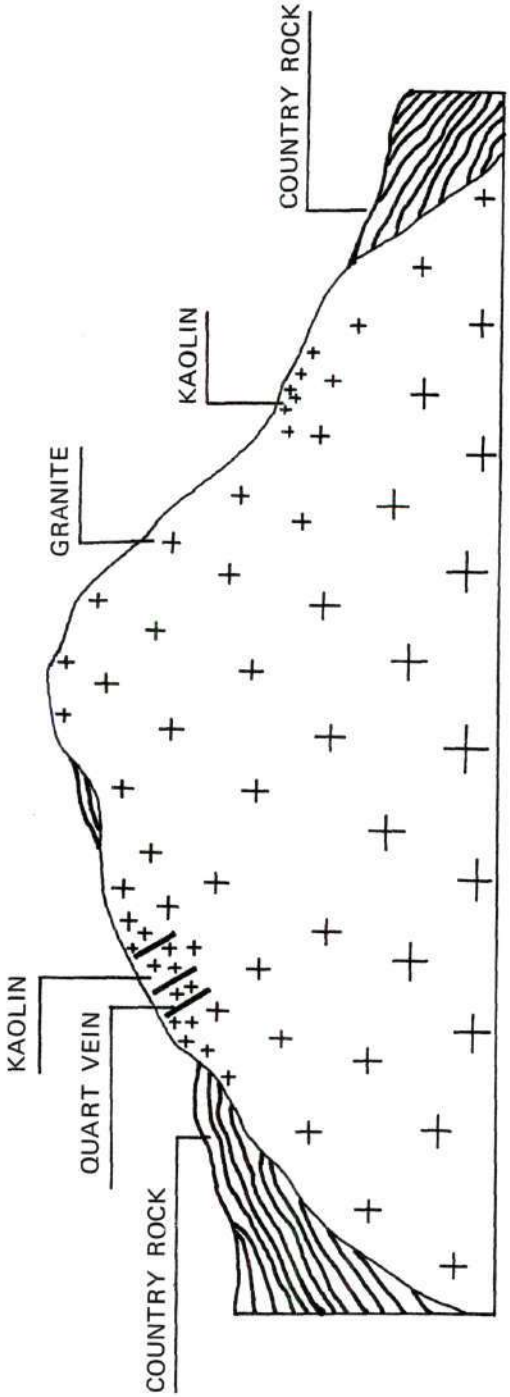

Figure 12. Ideal Section of Kaolin Deposits, Hadd Som Pan Area, Ranong Province, Thailand.

CHAPTER III

INSTRUMENTATION AND EQUIPMENT

X-ray Diffractometer

The X-ray diffraction analysis was carried out by using a Norelco diffractometer with copper radiation through a nickel filter. The dimensions of the angular aperture and the receiving slit were 1^{o} and 0.003 inch, respectively. The detector was a sealed proportional counter and the pulse height analyzer was set at 95 percent.

X-ray Spectrograph

The chemical element analysis was carried out by means of a Norelco Universal spectrograph with a tungsten tube. Both EDDT and LiF analyzing crystals (cut parallel to (200) plane) were used. A scintillation counter was used to detect the reflected fluorescent radiation from the LiF crystal and a gas flow proportional counter was used with the EDDT crystal.

Differential Thermal Analysis

The differential thermal analysis was carried out with a R. L. Stone Company "Controlled Environment DTA System" recorder-controller Model KA-H with a dynamic atmosphere sample holder SH-9A and a furnace Model F-1C.

Thermogravimetric Analysis

All the dehydration curves of Ranong clay were determined by using the R. L. Stone Company "Controlled Environment DTA System" recorder-

controller Model KA-H and a Cahn RG electrobalance with a Model F-1D furnace. The weight loss was determined in a vacuum of 23 inches of mercury.

Scanning Electron Microscope

The morphology of Ranong clay was investigated by a scanning electron microscope, Model Stereocan Mark IIa, by Cambridge Instrument Company, Cambridge, England. The resolution of this microscope is 200-600A°, and the range of useful magnification is 14X up to 30,000X.

Infrared Spectrophotometer

Identification was accomplished by a Perkin-Elmer spectrophotometer, Model 13, with a modified Leeds and Northrup Speedomax recorder, in the spectral region between 1 and 15.5 microns using NaCl prism. The instrument was manufactured by the Perkin-Elmer Corporation.

Atomic Adsorption Spectrophotometer

The Perkin-Elmer Corporation "Atomic Adsorption Spectrophotometer", Model 303, was used to determine the chemical analysis of Ranong clay.

Optical Spectrometer

All brightness and whiteness measurements were made with a Bausch and Lomb Spectronic 505. The instrument was made by the Pharr Instrument Company of Moline, Illinois.

Petrographic Microscope

The index of refraction of Ranong clay was determined by using a standard petrographic microscope and a standard set of oils. It was

also investigated for shape, crystallinity, and impurities.

Miscellaneous Equipments

Viscosimeters

All the viscosity determinations were done by a Stromer viscosimeter, Model 7649, by the Arthur M. Thomas Company, and a Brookfield viscosimeter, Model LVF, with a series of spindles and various RPM.

pH Meter

The pH determinations were accomplished by using a Beckmann Zeromatic pH meter with a Beckman Fiber Junction Electrode and a Beckman Glass Electrode. The pH meter was calibrated prior to each determination with the standard buffer solutions.

Particle Size Analysis

The particle size distribution was determined by an International Centrifuge, size 2, Type R, equipped with a No. 240 head and two trunnion rings (International No. 350), two 100 ml stainless steel shields (International No. 341), two rubber cushions (International No. 572), and six trunnion carriers (International No. 381), and the other conventional chemical apparatuses.

CHAPTER IV

PROCEDURE

Preparation of Specimens

Ranong water-washed clay was prepared and supplied from the Applied Scientific Corporation of Thailand, Bengkok, Thailand. It was investigated as received or with prior treatment, as specified in each test.

Fractionation of Ranong Clay

In order to study the clay minerals, the sample was fractioned into different size fractions by using the sedimentation and the centrifugal methods. A 20 percent weight suspension of Ranong washed clay, distilled water, and 5 grams of Tetrasodium Pyrophosphate (TSPP) per kilogram of clay, was blunged for 2 hours by a drill press blunger. The suspension was passed through a 325 mesh screen and the screen residues were saved. The suspension was allowed to settle and separate into the different size fractions by means of Jackson's method[30,31]. The fractions of clay were 20-44 microns, 10-20 microns, 5-10 microns, 2-5 microns, 1-2 microns, 0.5-1 micron, 0.25-0.50 micron, 0.1-0.25 micron, and less than 0.1 micron. These were used as the specimens in the subsequent experiments.

Data Collections

X-ray Diffraction Analysis

X-ray traces were run on the oriented and random powder specimens of each aforementioned particle size fractions of Ranong clay at 2θ of 2° to 66°. The x-ray diffraction patterns were interpreted and the results of the analysis were reported in terms of "d" spacing, 2θ degree, and relative peak height intensities. The nb/3 - crystallinity indexes of the specimens ranging from 1-2 microns to 20-44 microns, were determined by the method of Johns and Murray[7].

Determinations of Metal Impurities

Metal impurity determinations were done on bulk, 1-2 microns, and less than 0.1 micron fractions of Ranong clay. Each fraction was placed in the X-ray spectrograph sample holder. After the holder was covered with a 0.25 ml milar film, it was placed in a spectrographic unit. Spectrographic patterns were run on the specimens using LiF and EDDT analyzing crystals with W radiation. The impurities were reported in Table 35 of Appendix D.

Scanning Electron Microscopic Examinations

Each sample was mixed with distilled water to make a 1 percent suspension. Then, each suspension was dispersed with a small amount of TSPP and stirred until a noticeable turbidity was produced. The droplets of different sizes were placed on a metallic sample holder. After drying, the clay specimen on the sample holder was coated with evaporated metal to provide the conductive but transparent layers, and then was examined in the scanning electron microscope.

Differential Thermal Analysis

Each of the fractions of Ranong clay was run on the DTA units using alpha-alumina as the reference standard material. The differential thermal curves were run from 25°C to 1100°C at a constant rate of 15°C per minute. The amount of each sample was 25 milligrams for use in each experiment. DTA curves are illustrated in Figures 21 through 23 in Chapter V, showing the relations of temperatures and exothermic-endothermic reactions.

Thermogravimetric Analysis

The loss of water of each of the size fractions of Ranong clay was determined by the thermogravimetric analysis. Each sample was run on the thermogravimetric unit in the range between 25°C and 1000°C at a constant rate of 15°C per minute in a vacuum of 23 inches of mercury. The size of the samples varied from 6.7 to 13 milligrams. The results were reported as percent weight loss of water corresponding to each interval of temperature.

Infrared Spectroscopic Analysis

An amount of 10 grams of Ranong clay was ground in an agate mortar. The small amount of distilled water was added during the last few minutes before completion of grinding. The resulting thin paste of clay was washed with distilled water and transferred to a 1000 millimeter beaker. A part of the suspension was saved for serving as a bulk specimen fraction. The other part was mixed by a drill press mixer and classified according to particle sizes of 1-2 microns and less than 0.1 micron by centrifuging. One part of these clay fractions was saved for chemical analysis. After centrifuging, each clay fraction was washed with ethyl

alcohol several times to remove all noticeable water. The clay was shaken in a small amount of ethyl alcohol and some of the clay-alcohol suspension was dropped on the rock-salt plate adsorption cell. When the suspension was dry, the specimen was placed in an infrared spectroscopic unit. The infrared spectrum was run on the specimens in the spectral region between 1.5 and 15.0 micron using a NaCl prism.

Chemical Analysis

Samples saved from the previous analysis were used for chemical analysis. The analysis was carried out with an atomic adsorption spectrophotometer in accordance with the Analytical Methods for Atomic Absorption Spectrophotometry of Perkin-Elmer Corporation[32]. The results were reported as percent oxide contents.

Petrographic Microscopic Determinations

The screen residues obtained from the fractionation were immersed in a series of standard oils on glass slides. The slides were inspected under a petrographic microscope. Various minerals in screen residues were reported as impurities. The index of refraction of Ranong clay was determined by comparing with the standard oils until a match was obtained.

Estimation of Mineral Composition of Ranong Clay

First of all, the selection of standard minerals was performed. The standard components were selected for use in this analysis on the basis of their similar characteristics to those of the minerals in Ranong clay such as species of minerals, degree of crystallinity, particle size, etc. The standards were Georgia kaolinite, $2M_1$ muscovite, alpha quartz, and metahalloysite separated from Ranong clay. The X-ray

revealed that Georgia kaolinite has a well-crystallized character with very high purity. Scanning electron micrograph showed that the standard metahalloysite was rather pure.

Secondly, a series of mixtures containing various compositions of Georgia kaolinite, metahalloysite, alpha quartz, and $2M_1$ muscovite were prepared. X-ray traces were run on these mixtures at 2θ from 8° to 28°. They were also run on the bulk sample and the 80 percent less than 2 micron fraction of Ranong clay under the same 2θ degree conditions. All of the samples for X-ray analysis were in the form of random powder specimens.

The diffractometer settings were as follows:

kilovolts	35
milliamperes	20
scale factor	5×10^2
PHA	95 percent
time constant	8 seconds
chart speed	0.5 inch per minute
scanning speed	$1/8^{\circ}$ 2θ per minute

By comparing the X-ray diffraction traces of the bulk and 80 percent less than 2 micron fraction of Ranong clay with the traces of the series of mixtures of standard minerals, the mineral composition of each fraction of Ranong clay was determined.

Physical Tests

The particle size distribution of Ranong clay was determined in accordance with ASTM, Designation: D422-54T[33] in conjunction with a centrifuge-pipette method of Huber Clay Company[34]. It was reported as a cumulative percent finer than the specific size of particles correspond-

ing to the particle sizes of clay.

The moisture, pH, and screen residue of Ranong clay were measured in accordance with TAPPI Tetative Standard T-645 M-54[35]. The specific gravity was determined by means of ASTM, Designation: C329-56[36].

The brightness and whiteness of each Ranong clay fraction were measured with a Bausch and Lomb spectronic 505 in the spectral region between 400 and 700 millimicrons. The brightness was read at 457 millimicrons. The difference between the values of 700 and 400 millimicrons determined the whiteness value.

The viscosity determination was made with a Stromer viscosimeter with a falling weight of 150 grams. The time of weight fall, where a dial was traversed through 100 divisions by a pointer, was reported as an index of the viscosity. A 60.8 percent suspension of oven-dry clay and distilled water was mixed with a drill press mixer for 15 minutes prior to each determination. The suspension was titrated with 0.5 cc of 5 percent weight TSPP solution and the time of fall was recorded. This procedure was repeated until the minimum time of fall was obtained. The minimum viscosity of this clay was reported in seconds per 100 revolutions.

Preparation of Ranong Refined Clay

Ranong refined clay refers to Ranong clay which has a particle size of 80 percent less than 2 microns. This term will be used in the subsequent descriptions.

A 20 percent weight suspension of Ranong clay and distilled water was dispersed with 5 grams of TSPP per 1 kilogram of clay. The suspension

was mixed with the drill press mixer for 3 hours. Then the suspension was passed through a 325 mesh screen to remove any coarse materials such as mica and quartz. The suspension was allowed to settle down in the settling tanks in order to obtain a suspension of particle size less than 5 microns. The 5 micron suspension was separated to approximately 80 percent particle size finer than 2 microns. A part of the 80 percent finer than 2 micron suspension was saved for bleaching and the remainder was siphoned off and dried.

The portion of suspension saved from the previous separation was divided into two parts for bleaching. The first part was bleached with 30 percent hydrogen peroxide solution (5 percent by weight of clay). The second part diluted to 10 percent weight suspension, and bleached with sodium hydrosulphite (5 grams per 1 kilogram of clay) at pH range between 3.5 and 4.0. After bleaching, the top of each suspension was siphoned off and the bleached clay was dried.

Physical Evaluation Tests for Ranong Refined Clay

All the physical constants except the Brookfield viscosity and the Hercules viscosity were determined according to the same procedures as described in the previous section for physical tests.

The Hercules viscosity value, with the assistance of Dr. W. E. Moody of the School of Ceramic Engineering, Georgia Institute of Technology, was obtained from the Thiele Kaolin Company, Georgia.

The Brookfield viscosity was measured by a Brookfield viscosimeter using spindle No. 3. A suspension of 60.8 percent solid of Ranong refined clay was dispersed with 50 percent TSPP solution and various values

of viscosity were taken. The minimum Brookfield viscosity of completely deflocculated suspension was reported as the viscosity of Ranong refined clay.

CHAPTER V

DISCUSSION OF RESULTS

Identification of Ranong Clay, Thailand

X-ray Diffraction Analysis of Ranong Clay

The grit or particle size greater than 44 microns of this clay was found to be composed of muscovite, quartz, and a small amount of feldspar and touramline. The muscovite and quartz were identified as $2M_1$ muscovite and alpha quartz types, respectively. Figures 13 through 16 show the diagramatic representation of X-ray diffraction patterns of Ranong clay in both random powder and oriented specimens. In the random powder specimens, the X-ray traces are shown only for the fractions up to 1-2 microns since the traces of clay fractions larger than 2 microns are the same as those of the oriented samples, except for the few more diffraction lines which are of little significance for identification.

The clay fractions ranging from bulk to 10-20 microns gave the same results. The X-ray diffraction peaks at 7.1395A°, 3.5695A°, and 1.9976A° indicated the characteristic diffraction of kaolinite. The presence of $2M_1$ muscovite was detected by the characteristic peaks at 9.9917A° and 3.3386A°. The spacing at 4.2704A°, 2.462A° were attributed to alpha quartz and the strongest quartz peak was superimposed on the 3.3A° region of $2M_1$ muscovite. Potash feldspar was also found by the 3.2438A° reflection.

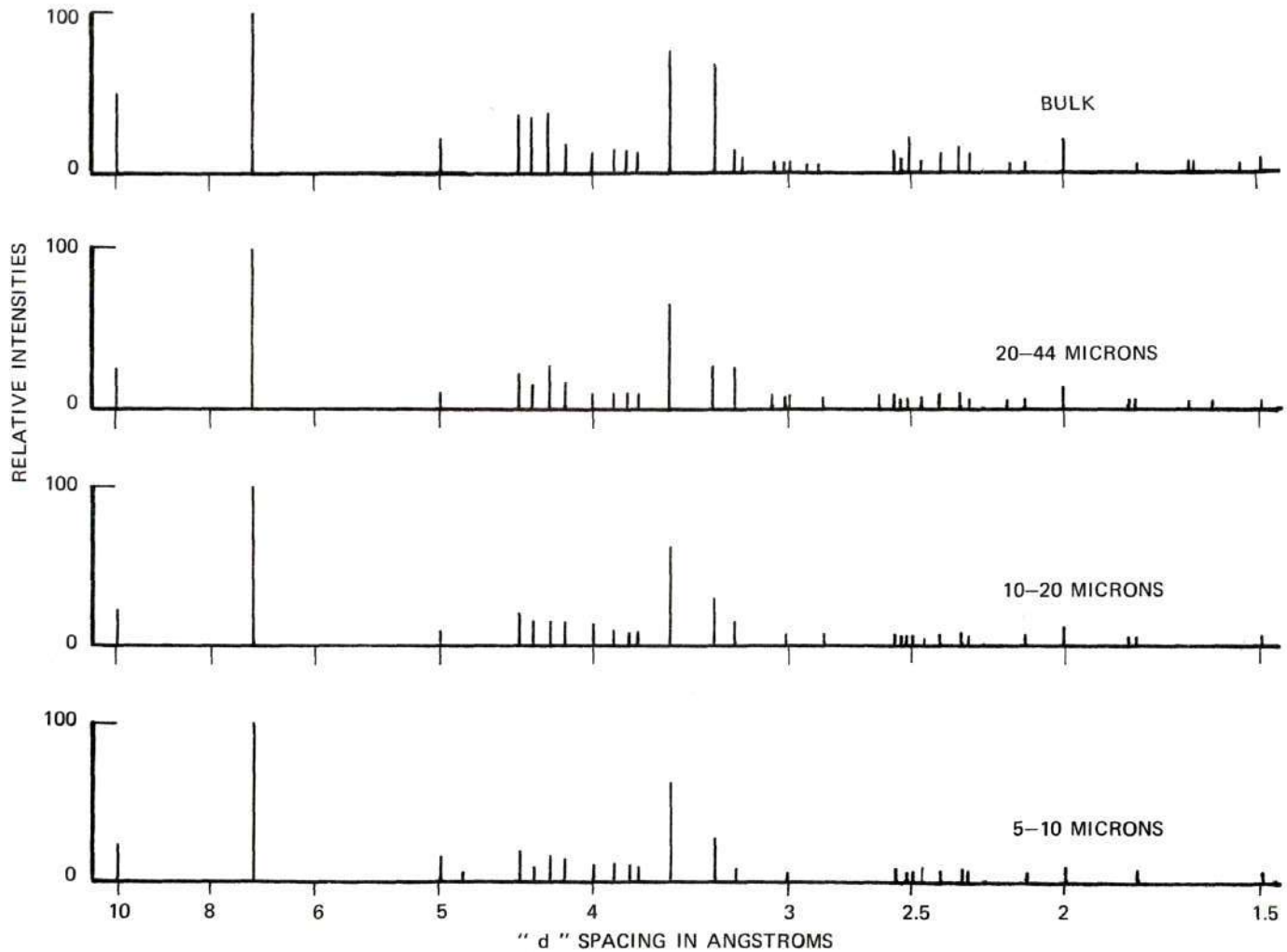

Figure 13. Diagramatic Representation of X-ray Diffraction Patterns of Oriented Sample of Ranong Clay.

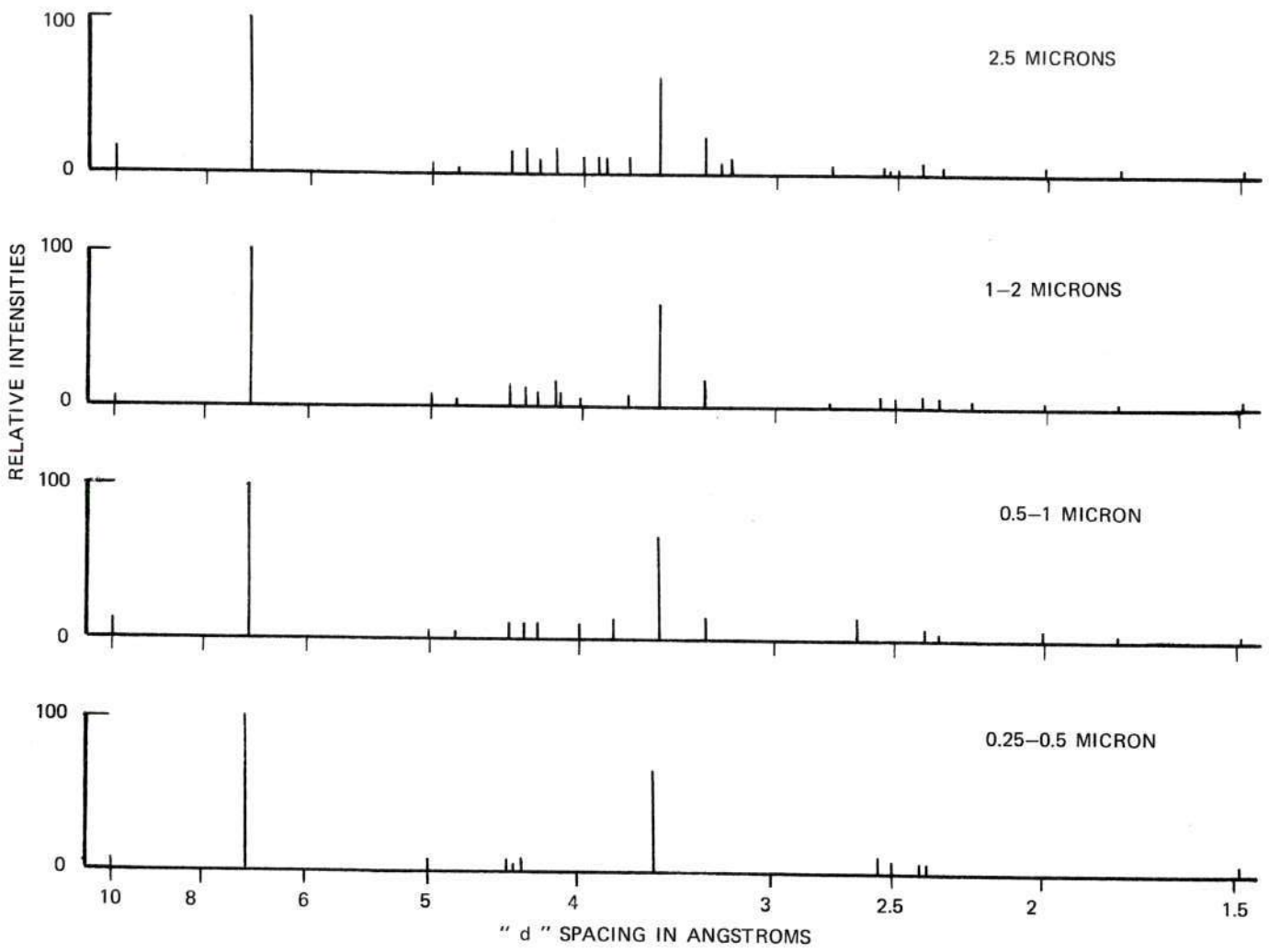

Figure 14. Diagramatic Representation of X-ray Diffraction Patterns of Oriented Sample of Ranong Clay.

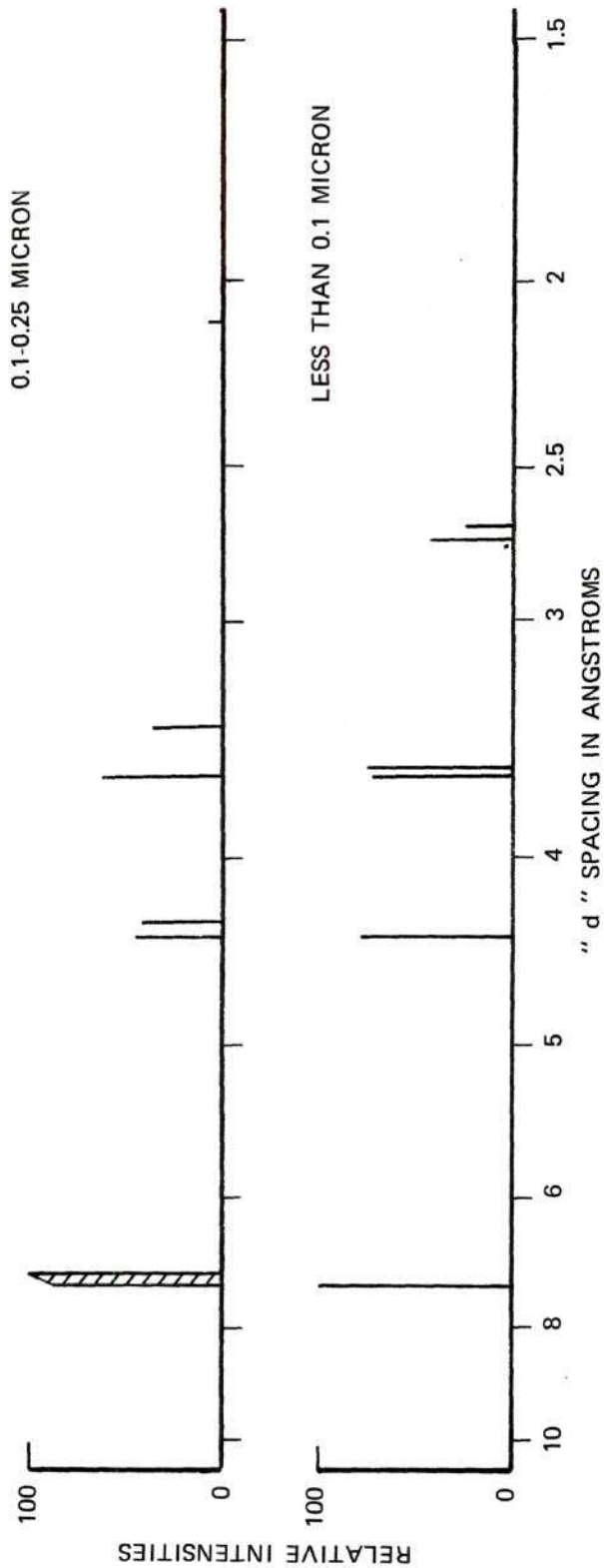

Figure 15. Diagramatic Representation of X-ray Diffraction Patterns of Oriented Sample of Ranong Clay.

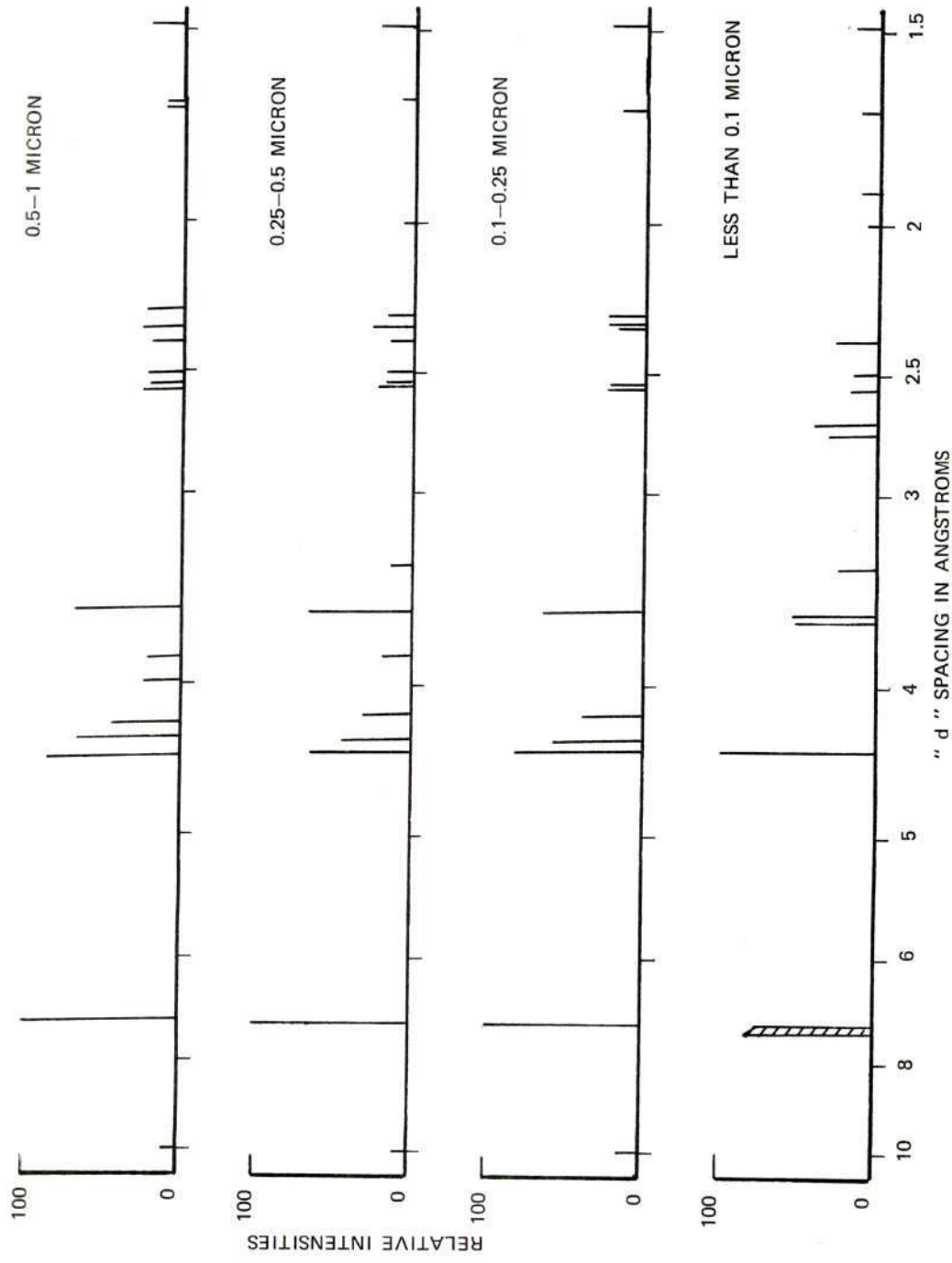

Figure 16. Diagramatic Representation of X-ray Diffraction of Random Powder Sample of Ranong Clay.

In 5-10 and 2-5 micron fractions, the diffraction patterns appeared similar to the patterns of the larger sized particles, except some variation in relative intensities which was due to the relative amounts of the minerals existing in each fraction. Gibbsite was found in these fractions. It was detected as only one very weak intensity peak at 4.8478A°.

In 1-2 micron fraction, the X-ray diffraction pattern seemed to be a representation of nearly pure kaolinite with a small amount of impurities, probably due to the pronounced concentration of kaolinite in this fraction. Alpha quartz, $2M_1$ muscovite, and gibbsite were also found. Potash feldspar became extinct in this fraction.

For the particle size of clay smaller than 1 micron, the X-ray diffraction patterns of the oriented samples were different from the randomly powder sample patterns.

In oriented samples, the X-ray diffraction patterns of 0.5-1 and 0.25-0.5 micron fractions were similar to the 1-2 micron fraction. In 0.1-0.25 micron fraction, the X-ray diffraction pattern was difficult to interpretate positively as it showed a tendency to separate into two peaks at 7.3750A° and 7.1668A°. This suggested the presence of a new mineral in this fraction and it was identified as metahalloysite by the presence of 7.3750A° peak, together with the new peaks at 4.4A° and 3.6A° regions, as shown in Figure 15. A positive identification could be given for the 7.1668A° peak, but due to its higher intensity it was more likely to be kaolinite than metahalloysite.

Referring to Figures 15 and 16, a marked increase in the relative intensities of all the reflections, except the (001) reflection, was

caused solely by a decrease in the intensity of (001) reflection, not by the increase in mineral concentrations, since the relative intensities were expressed with respect to the (001) reflection intensity. The pronounced decrease in the intensities of (001) and (002) reflections confirmed the rolled form of metahalloysite, since it gives little enhancement of basal reflections when in the rolled form. In the particle size less than 0.1 micron fraction of this clay, a new mineral, hematite, at 2.6984A° was found. The high background baseline of X-ray diffraction patterns of 0.1-0.25 and less than 0.1 micron fractions suggested the presence of amorphous materials (free alumina, silica, and iron oxides). The X-ray diffraction pattern of the 0.1 micron fraction seemed to represent metahalloysite with a small amount of kaolinite. In the oriented samples, both $2M_1$ muscovite and gibbsite and alpha quartz became extinct in the 0.1-0.25 micron and 0.25-0.5 micron fractions, respectively.

In random powder samples, the broad and asymmetrical X-ray diffraction patterns pointed out the characteristics of metahalloysite. However, some of the diffraction peaks corresponding to kaolinite were still found. Therefore, these clay fractions consisted of matahalloysite and kaolinite. For smaller particle size, the diffraction patterns showed the marked characteristics of metahalloysite, especially in the fraction of less than 0.1 micron in which there were two peaks at 7A° region and another high intensity peak at 4.4A° region ((002) reflection). This implied the increase of metahalloysite concentrations in Ranong clay when its particle size became smaller. The amorphous materials and hematite were also found in the less than 0.1 micron fraction. In the random powder samples, $2M_1$ muscovite, alpha quartz, and gibbsite were

extinct in the 0.1-0.25, 0.25-0.5, and 0.5-1 micron fractions, respectively.

The summary of the results of X-ray identification is shown in Table 4. The data of X-ray diffraction of Ranong clay corresponding to Figures 13 through 16 are tabulated in Tables 10 through 29 in Appendix A.

Attempts were made to confirm the type of halloysite. The saturation of ethylene glycol of an oriented sample was carried out. If this clay mineral was halloysite (endellite, $Al_2O_3 \cdot 2SiO_2 \cdot 4H_2O$), there would be a shift from 10.1A° to 10.5-11.0A° since the ethylene glycol molecule would be substituted for the water layer in the halloysite lattice and causes it to be modified. As there were no shifts in the diffraction patterns, the clay mineral was metahalloysite.

Montmorillonite which might be present in Ranong clay, was not found by the ethylene glycol test.

In order to determine the presence of chlorite that might associate with Ranong clay, the oriented samples were heat-treated at 550-600°C. The 7A° and 3.5A° region peaks of the heated specimens disappeared from the X-ray diffraction patterns. If there had been chlorite in this clay, such peaks would not have collapsed. Hence, there was no chlorite in Ranong clay.

The kaolinite as noted was a fairly well-crystallized kaolinite. Its X-ray diffraction trace is shown in Figure 17.

The region from 19.9° 2θ to 23.9° 2θ (3.57 to 2.56A°) gave four clear reflections; namely, (020) reflection, $(1\bar{1}0)$ reflection, $(11\bar{1})$ reflection, and $(02\bar{1})$ reflection. These four reflections implied a well-crystallized kaolinite. The crystallinity indexes of kaolinite

Table 4. Summary of Results of X-ray Identification of Ranong Clay

Clay Fraction	Kaolinite		$2M_1$ Muscovite		Alpha Quartz		Potash Feldspar		Tourmaline		Metahallosite		Gibbsite		Hermatite		Amorphous Materials	
	R*	0**	R	0	R	0	R	0	R	0	R	0	R	0	R	0	R	0
Screen residue	x	x	x	x	x	x	x	x	x	x								
Bulk	x	x	x	x	x	x	x	x										
20–44 microns	x	x	x	x	x	x	x	x										
10–20 microns	x	x	x	x	x	x	x	x										
5–10 microns	x	x	x	x	x	x	x	x										
2–5 microns	x	x	x	x	x	x	x	x					x	x				
1–2 microns	x	x	x	x	x	x							x	x				
0.50–1 micron	x	x	x	x	x	x							x	x				
0.25–0.50 micron	x	x	x	x							x			x				
0.10–0.25 micron	x	x									x	x		x				
Less than 0.1 micron	x	x									x	x			x	x	x	x

* Random sample
** Oriented sample

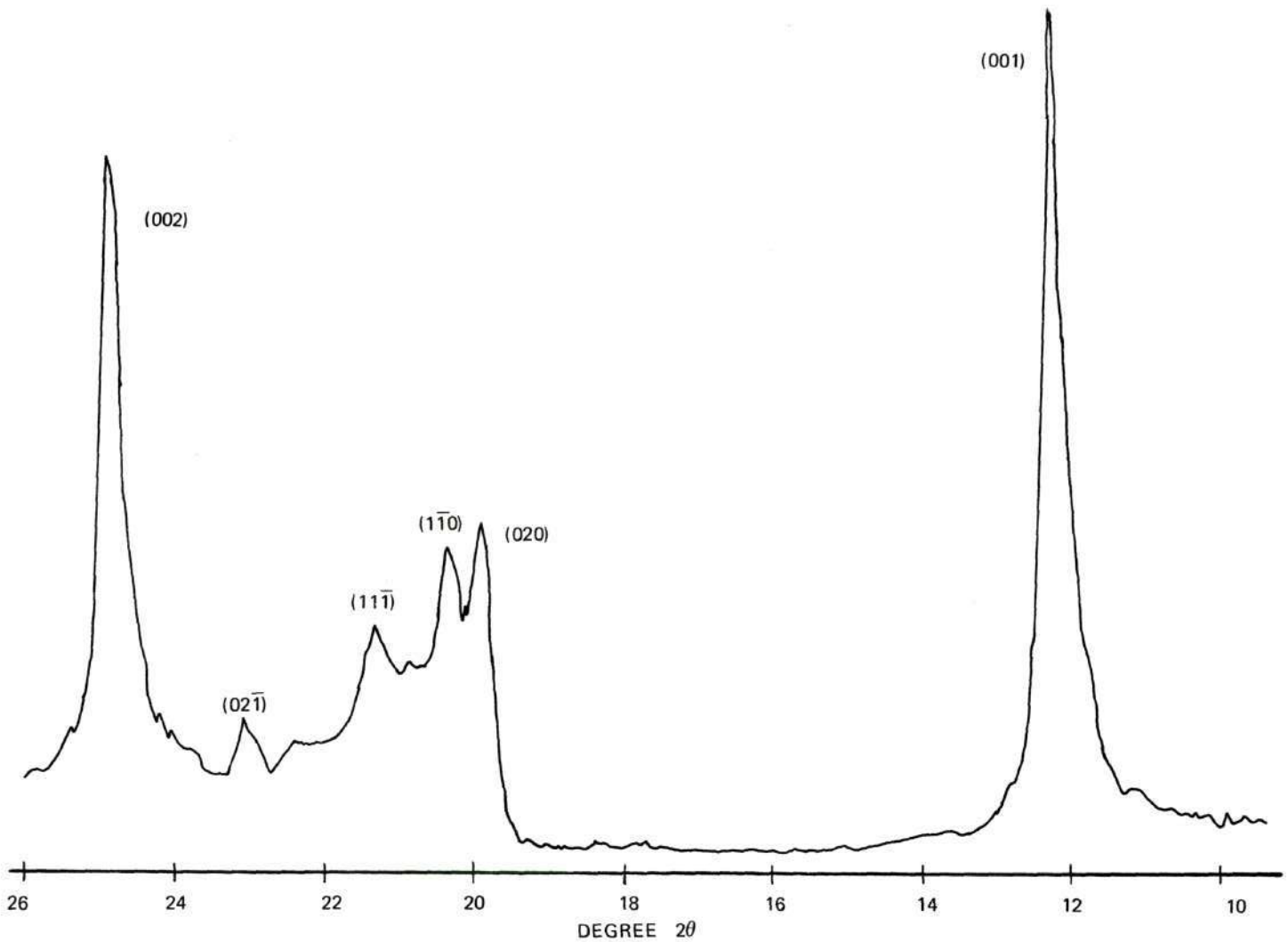

Figure 17. X-ray Diffraction Trace of Fairly Well-crystallized Kaolinite in Ranong Clay.

determined by using Johns and Murray's method are tabulated in Table 5. It may be observed that the kaolinite crystallinity index increased with decreasing particle size and was a maximum in the 1-2 micron fraction of clay. The crystallinity indexes of clay fractions below 1-2 microns were rendered undeterminable by the effect of the concentration of metahalloysite which markly modified the diffraction patterns. The effect of the interference of $2M_1$ muscovite on the (060) reflection may indicate that the kaolinite crystallinity indexes were lower than the expected values.

Apparently, Ranong clay belongs to the kaolin group. It is composed of kaolinite and metahalloysite with some impurities such as potash feldspar, $2M_1$ muscovite, alpha quartz, gibbsite, tourmaline, hematite, and amorphous materials. The kaolinite has a fairly well-crystallized character. The amount of metahalloysite in this clay increases with decreasing particle size. In the less than 0.1 micron fraction, Ranong clay is almost entirely composed of metahalloysite. Potash feldspar, alpha quartz, and $2M_1$ muscovite were not found in the 1-2, 0.25-0.5, and 0.1-0.25 micron fractions, respectively. Gibbsite was found in the range of fractions between 5-10 and 0.25-0.5 microns. Amorphous materials and hematite were found in the less than 0.1 micron fraction.

Scanning Electron Microscopic Analysis of Ranong Clay

Figures 18 through 20 show the scanning electron micrographs of the different size fractions of Ranong clay. Many large particles are easily seen in Figure 18, and they are referred to as stacks consisting of a variable number of plates. Stacks varied in thickness up to 30

Table 5. Data of Crystallinity Indexes for Kaolinite in Ranong Clay [7]

Clay Fraction	Crystillinity Index
Bulk	0.2234
20-44 microns	0.1415
10-20 microns	0.3214
5-10 microns	0.3264
2-5 microns	0.3426
1-2 microns	0.4940

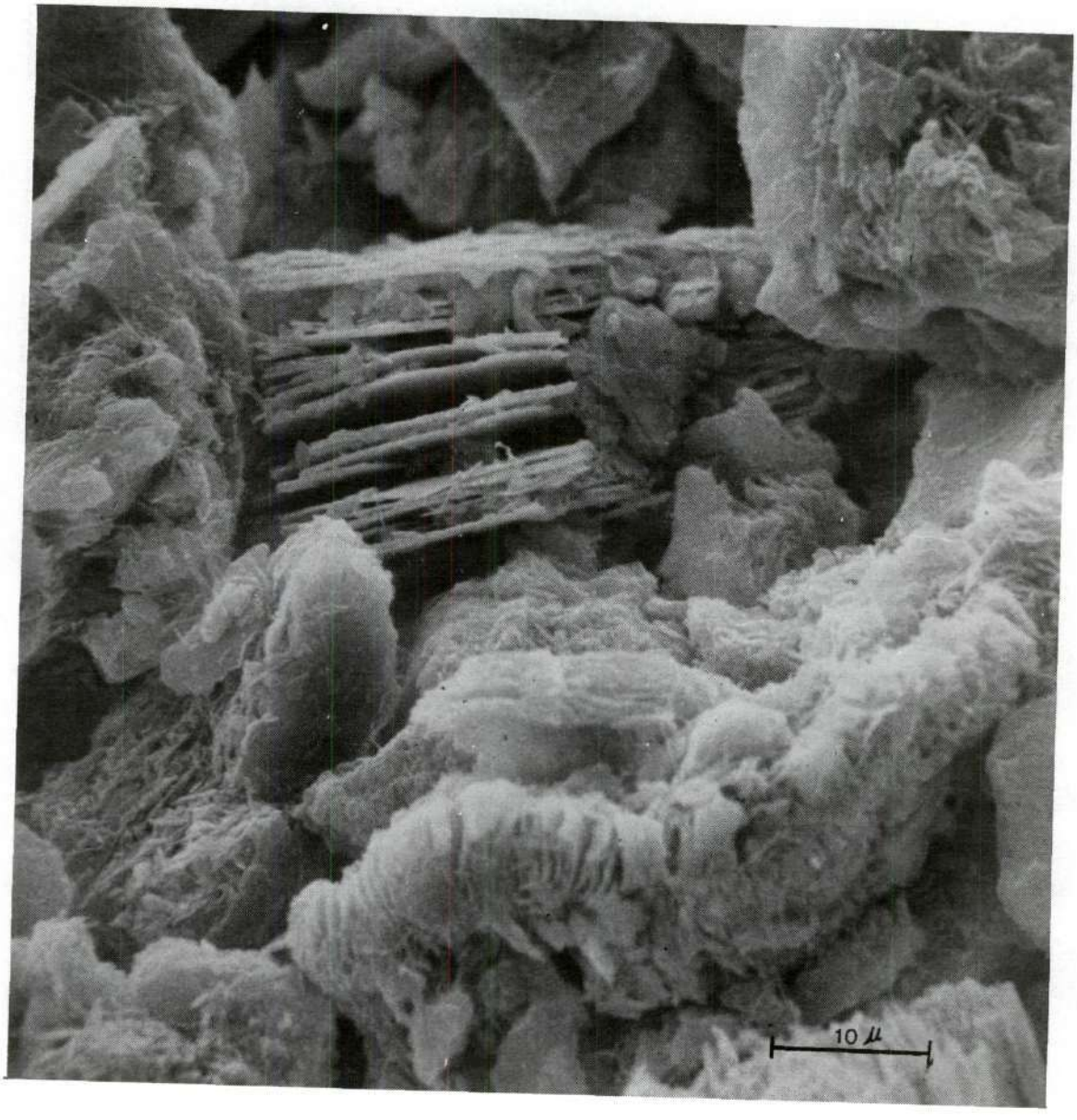

Figure 18. Scanning Electron Micrograph of Ranong Clay, Bulk.

microns. Some worms are also clearly seen. The stacks and worms are characteristic of kaolinite. The worm-shape particles are the so-called kaolinite worms. The development of kaolinite worms might be attributed to a great number of plates in which some of them were displaced laterally rather than all being stacked one above the other. The hexagonal outlines of kaolinite are partially seen. The worm shape and the hexagonal outlines of plates suggest the well-crystallized type of kaolinite, and this was further confirmed by the X-ray diffraction analysis.

Some of the rolled form or lath-like shape of particles seen in Figure 18 indicate the characteristic of metahalloysite. When the particle size of Ranong clay decreases to 2 microns, the kaolinite particles change their shapes from stacks to flat plates or flakes. Figure 19 shows the scanning electron micrograph of 1-2 micron fraction of Ranong clay. It can be seen that the shapes of kaolinite particles are flat and elongated flakes. Most of the particles are a single flake. The lateral dimensions of flake surfaces range from 0.8 to 4.3 microns and the thickness from 0.03 to 0.7 micron. The outline of kaolinite particles is not a well defined hexagon because of the mechanical damages done during clay processing. In this fraction, the rolled shape of metahalloysite could also be seen. Figure 20 shows the micrograph of Ranong clay for the less than 0.1 micron fraction. Evidently, this fraction contains metahalloysite. The shapes of particles in this micrograph are of rolled and curled forms. The outside diameters of these particles range from 0.05 to 0.13 micron. Particles vary in length up to 0.7 micron. There are few flakes of kaolinite which are difficult to observe.

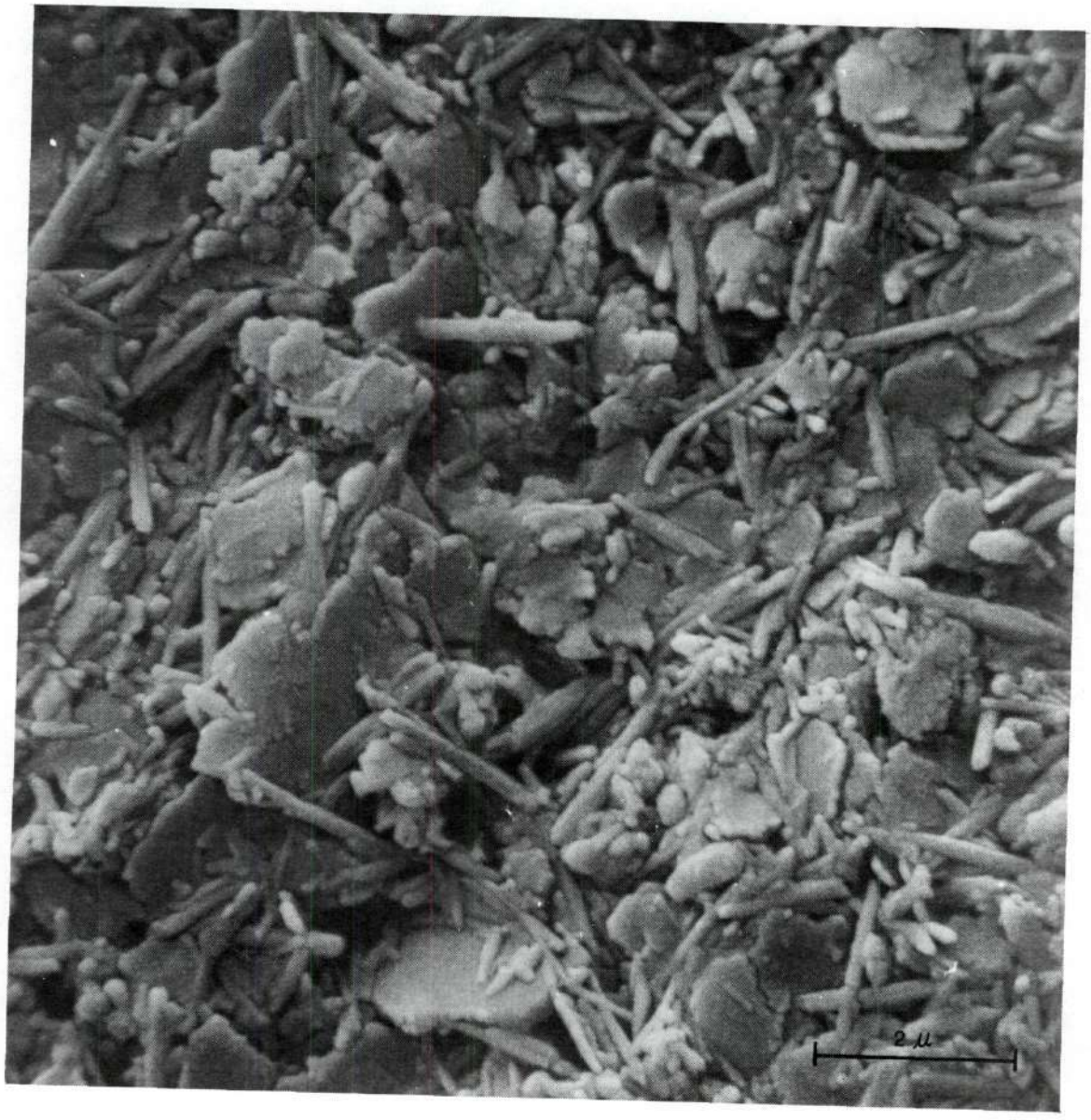

Figure 19. Scanning Electron Micrograph of Ranong Clay, 1-2 microns.

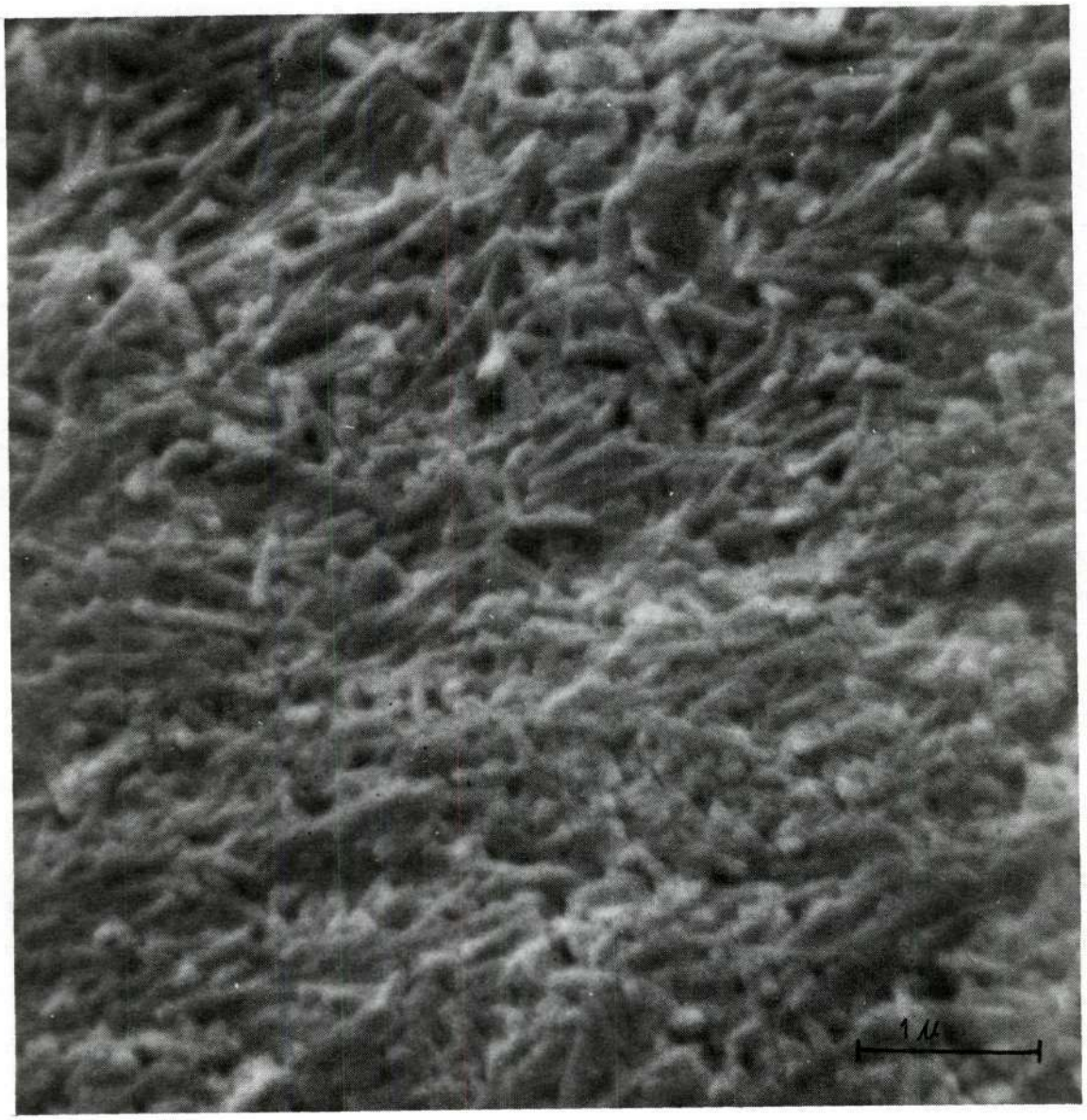

Figure 20. Scanning Electron Micrograph of Ranong Clay, Less than 0.1 micron.

Attempts were made to investigate all fractions of Ranong clay. Figures 32 through 41 in Appendix B show a series of scanning electron micrographs of Ranong clay. The low magnification scanning micrograph in Figure 32 shows the overall appearance of the bulk sample of Ranong clay. There are many stacks and kaolinite worms. The large particles could be kaolinite or muscovite, and some of the irregularly shaped particles might be attributed to quartz. Worm particles may be observed at higher magnifications to study the details of stacking of an individual plate, as shown in Figure 33. In the stacking of kaolinite worms, the irregularities in the form of gaps of maximum width 1.8 microns are observed. The maximum lateral dimensions and the thickness of kaolinite plates were 6.6 and 0.25 microns, respectively. Aggregates of metahalloysite were clearly seen in this electron micrograph. Figure 34 shows stacks of kaolinite in the 20-44 micron fraction of Ranong clay. The stacks were random in direction and positively show some fracture and shearing of the stacks.

Figure 35 displays the previous largest stacks of kaolinite, but at a higher magnification. A portion of the hexagonal outline of kaolinite is clearly seen. There are metahalloysite minerals deposited on most of the kaolinite stacks. Figure 36 displays the general features of 10-20 micron fractions of Ranong clay. Kaolinite stacks and worms, and metahalloysite aggregates were observed. The morphology of the clay is shown in more detail in Figure 37, which reveals the kaolinite stacks and probably also the metahalloysite aggregates. The shape of the metahalloysite might be likened to coconut candy bars. Referring to Figure 38, the scanning electron micrograph of 10-20 micron fractions reveals

the large kaolinite stacks. Mechanical damage may have occurred on the kaolinite particles as the edge appear to be fractured and highly irregular. The appearance of rolled or lath-like particles confirms the characteristic metahalloysite ($Al_2O_3 \cdot 2\ SiO_2 \cdot 2\ H_2O$) which is different from halloysite ($Al_2O_3 \cdot 2\ SiO_2 \cdot 4\ H_2O$). The amount of metahalloysite increased with decreasing particle size, and this was evident in Figures 39 through 41. Figure 41 reveals more information concerning metahalloysite. Metahalloysite varied in length and width up to 1.85 and 0.18 microns, respectively. There were also a large number of particles which were similar to a tube in shape. However, the shapes of these particles looked more similar to imperfected rolled form than to well-formed tubes.

From the scanning electron microscopic data, obviously, Ranong clay consists of a mixture of platy particles of kaolinite and of the imperfectly rolled form of metahalloysite particles. The intimate association of platy and rolled particles in Ranong clay might be the results of the weathering process acting on the platy kaolinite crystals and causing them to curl and roll into poorly formed metahalloysite particles.

Differential Thermal Analysis and Thermogravimetric Analysis of Ranong Clay

The thermal data of Ranong clay are reported in Tables 30 and 31 in Appendix C. Figures 21 through 23 show the differential thermal curves of the data from Table 30.

In the bulk sample, both the DTA and the TGA curves were reasonably symmetrical in the range of the loss of structural (hydroxyl) water at

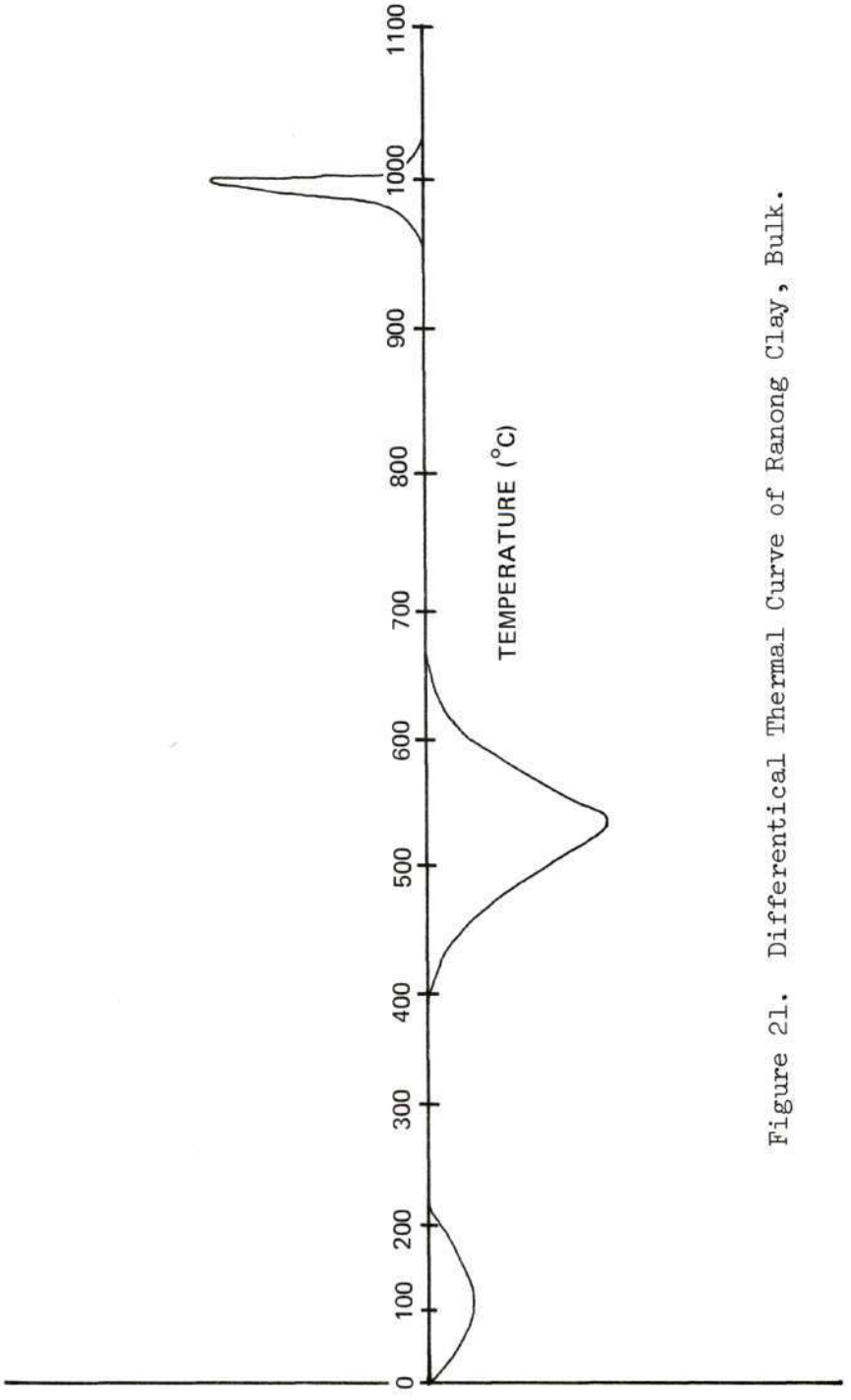

Figure 21. Differentical Thermal Curve of Ranong Clay, Bulk.

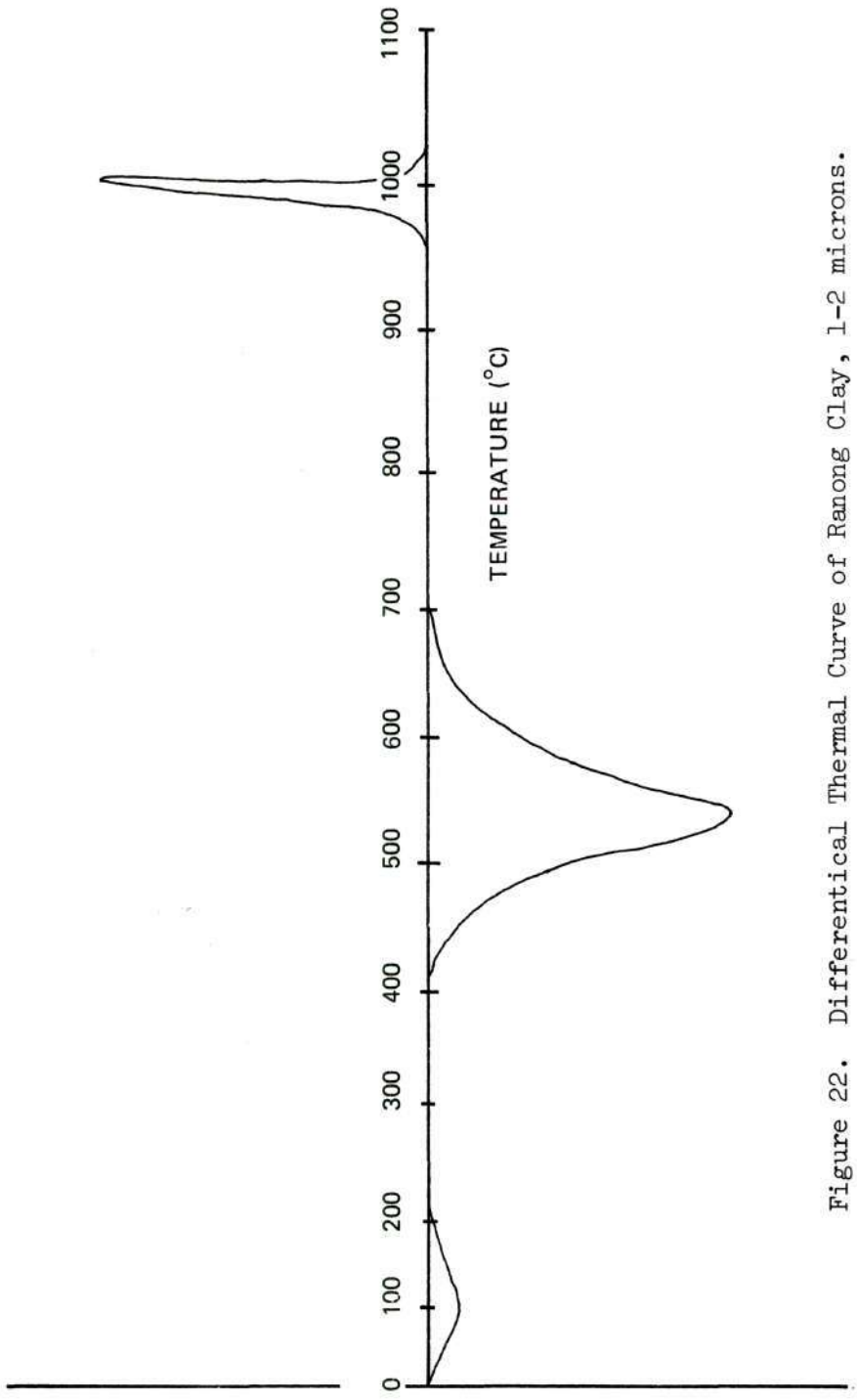

Figure 22. Differentical Thermal Curve of Ranong Clay, 1-2 microns.

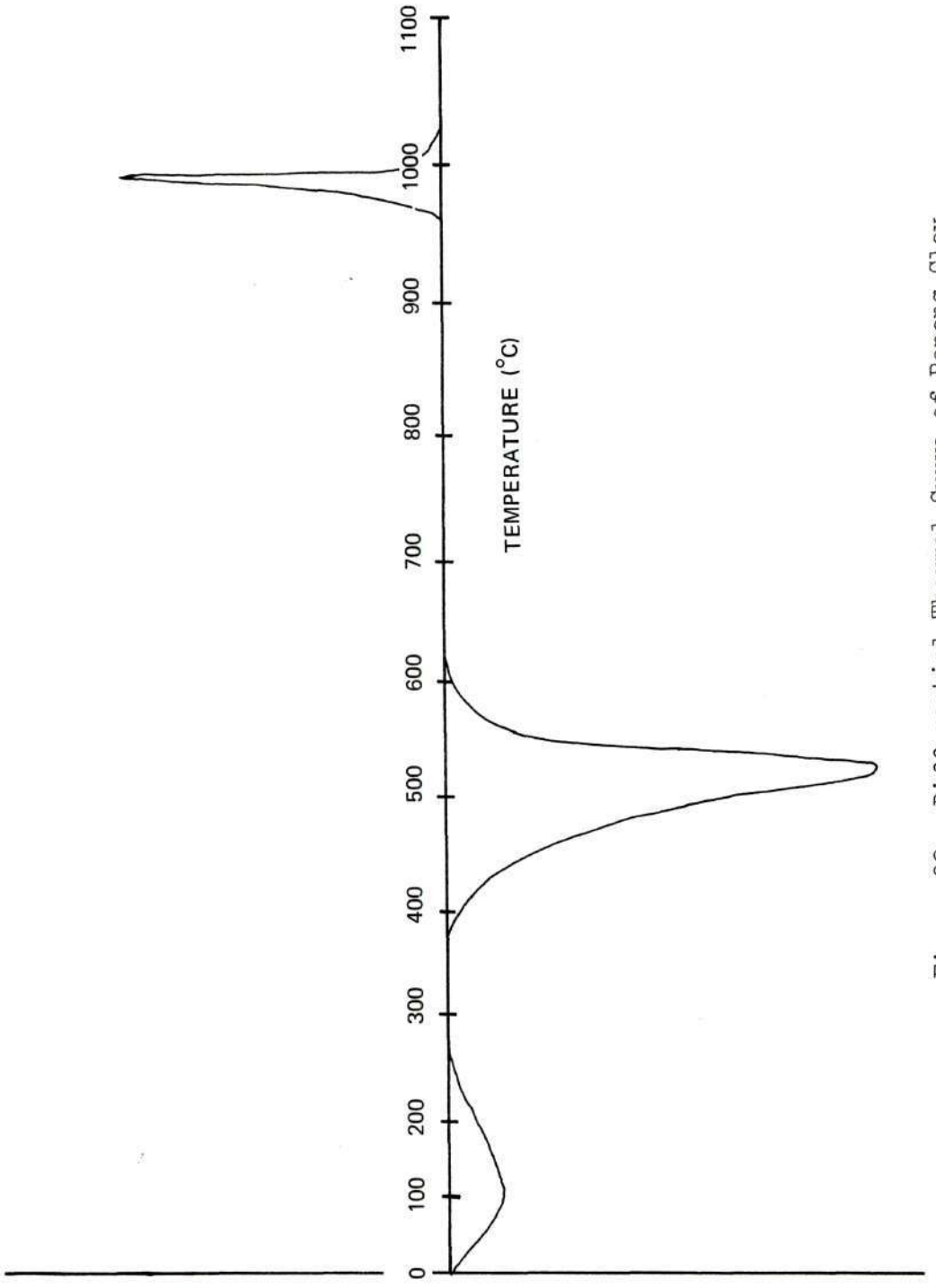

Figure 23. Differential Thermal Curve of Ranong Clay, Less than 0.1 micron.

540°C. The small amount of water, approximately 1 percent, liberated at a temperature below 300°C, was absorbed water. An inflection point occurred at 400°C on the TGA curve. The loss of water became rapid at about 450°C, as was evident on both thermal curves (Figures 21 and 24). The inflection point was the beginning of the crystalline water loss and a large amount of heat was required during the endothermic reaction. The reaction continued until the temperature reached about 800°C, (Figure 24), with a total water loss of 13.70 percent. Crystallization of the spinel phase was indicated by the exothermic reaction in the temperature range of 950 to 1020°C.

The thermograms for this clay ranging from the bulk to 2-5 micron fractions gave the same identification results. The thermal curves for the 1-2 micron fractions are shown in Figures 22 and 25. The total amount of water loss was 14.06 percent. Similar thermal curves were obtained for the 0.5-1 micron fraction. When the particle size of this clay decreased to less than 0.5 micron, the thermograms were more similar to halloysite rather than kaolinite since the peaks of structural water loss in the region of 400-665°C became asymmetrical, and this was particularly obvious in the clay fraction of less than 0.1 micron (Figure 23). In this fraction, both types of thermal curves (Figures 23 and 26) resembled the characteristic curves of metahalloysite. The amount of water loss at 320°C was 5.8 percent. The thermogravimetric curve indicated that the hydroxyl water began at 400°C. Both curves implied that the loss of hydroxyl water was not rapid until about 440°C. The total amount of water loss of this fraction was 18.462 percent. Again, the exothermic reactions in the range of 950 to 1010°C represented

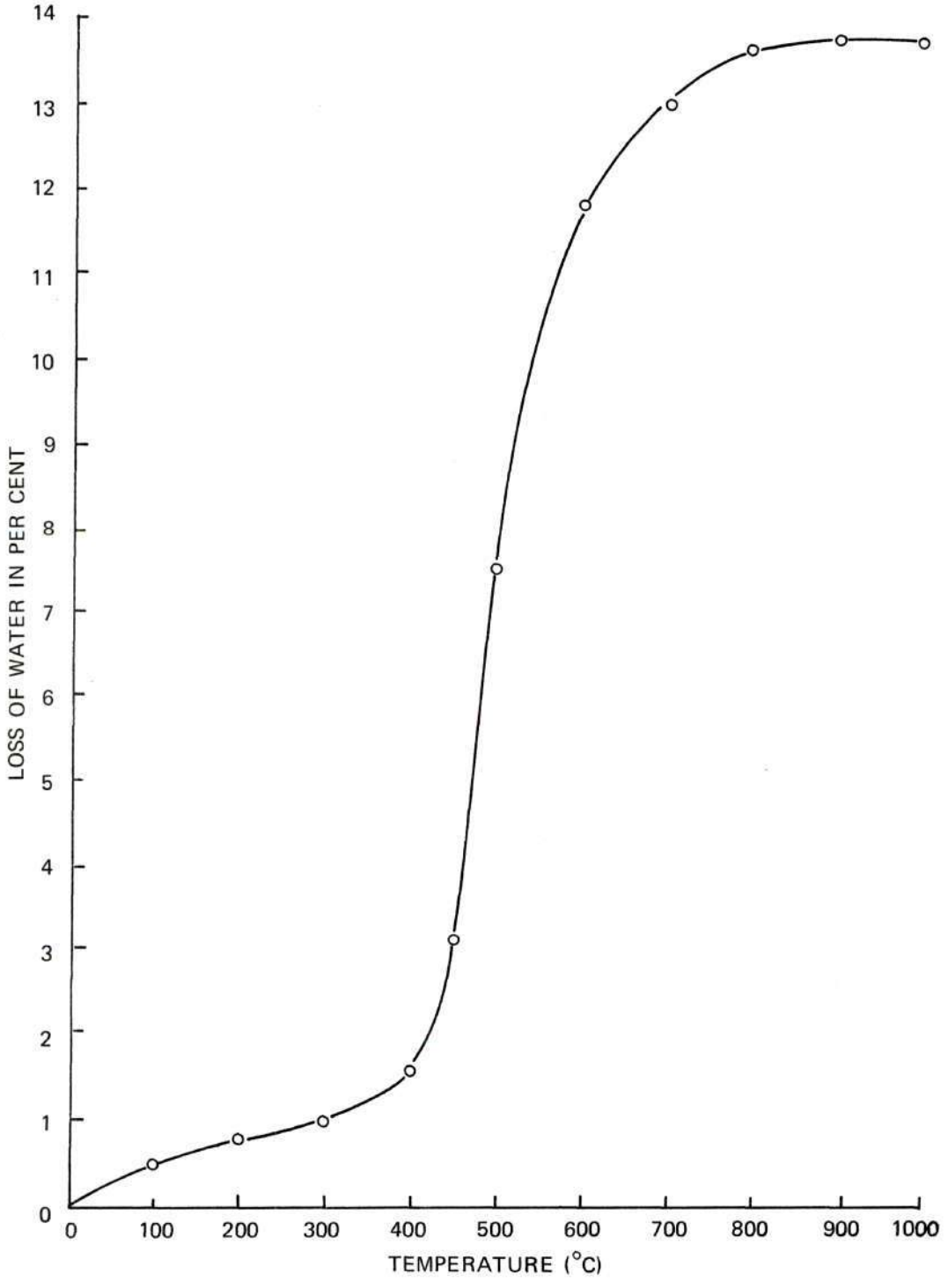

Figure 24. Dehydration Curve of Ranong Clay, Bulk.

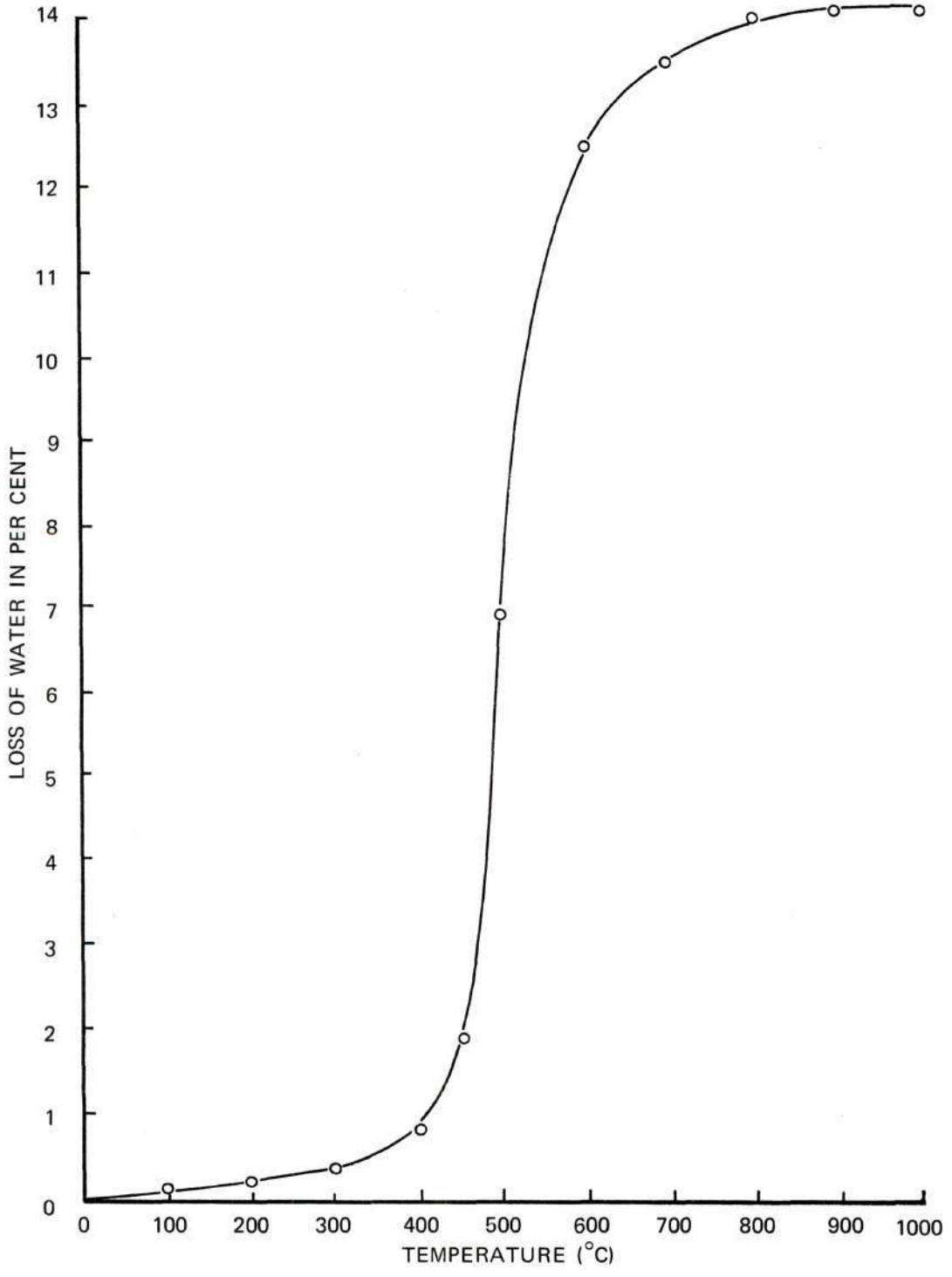

Figure 25. Dehydration Curve of Ranong Clay, 1-2 microns.

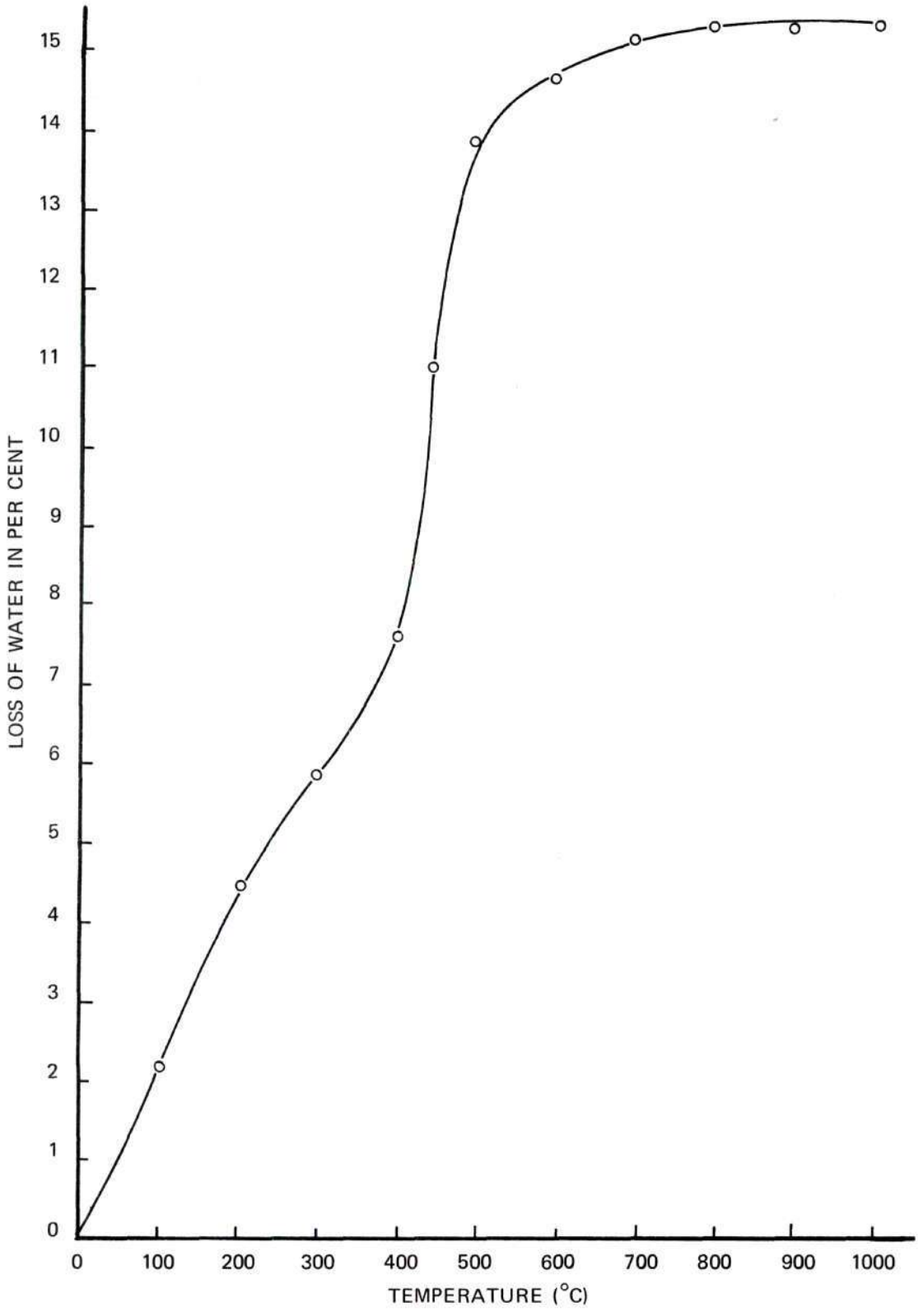

Figure 26. Dehydration Curve of Ranong Clay, Less than 0.1 micron.

the crystallization of the spinel phase.

In the clay fractions ranging from bulk to 1-2 microns, both DTA and TGA analyses reveal that the clay mineral was kaolinite. There was no clear identification for the fractions from 0.5-1 to 0.25-0.5 microns. However, the curves for the fine fraction of clay suggested the characteristic of halloysite, and that it should be meta-halloysite type as confirmed by X-ray diffraction and scanning electron microscopic analyses.

Infrared Spectroscopic Analysis of Ranong Clay

The adsorption spectra of different size fractions of Ranong clay are illustrated in Figures 27 through 29. Table 32 in Appendix C is the data of the observed adsorption bands corresponding to the aforementioned figures. The infrared spectra of Ranong clay in Figures 27 and 28 indicate the kaolinite mineral. They show adsorption bands at 2.7 microns region (3700 cm^{-1}), 6.0210 microns (1660.85 cm^{-1}), 8.9750 microns (1114.20 cm^{-1}), 9.6225 microns (1039.92 cm^{-1}), 10.6333 microns (940 cm^{-1}), 10.9500 microns (913.24 cm^{-1}), 12.5250 microns (798.40 cm^{-1}), 13.2125 microns (798.40 cm^{-1}), 13.2125 microns (756.85 cm^{-1}), 14.4250 microns (693.24 cm^{-1}), and 14.9875 microns (667.22 cm^{-1}). Absence of an adsorption band at 14.9875 microns for the 1-2 micron fractions of Ranong clay was also noted. The strong anti-symmetric adsorption band in the 2.70 micron region was attributed to the presence of free O-H bond or unbond OH. A low intensity adsorption band at 6.0210 microns was due to the deformation vibration of molecular water. The two intense bands at 8.9750 microns and 9.6225 microns resulted from lattice vibrations (Si-O stretching). All the remaining

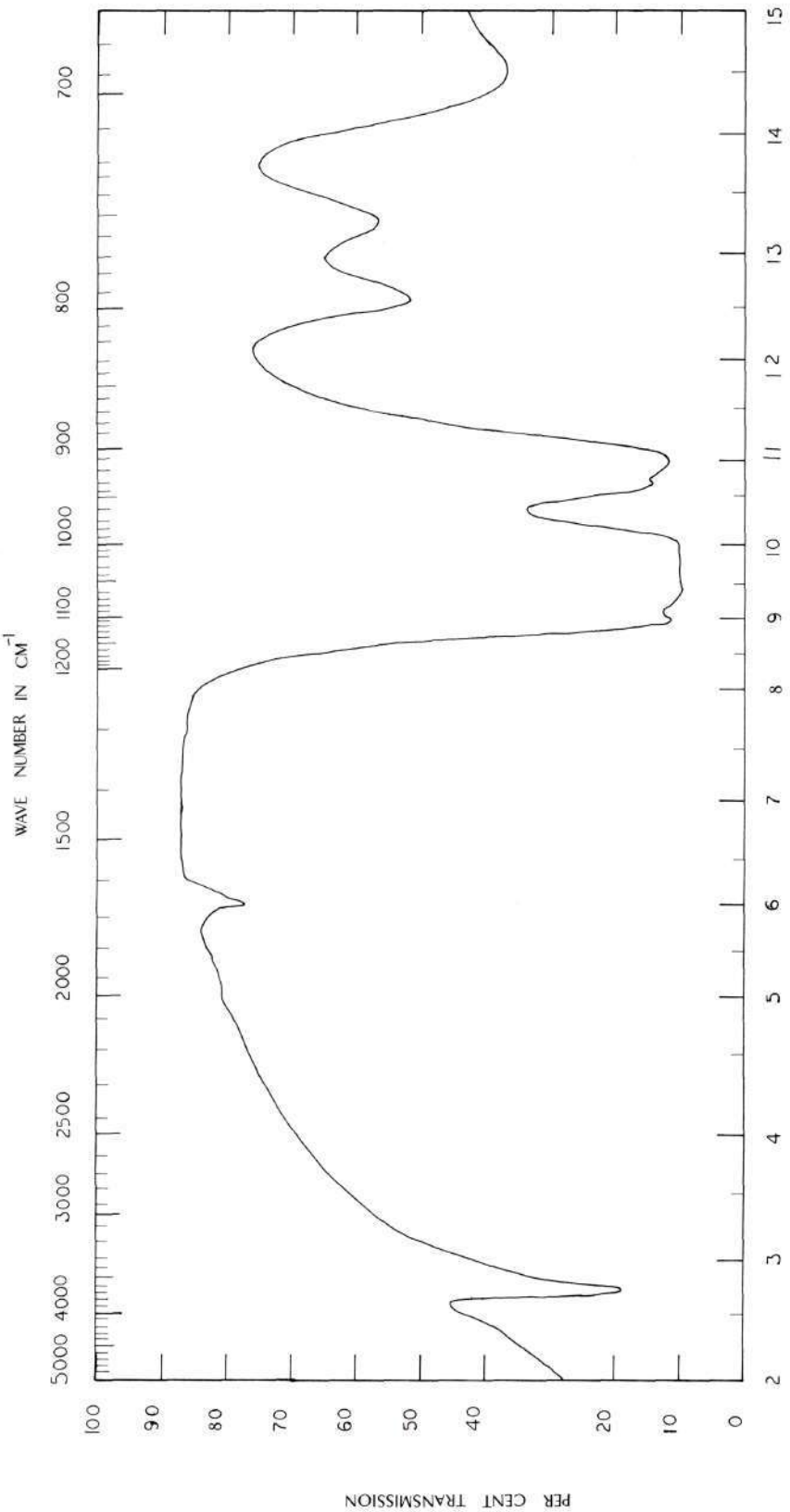

Figure 27. Infrared Spectrum of Ranong Clay, Bulk.

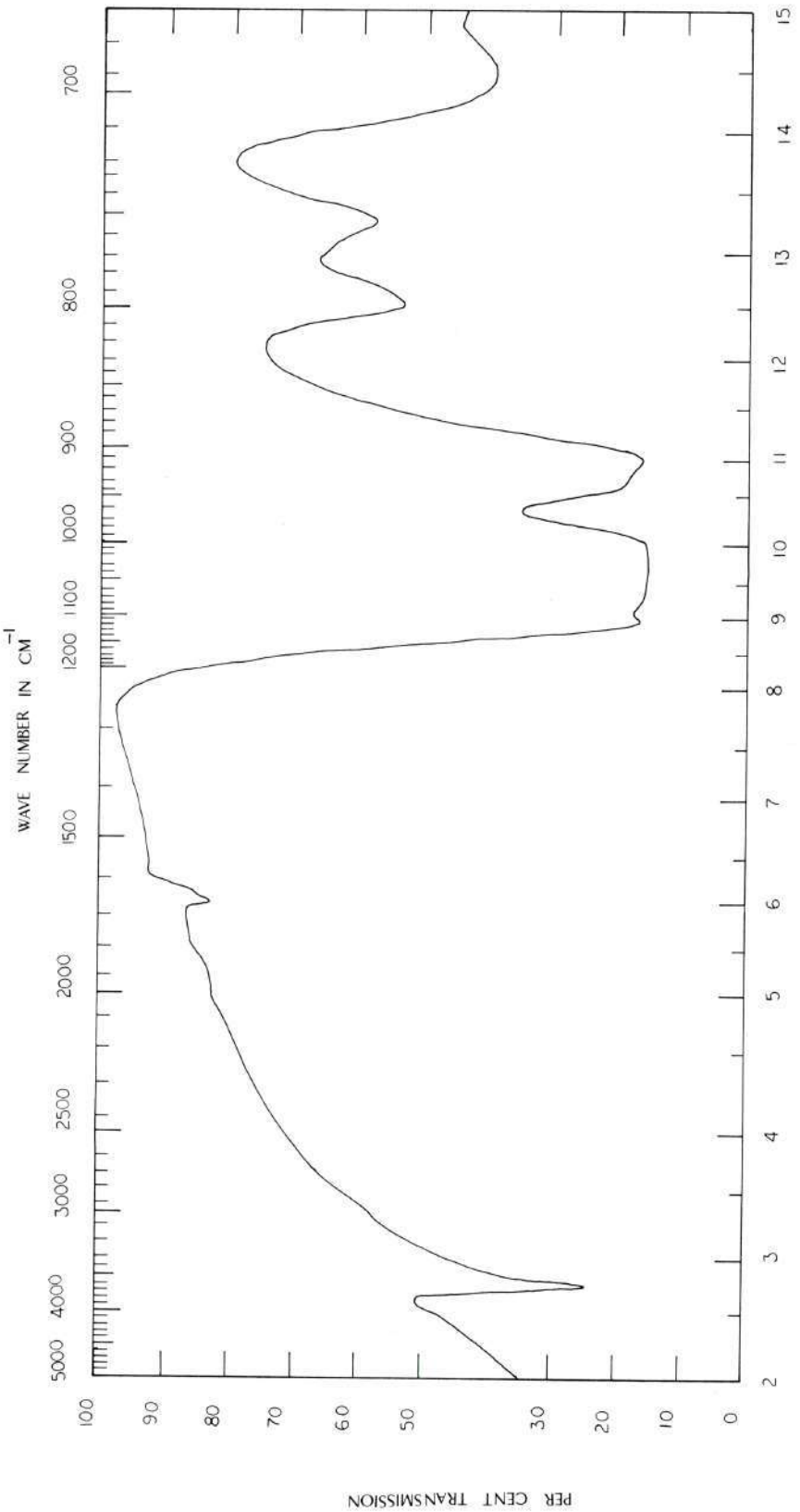

Figure 28. Infrared Spectrum of Ranong Clay, 1-2 microns.

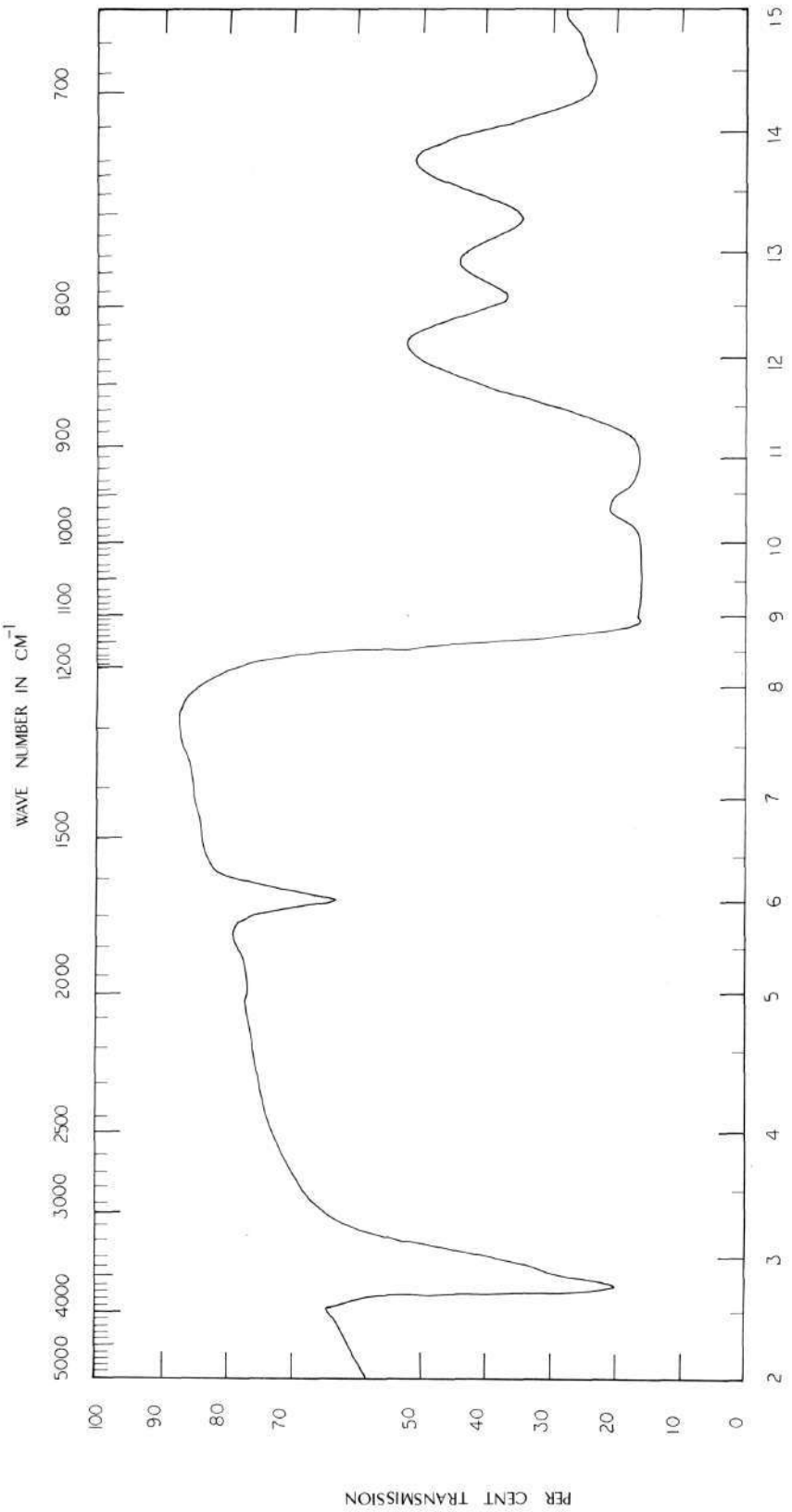

Figure 29. Infrared Spectrum of Ranong Clay, Less than 0.1 micron.

bands were caused by Al-O-H bending vibrations.

Figure 29 shows the infrared spectrum of Ranong clay in the fraction of less than 0.1 micron. The spectrum pattern was similar to the 1-2 micron fraction pattern. The absence of a 10.6333 micron adsorption band was noted. The characteristic of metahalloysite was suspected since this band generally does not show up in the metahalloysite spectrum according to Kerr and colleagues[37]. By comparing the infrared spectrum of the less than 0.1 micron fraction with the infrared spectra of metahalloysite, the spectrum of Ranong clay in this fraction was similar to metahalloysite rather than kaolinite.

Ranong clay was identified as kaolinite for its bulk and 1-2 micron fractions, and as metahalloysite in the fraction of less than 0.1 micron.

Chemical Analysis of Ranong Clay

The chemical analysis of Ranong clay, by an atomic adsorption spectrophotometer, is reported in Table 6. It would be seen that Ranong clay is relatively pure aluminum silicates with less than 0.5 percent of alkalies, and less than 0.4 percent of iron oxide. The high silica content of Ranong bulk sample was caused by free quartz and other impurities containing silica and alumina. The presence of K_2O indicated either muscovite, illitte, or feldspar or a small amount of each. However, from the X-ray diffraction analysis only muscovite and feldspare were found. No titanium was detected in any of the fractions of this clay.

X-ray Fluorescent Analysis of Ranong Clay

The metal impurities in Ranong clay are reported in Table 35 in

Table 6. Chemical Analysis of Ranong Clay

	Bulk	1-2 microns	Less than 0.1 micron
SiO_2	54.00	46.85	46.51
Al_2O_3	33.05	37.66	38.06
Fe_2O_3	0.28	0.28	0.29
MgO	0.01	trace	trace
CaO	0.02	0.01	0.01
K_2O	0.34	0.33	0.34
Na_2O	0.07	0.06	0.06
Ignition Loss	12.28	14.72	14.74
Total	100.05	99.91	100.01

Appendix D. These metals were Fe, K, Ca, Sn, Cr, Ba, Pb, Zn, and Ni. The presence of tin indicates the association of cassiterite with the Ranong clay deposits.

Petrographic Microscopic Analysis of Ranong Clay

The index of refraction of Ranong clay is reported as a value of 1.566. The impurities, from the screen residue on a 325 mesh screen, were identified as quartz, muscovite, hydromuscovite, tourmaline, potash feldspar, organic matter, and some unidentifiable materials. The grain size character of Ranong clay consists of a mixture of moderately coarse and fine grains. This clay contains worms, platy particles, and the aggregate materials. In the bulk sample of Ranong clay, the impurities are approximately 14 percent.

Mineral Composition of Ranong Clay

Ranong clay is composed of a mixture of kaolinite and metahalloysite. Alpha quartz and $2M_1$ muscovite are notably present in the clay. Petrographic microscope and X-ray revealed a small amount of other impurities.

The mineral composition of the bulk and the 80 percent particle size finer than 2 micron fractions are reported in Table 7. As can be seen, Ranong bulk clay consists mostly of kaolinite (79.2 percent) and 7.8 percent metahalloysite. The non-clay impurities are approximately 13 percent. In the 80 percent particle size finer than 2 micron fractions, Ranong clay is almost entirely composed of kaolinite and metahalloysite. The non-clay impurities are only 2.5 percent.

Table 7. Mineral Composition of Ranong Clay

	Bulk (%)	80% Particle Size Finer than 2 Microns Fraction (%)
Kaolinite	79.2	66.5
Metahalloysite	7.8	31.0
2 M_1 muscovite	5.5	1.5
Alpha quartz	7.5	1.0
Total	100.0	100.0

Properties of Ranong Clay, Thailand

Table 8 shows the physical properties of Ranong clay. The physical constants suggests that Ranong clay may be considered as a high quality clay. It has a small amount of grit, as small as only 0.41 percent. The brightness and whiteness were found to be 81 percent and 12, respectively, and these are relatively high values. The Stromer viscosity of this crude clay was reported as 56 seconds per 100 revolutions at 60.8 percent solids. The particle size of Ranong clay is moderately coarse with only 14 percent less than 2 microns. Figure 30 and Table 33 (in Appendix D) show the particle size distribution of Ranong clay. It may be seen that 50 percent of this clay is in the range of 5 to 20 microns. Table 36 in Appendix D shows the relation of particle size with brightness and whiteness. It may be seen that the brightness of this clay increases with decreasing particle size, but it is not true when the particle size decreases to 0.25-0.5 microns; this may be due to the increase in concentration of the dark color impurities such as iron materials. The brightness is remarkably reduced in the fraction of less than 0.25 micron. The main cause of reduction in brightness of this clay fraction is probably iron oxide which was detected by X-ray diffraction analysis.

Properties of Ranong Refined Clay, Thailand

The properties of Ranong refined clay are reported in Table 9. The brightness and whiteness values were found to be 77 percent and 12, respectively. These values are lower than those of the crude clay.

Attempts were made to improve the brightness and whiteness by a

Table 8. Properties of Ranong Bulk Clay

Properties	Values
Brightness	81
Whiteness	12
Particle Size Distribution, % less than 2 microns	14
Stormer Viscosity (Sec. per 100 revolution)	
150 gm. driving weight, 60.8% solid	56
Moisture (%)	0.82
Screen Residue on 325 mesh screen (%)	0.41
pH	4.61
Specific Gravity	2.52
Index of Refraction	1.566

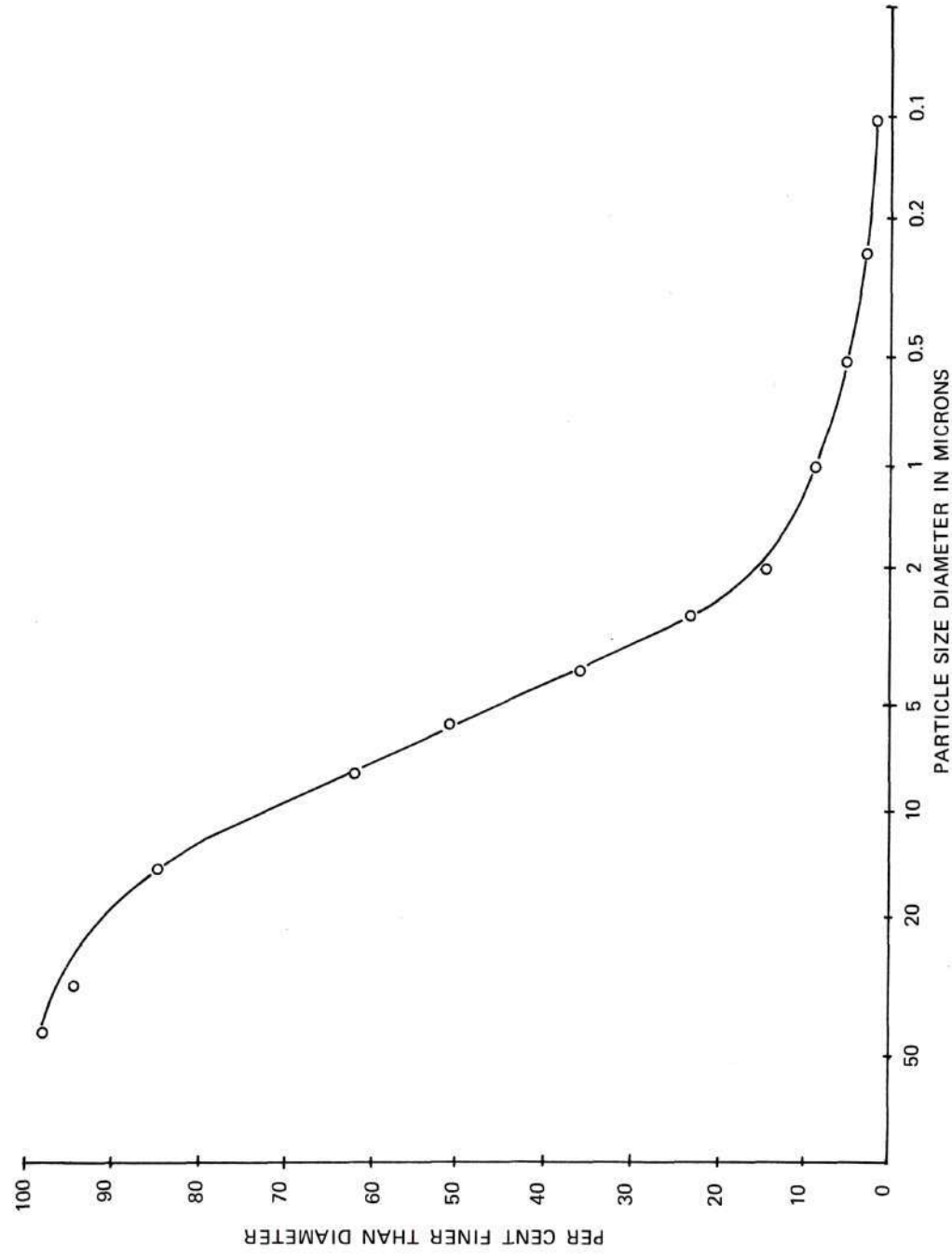

Figure 30. Particle Size Distribution of Ranong Clay.

Table 9. Summary of Properties of Ranong Refined Clay

Properties	Values
Brightness (%)	
Unbleaching	77.0
Hydrogen peroxide bleaching	77.5
Sodium hydrosulphite bleaching	83.0
Whiteness	
Unbleaching	13.2
Hydrogen peroxide bleaching	16.5
Sodium hydrosulphite bleaching	10.3
Particle size (%)	
Under 2 microns	80.0
2-5 microns	20.0
Viscosity, 60.8% solid	
Stormer (sec per 100 revolutions), 150 gm wt	17.0
Brookfield (cps), 60 rpm, spindle #3	670.0
*Hercules (dyne-cm x 10^{-5}) at 1100 rpm	6.3
Moisture (%)	1.3
Screen residue on 325 mesh screen (%)	0.1
pH	6.6
Specific gravity	2.56
Index of refraction	1.566

* Value was obtained from the Thiele Kaolin Company, Georgia.

chemical bleaching. It was found that sodium hydrosulphite gives a more effective bleaching than hydrogen peroxide, as indicated in Table 9. When bleached with sodium hydrosulphite, the brightness increases by 5.5 percent above the unbleached value, compared with the increase of 0.5 percent when bleached with hydrogen peroxide. The whiteness of sodium hydrosulphite bleached clay increases as indicated by the reduction of the whiteness values from 13.2 of unbleached clay to 10.3. On the other hand, the whiteness of hydrogen peroxide bleached clay decreases as indicated by the increase in the whiteness values from 13.2 to 16.5. Obviously, sodium hydrosulphite bleaching improves both whiteness and brightness of Ranong clay more than hydrogen peroxide bleaching.

The particle size of this clay was approximately 80 percent finer than 2 microns and 20 percent in the range of 2 to 5 microns. The particle size distribution of Ranong refined clay is shown in Figure 31 and Table 34 (in Appendix D).

The rheological property of the Ranong refined clay was found to be thioxtropic at 60.8 percent solid. Its viscosity decreases with an increase in the rate of shear or the spindle speed, as shown in Table 37 in Appendix D. The minimum viscosities of this clay as determined by various viscosimeters were reported as 17 seconds per 100 revolutions for Stromer viscosity, 670 centipoises for Brookfield viscosity, and 6.3 dyne-cm x 10^5 for Hercules viscosity, as shown in Table 9. These viscosity values are relatively high when compared to the accepted commercial coater clays. As Ranong clay is kaolin, having a well-crystallized kaolinite and no motmorillonite, its viscosity should have a low value according to Murray and Lyons[38]. However,

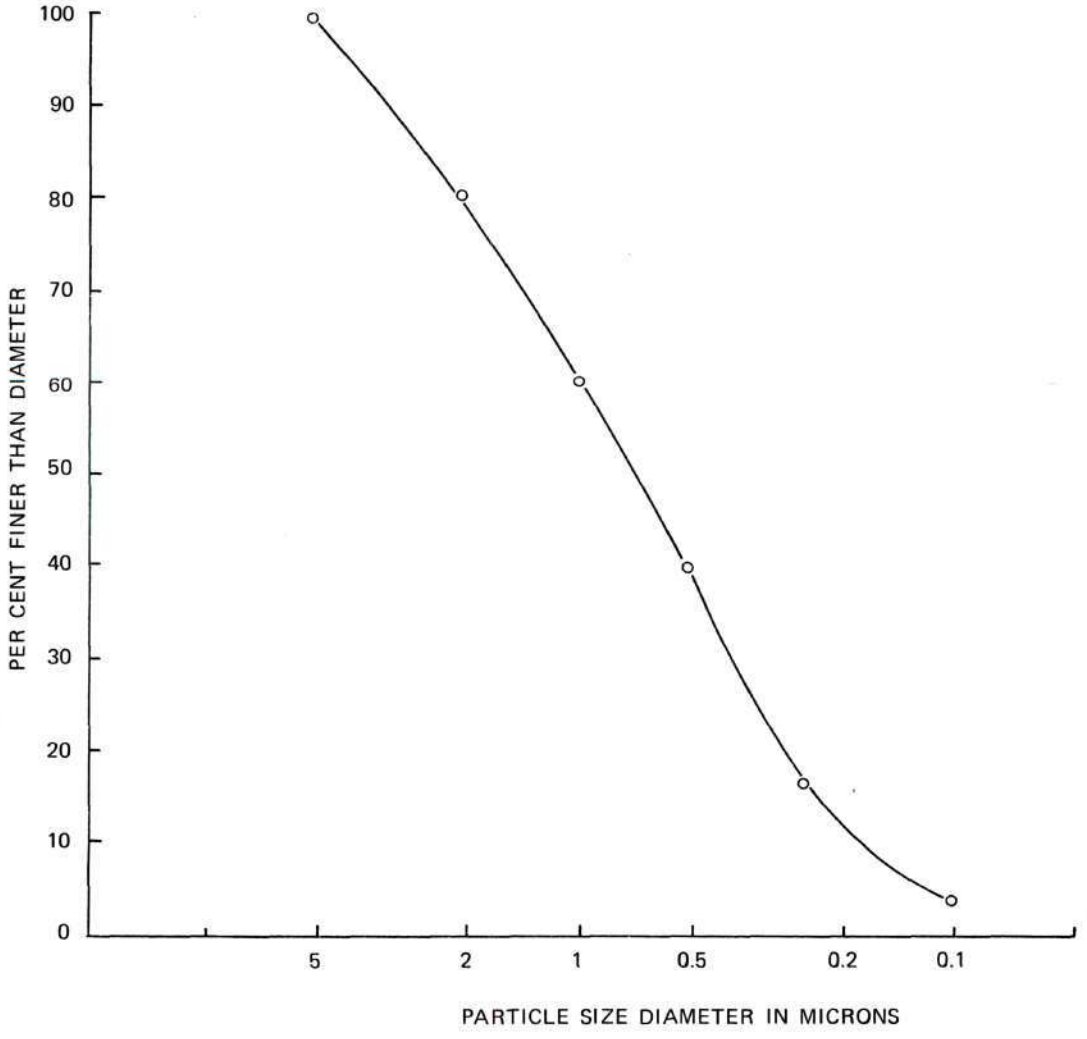

Figure 31. Particle Size Distribution of Ranong Refined Clay.

there are several factors affecting the viscosity, such as particle size and its distribution, particle shape, organic matters, and extraneous ions attaching to clay particles according to Mitchell and Poulos[39]. In this investigation, the author believes that the main causes of high viscosity of Ranong refined clay are attributed to the metahalloysite content in this clay. The anisotropic shape of the rolled metahalloysite is responsible for friction; therefore, the metahalloysite in Ranong clay will give it high viscosity.

The moisture content, pH, specific gravity and index of refraction were reported as 1.3 percent, 6.6, 2.56, and 1.566, respectively. The screen residue is relatively low and its maximum value was 0.1 percent.

Obviously, Ranong refined clay belongs to the kaolin group. It possesses good characteristics such as low grit content, good color, and controllable particle size, etc. Such characteristics may make Ranong refined clay suitable for use as a filler clay in the paper industry or ceramic clay. But it is unsuitable for use in the high speed coating equipment presently used in the paper industry, because of its high viscosity.

CHAPTER VI

CONCLUSIONS AND RECOMMENDATIONS

Conclusions

1. Ranong clay belongs to the kaolin group. It is composed of a mixture of kaolinite and metahalloysite with non-clay minerals of $2M_1$ muscovite and alpha quartz. The impurities of a small amount are potash feldspar, tourmaline, gibbsite, hydromuscovite, organic matter, hematite, and amorphous materials. The mineral composition of the clay is approximately 79.2 percent kaolinite, 7.8 percent metahalloysite, 7.5 percent quartz, and 5.5 percent muscovite.

2. Kaolinite in Ranong clay is a fairly well-crystallized type and its degree of crystallinity increases with decreasing particle size.

3. The range of the lateral surfaces of kaolinite plates is 0.8 to 6.6 microns and the thickness varies from 0.03 to 0.7 micron. For metahalloysite, the outside diameter of rolled form is between 0.05 and 0.18 micron. The length of this form varies from 0.7 to 1.85 microns.

4. Ranong refined clay consists of 66.5 percent kaolinite, 31 percent metahalloysite, 1.5 percent muscovite, and 1.0 percent quartz. It is a high quality clay with low grit content, a small amount of impurities, controlled particle size, and good color.

5. Ranong refined clay may be suitable for uses as a filler clay in the paper industry or as a ceramic clay in the ceramic industry.

6. Metahalloysite is responsible for the high viscosity of

Ranong refined clay and consequently makes it unsuitable for use in the high speed coating equipment currently used in the paper industry.

7. The brightness of Ranong clay increases with decreasing particle size.

8. Sodium hydrosulphite bleaching improves brightness and whiteness of Ranong refined clay more than hydrogen peroxide bleaching.

Recommendations

It is recommended that the relationship of the viscosity of the clay-water system to metahalloysite content in certain Ranong clays be studied. Also, the possibility for production of a coating clay by means of fracturing the kaolinite stacks should be determined.

APPENDICES

APPENDIX A

X-RAY DATA

Table 10. X-ray Diffraction Data for Oriented Sample of Ranong Clay, Bulk

"d" Spacing in Angstroms	Relative Intensities
9.9917	49
7.1395	100
4.9884	19
4.4502	36.5
4.3744	3.5
4.2704	37.5
4.1520	19.5
3.9864	11.5
3.8667	12.5
3.8338	11.5
3.7385	11.5
3.5758	75.5
3.3386	68
3.2433	13
3.2090	7.5
3.0598	5.5
3.0278	5.5
2.9882	5.5
2.8666	5.5
2.8225	4
2.5636	15
2.5355	9.5
2.5014	15
2.4610	7
2.3846	9.5
2.3382	14
2.2924	9
2.1669	3.5
2.1298	3.5
1.9976	19
1.7874	3.5
1.6670	5.5
1.6556	5.5
1.5441	3.5
1.4881	8

Table 11. X-ray Diffraction Data for Oriented Sample of Ranong Clay, 20-44 microns

"d" Spacing in Angstroms	Relative Intensities
9.9917	37.5
7.1395	100
4.9884	13.5
4.4502	20.5
4.3532	18
4.2704	27
4.1882	15
3.9515	9
3.8813	9
3.8334	10
3.7385	9
3.5695	65
3.3396	46.5
3.2428	24.5
3.0861	8.5
3.0178	4
2.9785	4.5
2.8488	4
2.6217	3
2.5671	8
2.5286	6
2.5014	10
2.4616	4
2.3846	7
2.3382	9
2.2924	5
2.1609	3
2.1298	3
1.9976	16.5
1.8207	3
1.7879	3
1.6667	5
1.6182	2.5
1.4881	6

Table 12. X-ray Diffraction Data for Oriented Sample of Ranong Clay, 10-20 microns

"d" Spacing in Angstroms	Relative Intensities
9.9917	40
7.1395	100
4.9884	15.5
4.4502	19
4.3532	17.5
4.2704	19
4.1882	13
3.9515	10.5
3.8813	9
3.8338	9.5
3.7540	9.5
3.5695	63
3.3264	46.5
3.2433	13.5
3.0480	5
2.8448	5
2.5671	7
2.5565	7
2.5286	5
2.4985	10
2.4487	4.5
2.3846	6
2.3330	6.5
2.2924	4.5
2.1298	2.5
1.9976	14.17
1.8309	1.89
1.7879	3.15
1.4900	4.72

Table 13. X-ray Diffraction Data for Oriented Sample of Ranong Clay, 5-10 microns

"d" Spacing in Angstroms	Relative Intensities
9.9917	22.5
7.1395	100
4.9884	13.5
4.8478	3.5
4.4502	19.5
4.3532	19
4.2702	19.5
4.1520	14
3.9694	9.5
3.9001	9.5
3.8590	10
3.7385	9
3.5695	63
3.3486	29.5
3.2634	8.5
3.0374	4.5
2.5565	7.5
2.5286	6
2.4980	8
2.4616	3
2.3848	6
2.3318	6.5
2.2924	3.5
2.1317	3
1.9935	9.5
1.7890	3
1.4881	4

Table 14. X-ray Diffraction Data for Oriented Sample of Ranong Clay, 2-5 microns

"d" Spacing in Angstroms	Relative Intensities
9.9917	15
7.1395	100
4.9828	6
4.8240	4
4.4504	15
4.3532	15
4.2704	12
4.1713	12.5
3.9864	9.5
3.9171	10
3.8667	10
3.7385	10
3.5695	61.5
3.3411	22.5
3.2503	8
3.2090	7.5
2.7540	3.5
2.5425	3.5
2.5218	3
2.4980	3.5
2.3846	5.5
2.3318	4
1.9935	5.5
1.7890	1.5
1.4903	2

Table 15. X-ray Diffraction Data for Oriented Sample of Ranong Clay, 1-2 Microns

"d" Spacing in Angstroms	Relative Intensities
9.9917	6
7.1395	100
4.9884	3
4.8230	3
4.4502	14
4.3532	12
4.2704	8.5
4.1810	15.5
4.1329	9.5
4.0220	6.5
3.7385	7.5
3.5695	64
3.2181	14.5
2.7631	2
2.5636	5
2.4985	5
2.3846	6
2.3330	5.5
2.2325	3
1.9852	2.5
1.7874	2
1.4860	2.5

Table 16. X-ray Diffraction Data for Oriented Sample of Ranong Clay, 0.5-1 Micron

"d" Spacing in Angstroms	Relative Intensities
9.9917	11
7.1437	100
4.9884	5
4.8240	6
4.4504	10
4.3551	10
4.2704	9.5
3.9515	10
3.8176	11
3.5635	64
3.3264	13.5
2.6450	13
2.3799	5.5
2.3384	2
1.9935	5
1.7874	2
1.4881	1.5

Table 17. X-ray Diffraction Data for Oriented Sample of Ranong Clay, 0.25-0.5 micron

"d" Spacing in Angstroms	Relative Intensities
9.9917	5
7.1668	100
5.0107	5
4.4504	2
4.4175	22
4.3427	19
3.5845	65
2.5636	9.5
2.5014	7
2.3921	4.5
2.3798	5
1.4889	4

Table 18. X-ray Diffraction Data for Oriented Sample of Ranong Clay, 0.1-0.25 micron

"d" Spacing in Angstroms	Relative Intensities
7.3750	90
7.1668	100
4.4175	43.5
4.3427	43
3.6479	61.5
3.4399	38
2.1175	7

Table 19. X-ray Diffraction Data for Oriented Sample of Ranong Clay, Less than 0.1 micron

"d" Spacing in Angstroms	Relative Intensities
7.3750	100
4.4175	79
3.6479	71
3.6043	75
2.7385	43.5
2.6944	44

Table 20. X-ray Diffraction Data for Random Powder Sample of Ranong Clay, Bulk

"d" Spacing in Angstroms	Relative Intensities
9.9917	42
7.1395	100
4.9884	12.5
4.4615	37
4.3744	27.5
4.2704	31.5
4.1907	22
3.9864	13
3.8502	12.5
3.7231	15
3.5758	76.5
3.4930	16.5
3.3386	51
3.2491	13.5
3.2033	7
2.9980	7
2.5636	23
2.5218	13.5
2.5014	16
2.4551	7
2.3846	11.5
2.3330	21
2.2981	12.5
2.2378	5.5
2.1910	3.5
2.1317	4
1.9976	13.5
1.8207	3.5
1.7874	3
1.6808	7
1.6667	9
1.6502	7.5
1.5441	4
1.4881	15

Table 21. X-ray Diffraction Data for Random Powder Sample of Ranong Clay, 20-44 microns

"d" Spacing in Angstroms	Relative Intensities
9.9917	32
7.1395	100
4.9884	10
4.4615	38
4.3744	34.5
4.2704	37
4.1907	24.5
3.9864	12.5
3.8833	15
3.8502	13.5
3.7385	12.5
3.7231	13.5
3.5758	77
3.3510	93
3.3022	15
3.2491	13
3.2033	8.5
3.0379	3.5
2.9039	3
2.8666	3
2.7968	6
2.7549	2.5
2.5636	25
2.5218	13.5
2.5014	20
2.4616	9
2.3846	11.5
2.3330	25
2.2981	15
2.2378	7
2.1961	3.5
2.1599	4.5
2.1317	6
1.9976	16.5
1.8207	4
1.8072	3
1.7874	3.5
1.6751	8.5
1.6667	12.5

Table 21. (continued)

"d" Spacing in Angstroms	Relative Intensities
1.6612	10
1.6502	9
1.6234	5.5
1.5441	7
1.5234	3.5
1.4903	16
1.4881	17

Table 22. X-ray Diffraction for Random Powder Sample of Ranong Clay, 10-20 microns

"d" Spacing in Angstroms	Relative Intensities
9.9917	32
7.1395	100
4.9884	9.5
4.4615	31
4.3744	26
4.3532	25.5
4.2704	32
4.1907	11.5
3.9864	12.5
3.8667	14
3.8502	10.5
3.7385	11
3.7231	11.5
3.5758	81.5
3.4930	12.5
3.4796	12.5
3.3510	62
3.2549	11.5
3.1977	6.5
2.9980	6.5
2.9629	2.5
2.8666	3.5
2.7968	3
2.7549	2
2.5636	19.5
2.5218	11.5
2.5014	18
2.4616	9.5
2.3846	11.5
2.3441	21
2.2924	11.5
2.2378	5.5
2.1609	3
2.1317	5.5
1.9976	13
1.8483	3
1.8207	6
1.8072	2.5
1.7874	3.5
1.6695	10.5
1.6612	10.5

Table 22. (continued)

"d" Spacing in Angstroms	Relative Intensities
1.6502	7.5
1.6234	5
1.5441	6
1.4881	13

Table 23. X-ray Diffraction Data for Random Powder Sample of Ranong Clay, 5-10 microns

"d" Spacing in Angstroms	Relative Intensities
9.9917	20
7.1395	100
4.9884	6
4.8478	2
4.4615	31.5
4.3540	26
4.2704	26
4.1907	20
3.9689	10.5
3.9001	11
3.8502	11.5
3.7385	10.5
3.5758	80.5
3.4930	12.5
3.3510	50.5
3.2903	7.5
3.2433	7
3.2090	6
2.9882	4.5
2.8666	2.5
2.8053	3
2.5636	17.5
2.5218	11.5
2.5014	15
2.4616	7
2.3846	11
2.3330	20
2.2981	12
2.2432	3
2.1961	3.5
2.1659	2.5
2.1317	4.5
2.0018	10
1.8207	5
1.7874	3
1.6695	9
1.6639	8.5
1.6502	6
1.6287	4
1.5441	5.5
1.4903	13

Table 24. X-ray Diffraction Data for Random Powder Sample of Ranong Clay, 2-5 microns

"d" Spacing in Angstroms	Relative Intensities
9.9917	12
7.1395	100
5.0107	3.5
4.8478	4.5
4.4615	33.5
4.3744	32.5
4.2704	26
4.1907	23.5
3.9689	12
3.9001	12
3.8502	12.5
3.7540	13
3.5758	11
3.4930	90.5
3.3510	43.5
3.2903	6.5
3.2541	6
3.2090	6
2.9980	5
2.8756	2
2.8053	3
2.5636	20
2.5218	12
2.5014	19.5
2.4616	8
2.3846	14
2.3330	23
2.2981	14
2.2432	4
2.1910	5
2.1609	3.5
2.1317	4
1.9976	9.5
1.8207	3.5
1.7874	4.5
1.6695	10
1.6612	10
1.6556	9
1.6234	5
1.5441	5.5
1.4903	9

Table 25. X-ray Diffraction Data for Random Powder Sample of Ranong Clay, 1-2 micron

"d" Spacing in Angstroms	Relative Intensities
9.9917	9
7.1395	100
4.9884	2.5
4.8478	2.5
4.4504	27
4.4175	22
4.3540	26
4.2704	19.5
4.1713	20
3.9515	9.5
3.8334	10.5
3.7385	10
3.5785	81
3.4530	8.5
3.3510	24.5
2.9882	2.5
2.8666	1.5
2.5565	15
2.5286	10
2.5218	16
2.4616	5
2.3846	12.5
2.3330	18.5
2.2981	12.5
2.2432	3
1.9935	6.5
1.8842	2
1.8207	2
1.7906	3
1.6695	8.5
1.6612	7.5
1.5418	3
1.4881	10

Table 26. X-ray Diffraction Data for Random Powder Sample of Ranong Clay, 0.5-1 micron

"d" Spacing in Angstroms	Relative Intensities
9.9917	10
7.2527	100
4.4615	85
4.3572	67
4.2502	43
3.9864	22
3.8502	20.5
3.6043	68
2.5707	24
2.5565	22.5
2.5286	23
2.3982	19.5
2.3500	26
2.2869	20.5
1.6806	10.5
1.6751	10.5
1.4860	20.5

Table 27. X-ray Diffraction Data for Random Powder Sample of Ranong Clay, 0.25-0.5 micron

"d" Spacing in Angstroms	Relative Intensities
9.9917	9
7.2545	100
4.4394	63.5
4.3532	46
4.1907	31
3.8338	18
3.5906	64.5
3.3510	12
2.5565	20.5
2.5355	17.5
2.4947	18
2.3921	17.5
2.3441	26
2.2981	15
1.9976	7.5
1.6667	10
1.4881	20.5

Table 28. X-ray Diffraction Data for Random Powder Sample of Ranong Clay, 0.1-0.25 micron

"d" Spacing in Angstroms	Relative Intensities
9.9917	15
7.2527	100
4.4175	81
4.3532	57
4.1907	39
3.5906	64
2.5636	23
2.4880	23
2.3441	19
2.3324	23
2.3037	23
1.6836	16
1.4881	20.5

Table 29. X-ray Diffraction Data for Random Powder Sample of Ranong Clay, Less than 0.1 micron

"d" Spacing in Angstroms	Relative Intensities
7.3750	81.5
7.2527	78
4.4175	100
3.6332	51
3.6043	53
3.3759	26
2.7385	31
2.6984	40.5
2.5636	17.5
2.4880	15.5
2.3799	29
2.0804	9.5
1.9217	10.5
1.6836	10.5
1.4839	14.5

APPENDIX B

SCANNING ELECTRON MICROGRAPHS

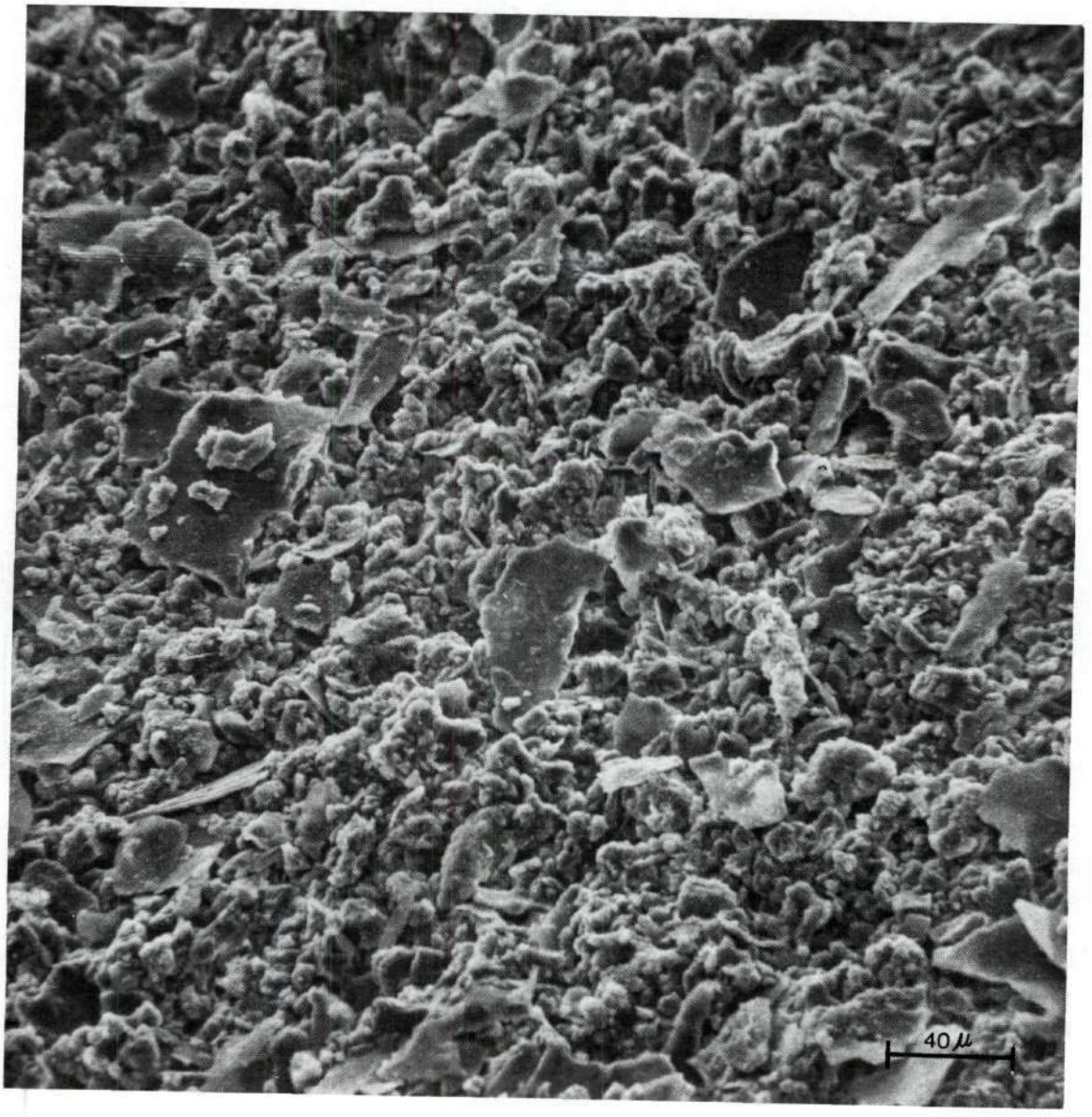

Figure 32. Scanning Electron Micrograph of Ranong Clay, Bulk.

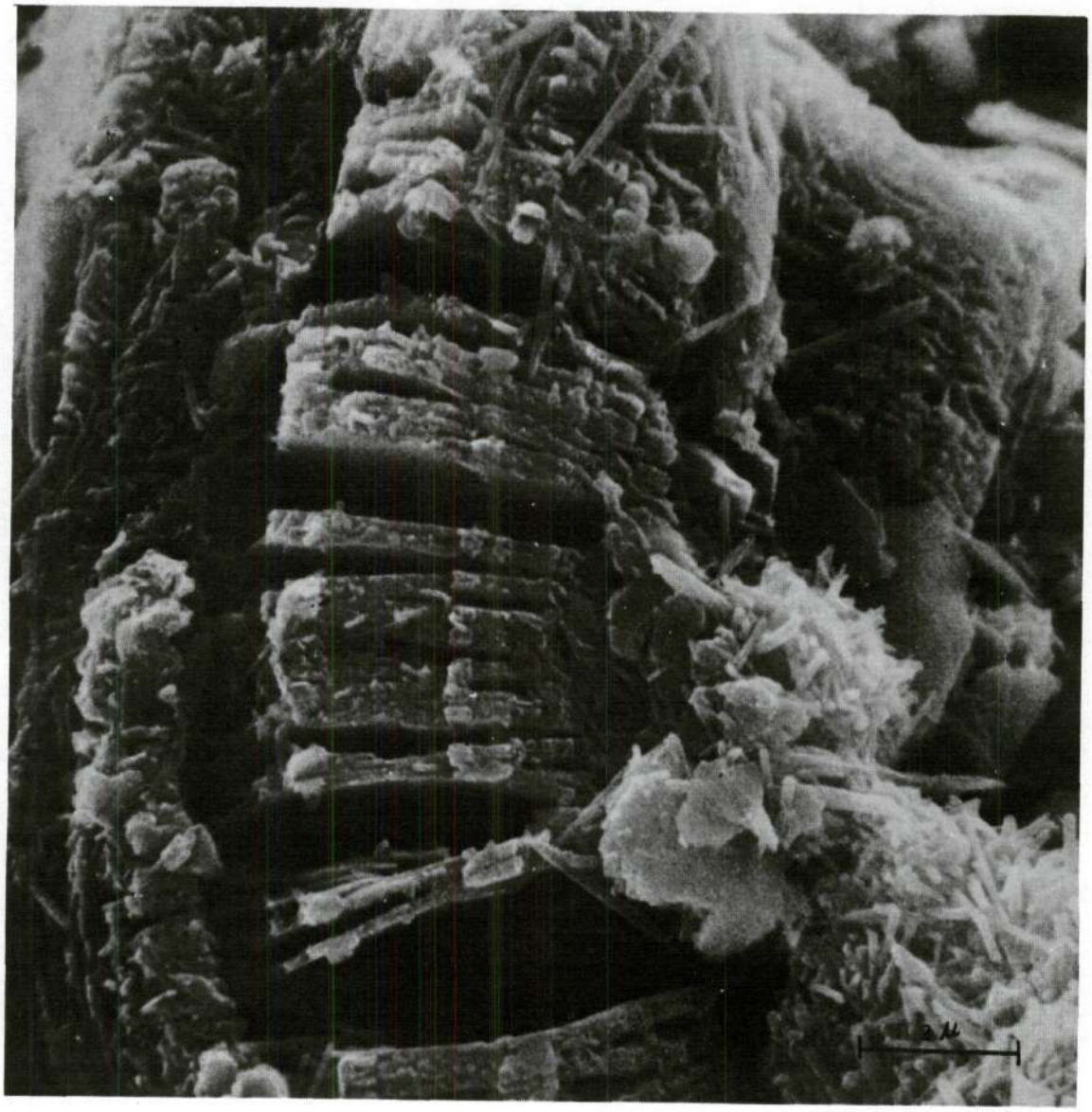

Figure 33. Scanning Electron Micrograph of Ranong Clay, Bulk.

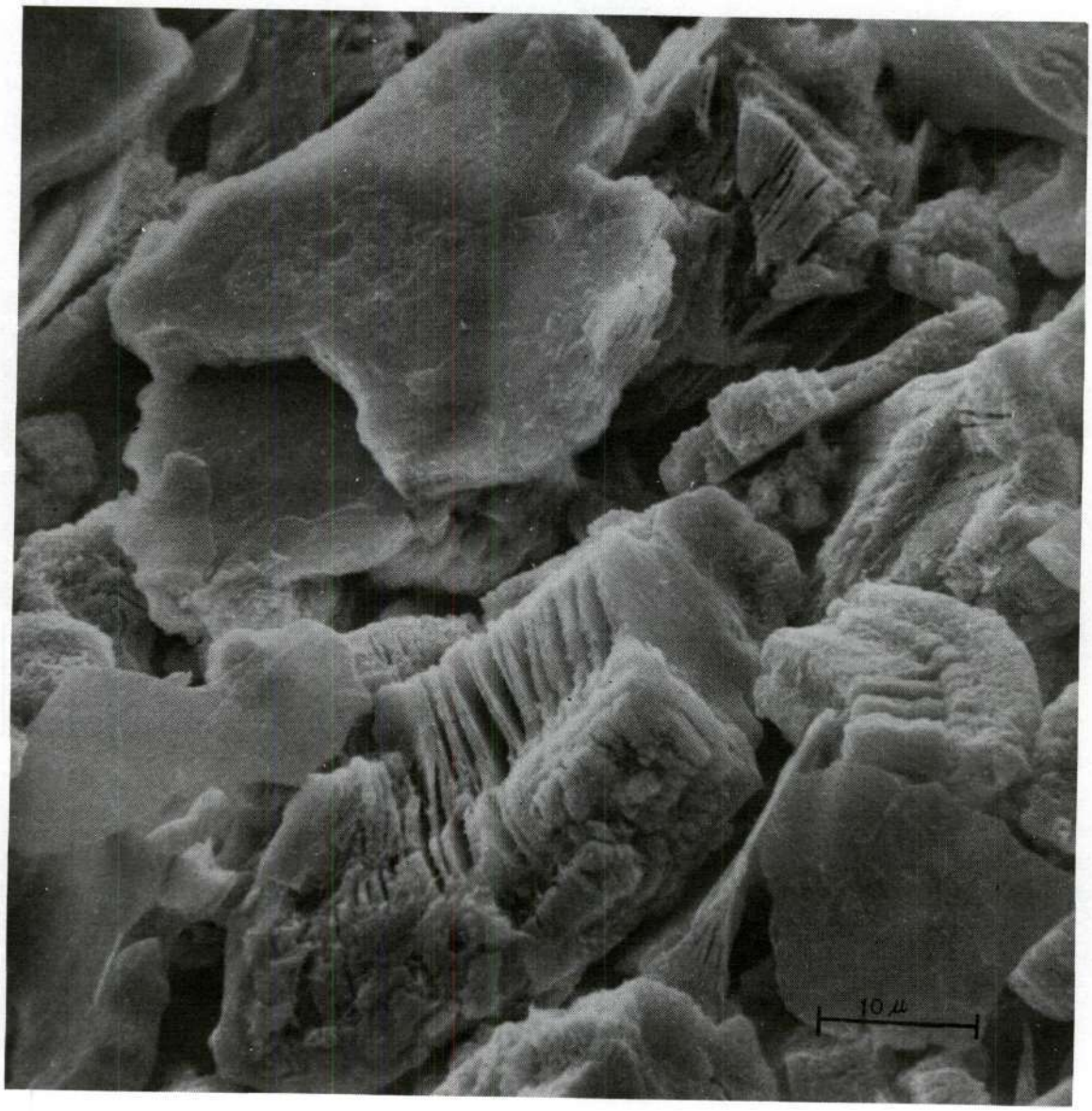

Figure 34. Scanning Electron Micrograph of Ranong Clay, 20-44 microns.

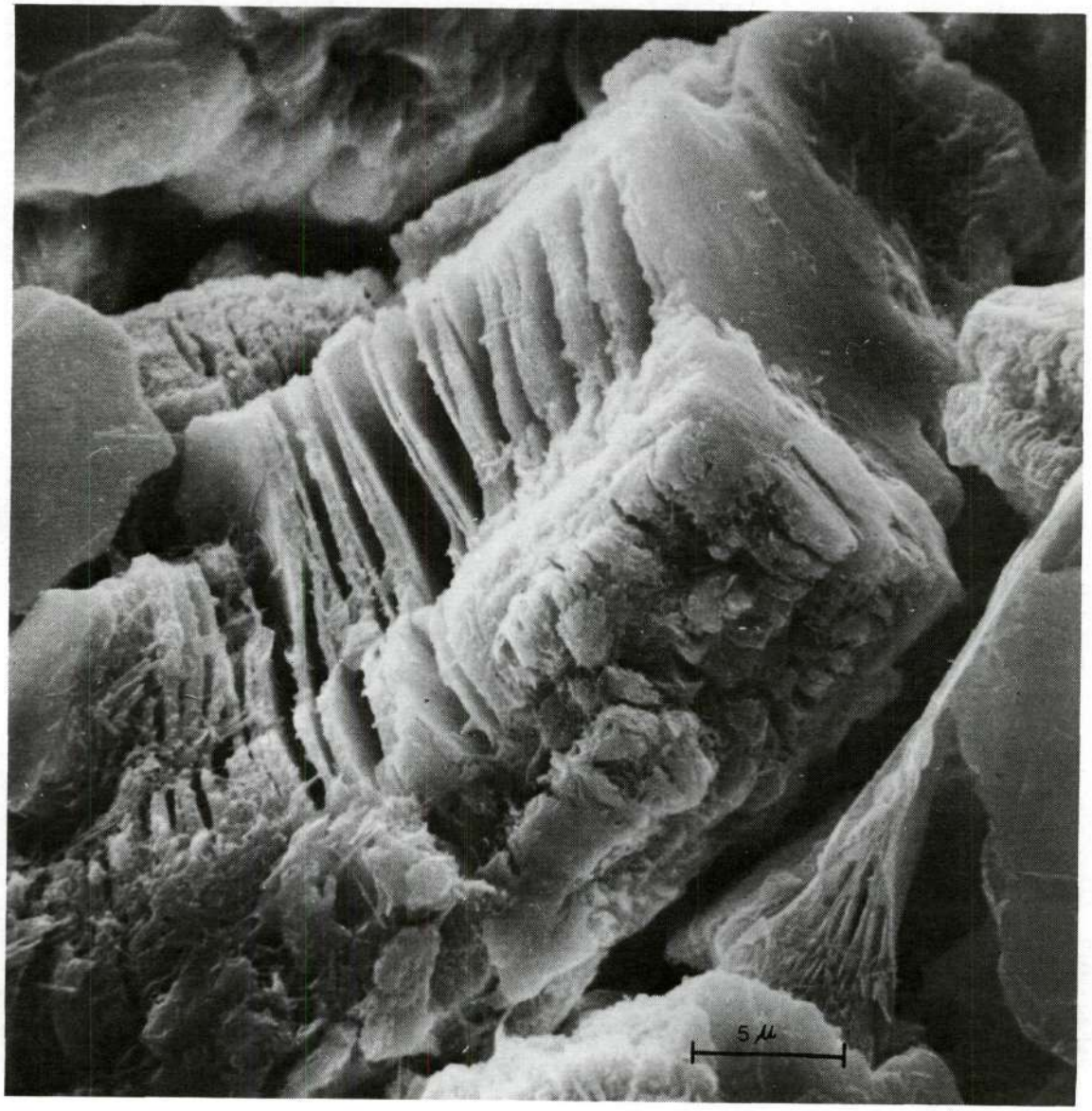

Figure 35. Scanning Electron Micrograph of Ranong Clay, 20-44 microns.

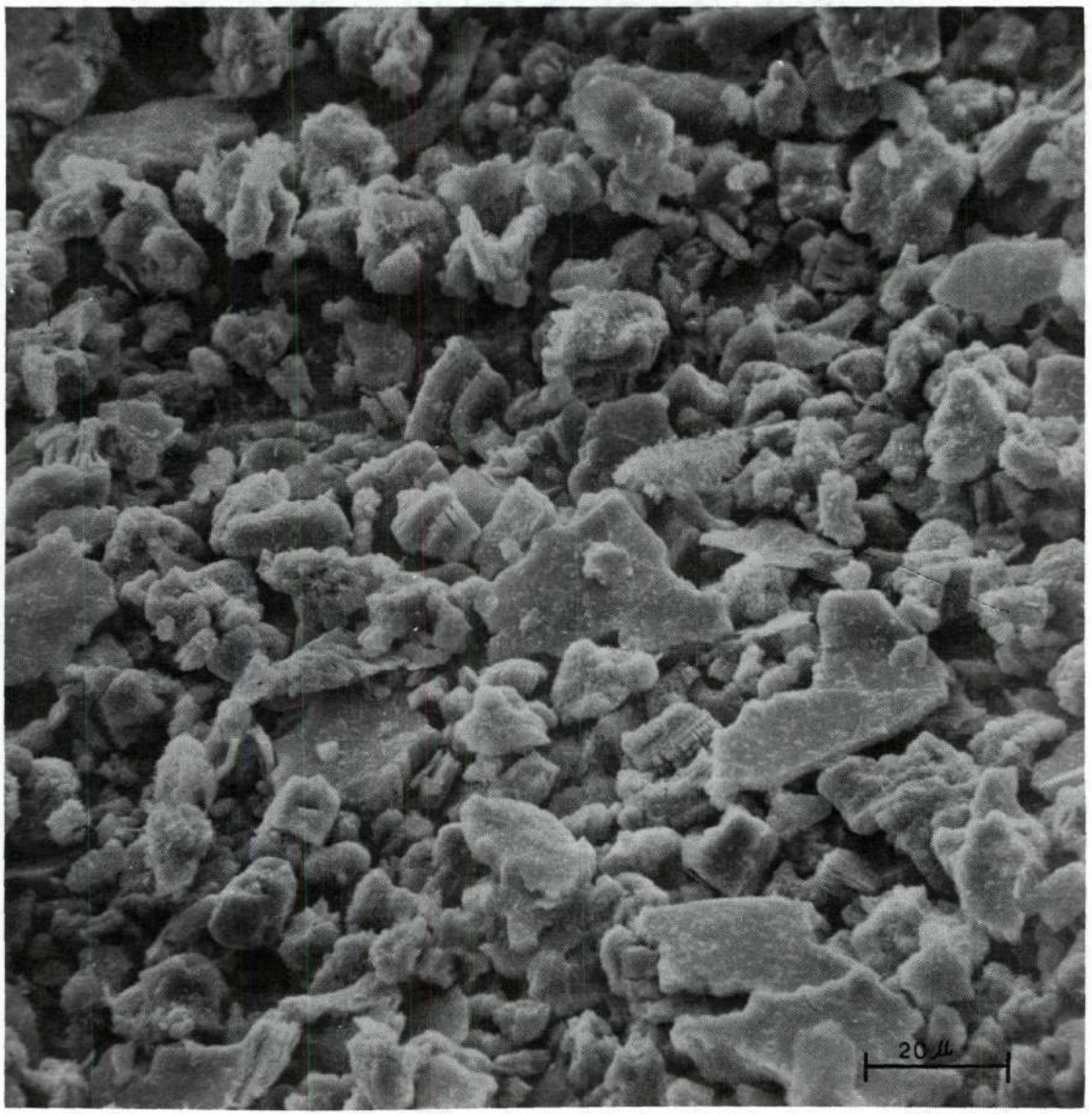

Figure 36. Scanning Electron Micrograph of Ranong Clay, 10-20 microns.

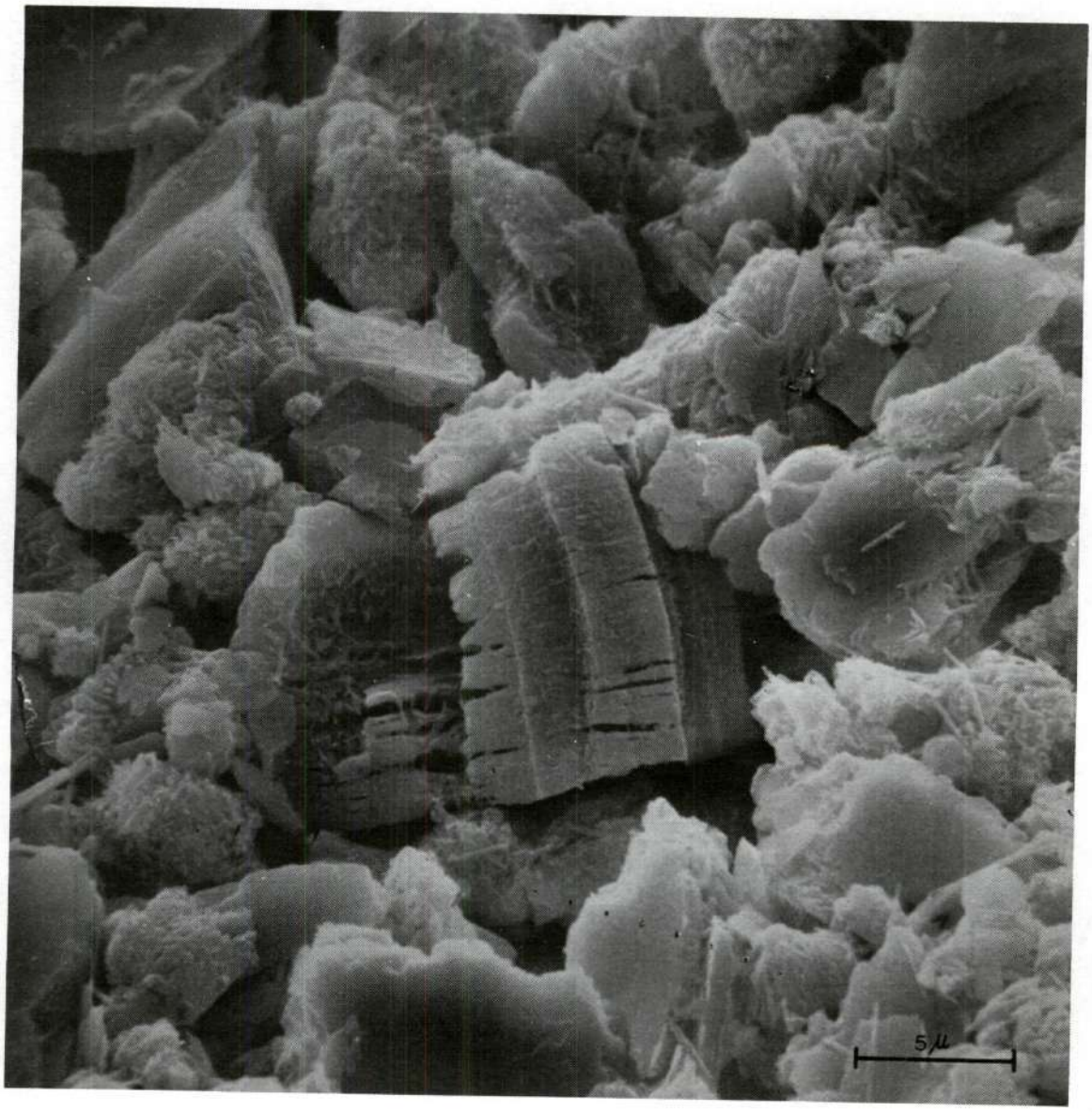

Figure 37. Scanning Electron Micrograph of Ranong Clay, 10-20 microns.

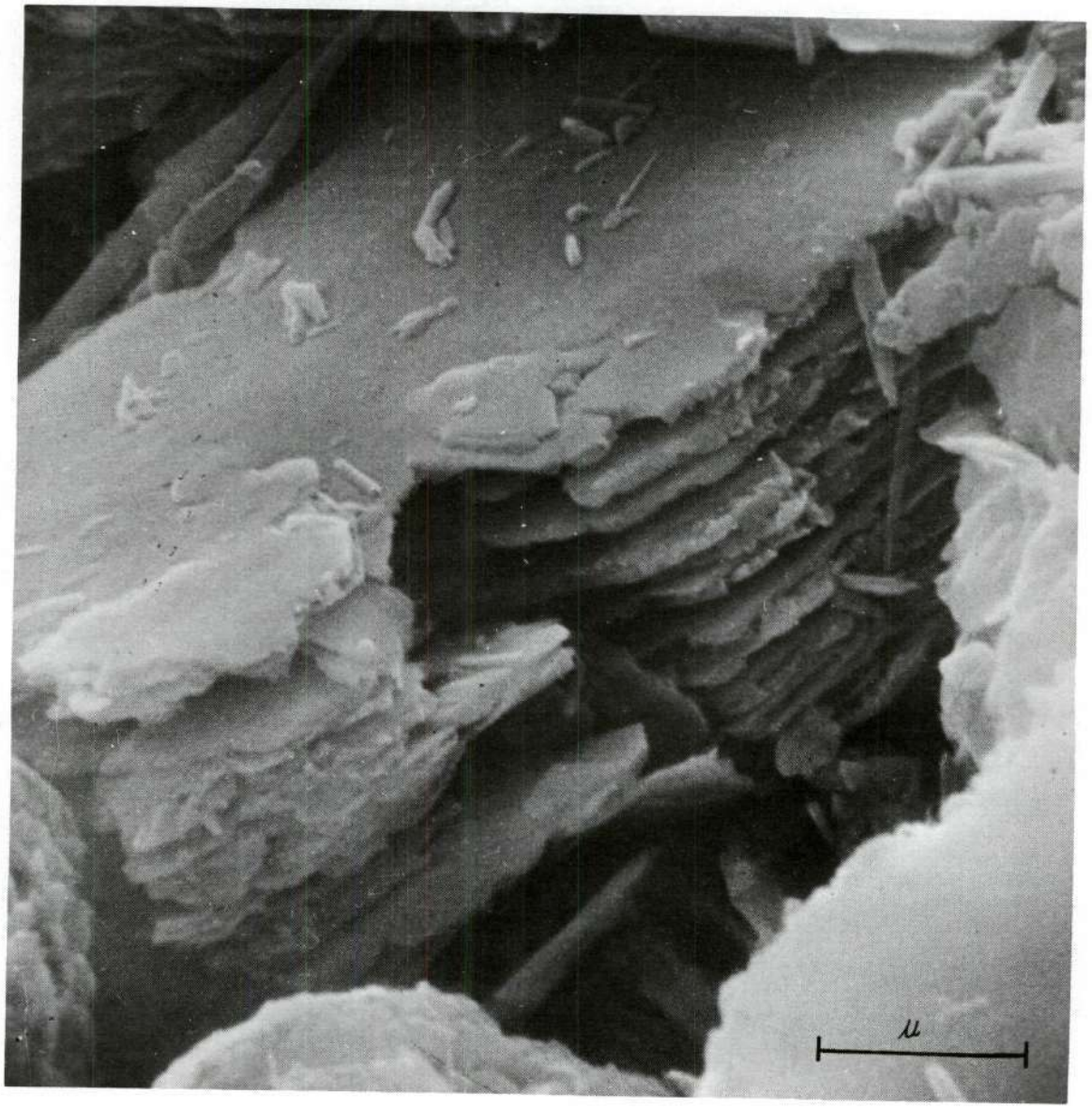

Figure 38. Scanning Electron Micrograph of Ranong Clay, 10-20 microns.

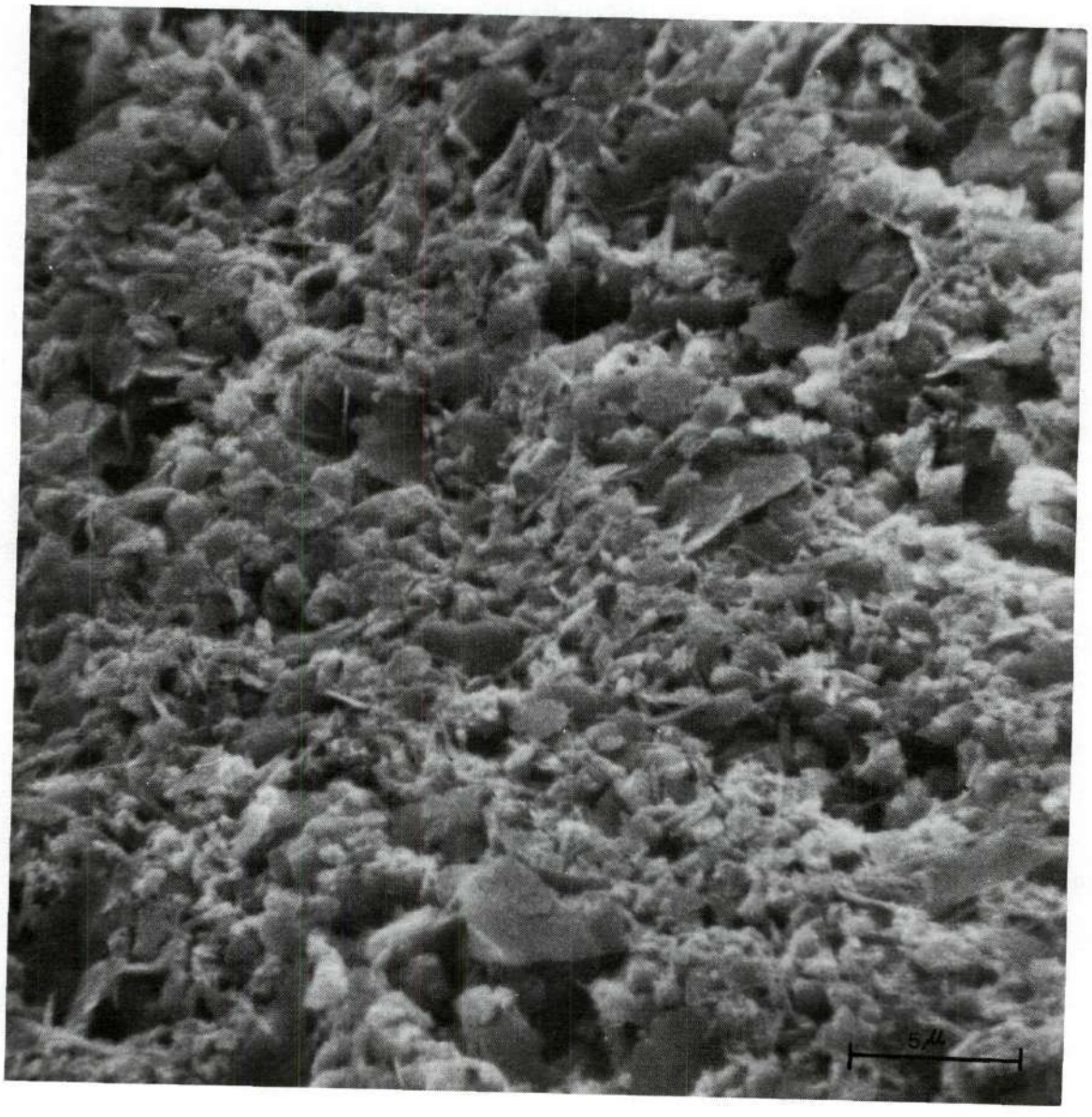

Figure 39. Scanning Electron Micrograph of Ranong Clay, 1-2 microns.

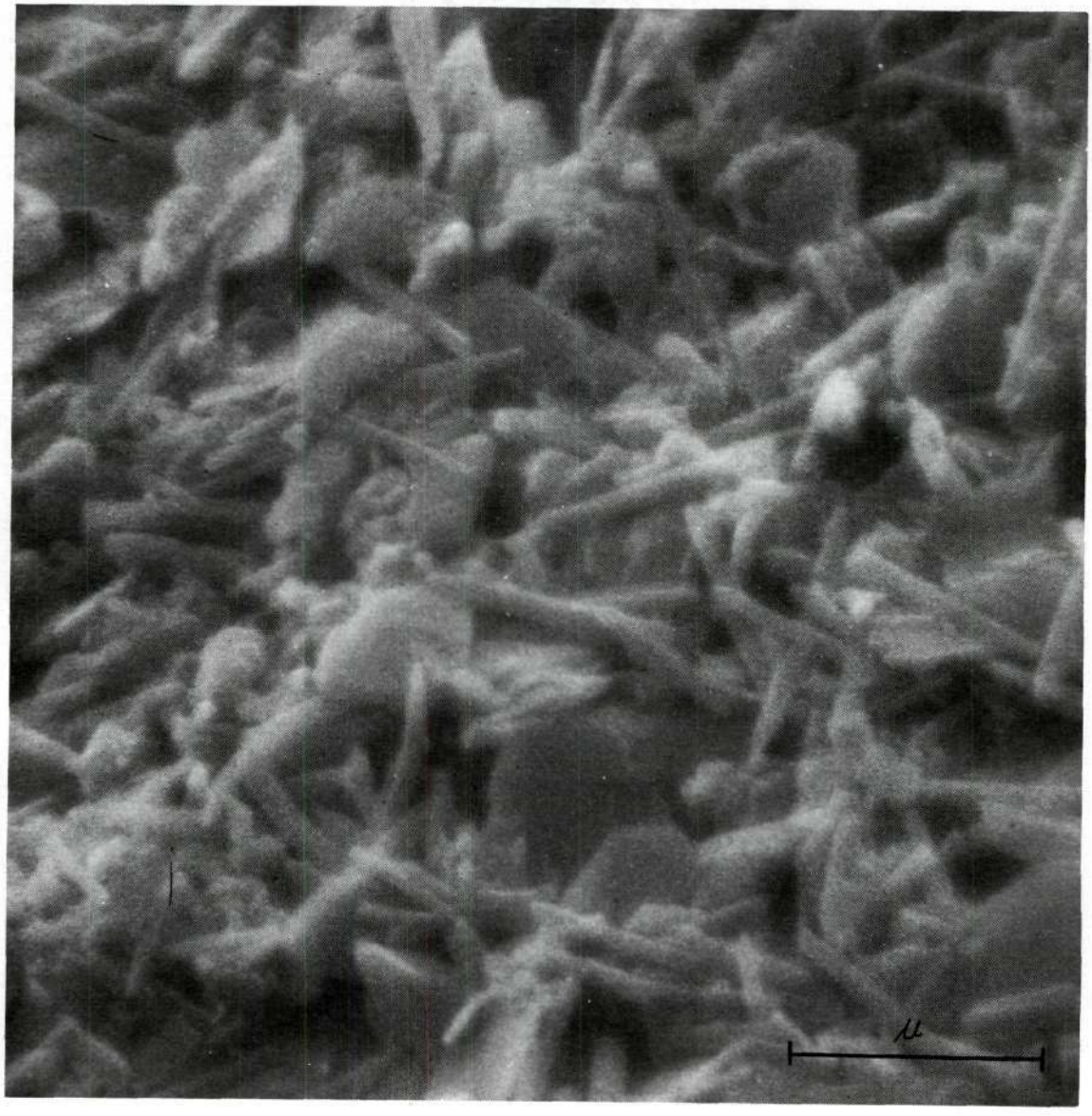

Figure 40. Scanning Electron Micrograph of Ranong Clay, Less than 2 microns.

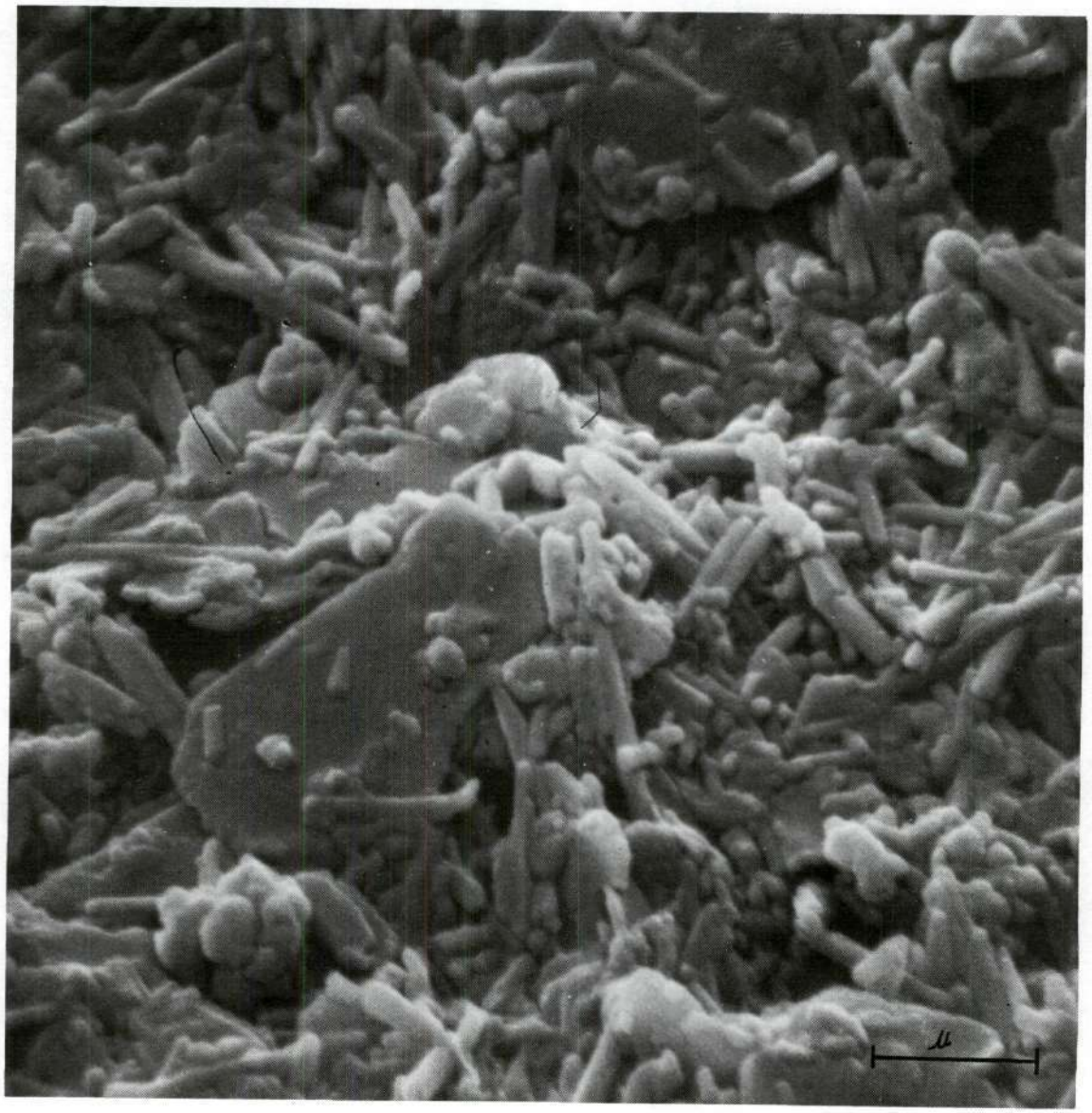

Figure 41. Scanning Electron Micrograph of Ranong Clay, Less than 2 microns.

APPENDIX C

DTA, TGA, AND INFRARED DATA

Table 30. Differential Thermal Data for Ranong Clay

Clay Fraction	Endothermic Peak (°C)				Exothermic Peak (°C)	
	Range	Maximum Peak	Range	Maximum Peak	Range	Maximum Peak
Bulk	0-210	98	400-665	545	950-1020	993
20-44 microns	0-210	98	400-665	545	950-1020	993
10-20 microns	0-210	100	400-665	547	950-1020	993
5-10 microns	0-210	104	400-665	548	950-1020	993
2-5 microns	0-210	98	400-665	547	950-1020	993
1-2 microns	0-210	98	400-685	547	950-1020	993
0.5-1 micron	0-210	96	400-625	547	950-1020	993
0.25-0.5 micron	0-210	95	400-625	547	950-1010	993
0.1-0.25 micron	0-210	95	400-625	540	950-1010	990
Less than 0.1 micron	0-210	95	400-625	520	950-1010	980

Table 31. Data of Dehydration Temperature of Selected Size-Fractions of Ranong Clay

Bulk Clay		Clay, 1-2 microns		Clay, Less than 0.1 micron	
Temp. (°C)	% Loss of Water	Temp. (°C)	% Loss of Water	Temp. (°C)	% Loss of Water
100	0.498	100	0.031	100	2.184
200	0.692	200	0.153	200	4.467
300	0.968	300	0.305	300	5.856
400	1.522	400	0.763	400	7.543
450	3.183	450	1.831	450	11.123
500	7.474	500	6.865	500	15.682
600	11.900	600	12.510	600	17.271
700	13.010	700	13.425	700	18.164
800	13.700	800	14.035	800	18.462
900	13.700	900	14.035	900	18.462
1000	13.700	1000	14.035	1000	18.462

Table 32. Observed Adsorption Bands* of Selected Size-Fractions of Ranong Clay

Clay Fraction	Wavelengths in microns									
	1	2	3	4	5	6	7	8	9	10
Bulk	2.7150	6.0210	8.9750	9.6225	10.6333	10.9500	12.5250	13.2125	14.4250	14.9875
	3683.24	1660.85	1114.20	1039.92	940.00	913.24	798.40	756.85	693.24	667.22
1-2 microns	2.7125	6.0210	8.9750	9.6625	10.6333	10.9500	12.5250	13.2125	14.4250	----
	3686.63	1660.85	1114.20	1032.92	940.00	913.24	798.40	756.85	693.24	----
Less than 0.1 micron	2.7250	6.0210	8.9750	9.6225	----	10.8750	12.5250	13.2125	14.4250	----
	3669.72	1660.85	1114.20	1032.92	----	919.54	798.40	756.85	693.24	----

* Wavenumbers(cm^{-1}) are given below the corresponding wavelength values in microns.

APPENDIX D

MISCELLANEOUS DATA

Table 33. Particle Size Distribution of Ranong Clay

Particle Size (microns)	Cumulative Percent Finer
44.00	99.59
42.54	95.08
30.06	94.01
21.28	93.60
13.45	84.50
7.76	61.75
5.49	51.02
3.88	35.69
2.74	23.72
2.34	20.19
2.10	18.50
2.00	14.00
1.00	8.60
0.50	5.20
0.25	2.47
0.10	0.18

Table 34. Particle Size Distribution of Ranong Refined Clay, (80 Percent finer than 2 microns)

Particle Size (microns)	Cumulative Percent Finer
5	99.90
2	80.00
1	59.94
0.50	39.89
0.25	16.61
0.10	3.56

Table 35. Metal Impurities in Ranong Clay from X-ray Fluorescent Analysis and Atomic Adsorption Spectrophometric Analysis

	Metal Impurities, Trace Quantities
X-ray Fluorescent Analysis	Fe
	K
	Ca
	Sn
	Cr
	Ba
	Pb
	Zn
	Ni
Atomic Adsorption Spectrophotometric Analysis	Fe
	K
	Ca
	Na
	Mg

Table 36. Brightness and Whiteness of Various Particle Size Fractions of Ranong Clay

Clay Fraction	% Brightness	Whiteness
Bulk	81.0	12.0
20-44 microns	78.5	13.5
10-20 microns	79.0	13.2
5-10 microns	80.5	12.0
2-5 microns	81.5	10.5
1-2 microns	81.8	11.0
0.5-1 micron	82.0	9.5
0.25-0.5 micron	81.0	11.0
less than 0.25 micron	76.2	14.0

Table 37. Viscosity of Ranong Refined Clay

RPM (Rate of shear)	Viscosity* in centipoises
6	4,000
12	2,170
30	1,260
60	670

* Brookfield viscosity was measured at maximum fluidity with TSPP (o.55%) using spindle #3, 60.8% solids.

BIBLIOGRAPHY*

1. Grim, R. E., Clay Mineralogy, Second edition, McGraw-Hill, New York, 1968
Grim (II), as published in this reference.

2. White, W. A., "Allophane from Lawrence Country, Indiana," American Mineralogist 38, 634-642 (1953).

3. Ross, C. S. and Kerr, P. F., "Halloysite and Allophane," U. S. Geol. Survey, Prof. Paper 185-G, 135-138, (1934).

4. Ross, C. S. and Kerr, P. F., "The Kaolin Minerals," U. S. Geol. Survey, Prof. Paper 165-E, 151-180, (1931).

5. Brindley, G. W., X-ray Identification and Structure of the Clay Minerals, Mineralogical Society of Great Britain Monograph, 32-75, 1951.

6. Brindley, G. W. and Robinson, K., "Randomness in the Structure of Kaolinite Clay Minerals," Transactions of the Faraday Society 42B, 198-205, (1946).

7. Johns, W. D. and Murray, H. H., "An Empirical Index for Kaolinite Crystallinity," Paper presented at Meeting of Mineralogical Society of America, 1959.

8. Hoffman, U., Endell, K., and Wilm, D., "Rontgenographische and Kolloidchemische Untersuchungen Uber Tun," Angew. Chem. 47, 539-547, (1937).

9. Hendricks, S. B. and Jefferson, M. E., "Structure of Kaolin and Talc-Pyrophyllite Hydrates and Their Bearing on Water Sorption of the Clays," American Mineralogist 23, 863-875, (1938).

10. Bates, T. F., Hildebrand, F. A., and Swinford, A., "Morphology and Structure of Endellite and Halloysite," American Mineralogist 35, 463-484, (1950).

11. Collins, B. J. S., "Textural and Morphological Studies of Some Clay Minerals," Ph.D. Thesis, University of Illinois, 1955.

---

* Abbreviations used herein follow the form employed by Chemical Abstracts (1965).

12. Marshall, C. E., "Layer Lattices and Base-Exchange Clay," Z. Krist. 91, 443-449, (1935).

13. Grim, R. E., Bray, R. H., and Bradley, W. F., "The Mica in Argillaneous Sediments," American Mineralogist 22, 813-829, (1937).

14. Pauling, L., "The Structure of Chlorite," Proc. Natl. Acad. Sci. 16, 123-129, (1930).

15. McMurchy, R. G., "Structure of Chlorites," Z. Krist 91, 443-449, (1935).

16. Hathaway, J. C., "Some Vermiculite-tupe Clay Minerals," Natl. Acad. Sci., Publ. 395, 74-86, (1955).

17. Gruner, J. W., "Vermiculite and Hydrobiotite Structures," American Mineralogist 19, 557-575,(1934).

18. Bradley, W. F., "The Structural Scheme of Attapulgite," American Mineralogist 25, 405-410, (1940).

19. Nagy, B. and Bradley, W. F., "Structure of Sepiolite," American Mineralogist 40, 885-892, (1955).

20. Brauner, K. and Preisinger, A., "Structure of Sepiolite," Mineral. Petrog. Mitt. 6, 120-140, (1956).

21. Huggins, C. W., Denny, M. V., and Shell, H. R., "Properties of Palygorskite, An Asbesti-form Mineral," U. S. Bur. Mines, Rept. Invest. 6071, 17, (1962).

22. Mielenz, R. C. and King, M. E., "Physical-Chemical Properties and Engineering Performance of Clays," Calif. Dept. of Natural Resources, Div. of Mines, Bull. 169, 196-254, (1955).

23. Grim, R. E., "Petrographic Study of Clay Materials," Calif. Dept. of Natural Resources, Div. of Mines, Bull. 169, 101-104, (1955).

24. Piller, H., "Phase Contrast Microscopy Applied to the Determination of Fine-grained, Thin Transparent Minerals," Heidelberg Beitr. Min. 3, 307-334, (1955).

25. Kelly, W. P., "Interpretation of Chemical Analysis of Clays," Calif. Dept. of Natural Resources, Div. of Mines, Bull. 169, 92-94, (1955).

26. Grim, R. E., Applied Clay Mineralogy, McGraw-Hill, New York, 1962.

27. Iannicelli, J. and Millman, N., "Relation of Viscosity of Kaolin-Water Suspensions to Montmorillonite Content of Certain Georgia Clay," Clay and Clay Minerals, Proc. 14th Conf., Pergamon Press, New York, 347, (1966).

28. Thate, H., "The Chemical Industry in Thailand," Rept. submitted to the Board of Investment, Bangkok, Thailand, 1966.

29. Arunyakanondha, P., "Occurrence of Thai Kaolin from Granite by Pneumatolytic Action," Dept. of Mineral Resources, Ministry of Development, Bangkok, Thailand, Personal communication, 1969.

30. Jackson, M. L., Soil Chemical Analysis-Advanced Course, published by the author, Dept. of Soil Science, University of Wisconsin, Madison, Wis., 114-115, 1956.

31. Jackson, M. L., Soil Chemical Analysis-Advanced Course, published by the author, Dept. of Soil Science, University of Wisconsin, Madison, Wis., 127-145, 1956.

32. "Analytical Methods for Atomic Adsorption Spectrophotometry," Perkin-Elmer Corporation, Norwalk, Connecticut, 1969.

33. "1968 Book of ASTM Standards with Related Material," Part II, ASTM, Philadelphia 3, Pennsylvania, 1968.

34. "Kaolin Clays and Their Industrial Uses," J. M. Huber Corporation, New York, 156-158, 1955.

35. TAPPI, "Analysis of Clay," TAPPI Standard T-645m-54, New York, TAPPI, 1968.

36. "1968 Book of ASTM Standards with Related Material," Part XIII, ASTM, Philadelphia 3, Pennsylvania, 1968.

37. Kerr, P. F., Adler, H. H., Bray, E. E., Steven, N. P., Hunt, J. M., Keller, W. D., and Pickett, E. E., "Infrared Spectra of Reference Clay Minerals," Amer. Petrl. Inst. Project 49, Rept. 8, Columbia University, New York, (1950).

38. Murray, H. H. and Lyons, S. C., "Correlation of Paper-coating Quality with Degree of Crystal Perfection of Kaolinite," Clays and Clay Minerals, Natl. Acad. Sci., Natl. Res. Council Pub. 456, 39, 97-108, (1950).

39. Mitchell, L. and Poulos, N. E., "The Relationship of Structure of Georgia Kaolin to Its Viscosity," Engineering Experiment Station, Bull. 23, Georgia Institute of Technology, Atlanta, Ga., 1959.